OPTIMIZATION OF CURDLAN BIOSYNTHESIS IN THE GRANULE MATRIX DURING WASTEWATER TREATMENT IN AEROBIC GRANULAR SLUDGE SYSTEMS

by

Adedoyin Adekunle
B.Sc., Covenant University, 2017
M.Sc., Cranfield University, 2022

THESIS SUBMITTED IN PARTIAL FULFILLMENT OF
THE REQUIREMENTS FOR THE DEGREE OF
MASTER OF APPLIED SCIENCE
IN
ENGINEERING

UNIVERSITY OF NORTHERN BRITISH COLUMBIA

April 2025

Abstract

Aerobic granular sludge (AGS) biotechnology has been extensively studied for wastewater treatment over the past two decades, gaining increased interest due to its enhanced treatment performance and potential for resource recovery. This research focused on optimizing curdlan biosynthesis in the aerobic granule matrix during wastewater treatment. Using Taguchi fractional factorial design, nine experimental runs were conducted to determine the effect of carbon-to-nitrogen (C/N) ratio (carbon measured in form of chemical oxygen demand – COD), organic loading rate (OLR), and feeding strategy on curdlan biosynthesis in the aerobic matrix. These factors were tested at three levels: C/N ratios of 10, 20, and 30; OLRs of 0.8, 1.5, and 2.1 kg COD/m³·d, and feeding strategies of 60 min feeding, 30 min feeding followed by 30 min resting phase, as well as 10 min pulse feeding followed by 50 min resting phase. Results indicate that C/N ratio had no effect on curdlan yield. Pearson correlation analysis revealed no correlation ($r = -0.07$) between C/N ratio and curdlan yield. This result was not statistically significant at 95% confidence level ($p=0.516$). The OLR was identified as the most influential factor. Curdlan yield increased with increasing OLR, attaining an optimum yield of 74 ± 6 mg curdlan/g biomass. Findings show a significant positive correlation ($r = 0.82$) between OLR and curdlan yield; and this was statistically significant at 95% confidence level ($p=0.007$). The feeding strategy showed minimal effect on curdlan yield with a weak negative Pearson correlation ($r = -0.25$) between feeding strategy and curdlan yield. However, this result was not statistically significant at 95% confidence level ($p = 0.852$. From mean effect analysis, OLR of 2.1 kg COD/m³·d, C/N ratio of 10, and feeding strategy of 30 min feeding followed by 30 min resting phase were optimal for curdlan production. The AGS system achieved stability throughout the duration of the experiments as both SVI_5 and SVI_{30} values in all the experimental runs were in the range 16 ± 2 – 43 ± 1 mL/g, and the

SVI_{30}/SVI_5 ratio was consistently between 0.9 and 1.0. Additionally, the AGS system achieved organic matter, ammonia-nitrogen, and phosphorus removal efficiencies reaching 99.6 ± 0.6%, 97 ± 1%, and 91 ± 6%, respectively. These findings look promising to enhance the sustainability of AGS-based wastewater treatment plants contributing to the attainment of circular economy in the wastewater management industry.

Table of Contents

List of Tables

List of Figures

Glossary

AGS	Aerobic granular sludge
ALE	Alginate-like exopolysaccharide
CAS	Conventional activated sludge
C/N	Carbon-to-Nitrogen ratio
COD	Chemical oxygen demand
DO	Dissolved oxygen
DOE	Design of experiment
EPS	Extracellular polymeric substances
FT-IR	Fourier Transform Infrared
GAOs	Glycogen-accumulating organisms
HRT	Hydraulic retention time
HSQC	Heteronuclear single quantum coherence
MLSS	Mixed liquor suspended solids
MLVSS	Mixed liquor volatile suspended solids
NaAc	Sodium acetate
NaPr	Sodium propionate
NH_3-N	Ammonia nitrogen
NMR	Nuclear Magnetic Resonance
NO_3-N	Nitrate nitrogen
NO_2-N	Nitrite nitrogen
OLR	Organic loading rate

PHA	Polyhydroxyalkanoate
$PO_4^{3-}P$	Phosphate phosphorus
PAOs	Phosphate-accumulating organisms
RAS	Return activated sludge
SBR	Sequencing batch reactor
SRT	Solids retention time
SVI	Sludge volume index
SWW	Synthetic wastewater
WWTPs	Wastewater treatment plants

Acknowledgments

I would like to acknowledge my sincere appreciation for all those who made the journey on this thesis a fruitful and exciting experience. I am grateful to the Almighty God for seeing me through my research. I would like to thank my supervisor, Dr Oliver Iorhemen from the School of Engineering, who oversaw my research work, for his commitment to this research, challenging and creative contribution and his pragmatic approach to keeping the project on track. Through your efforts and encouragement, I never lost the enthusiasm to see the project through to the conclusion. My appreciation goes to our research collaborator, Professor Andre Santos from the Federal University of Fortaleza, Ceara, Brazil for the advice and insightful contributions, particularly in the early stages of this work. I am grateful to Dr Kalindi Morgan and Dr Ron Thring for their immense contributions and support throughout this research.

I acknowledge Stefan Smulik for his support throughout my experimental work. His support and availability throughout my experiment was helpful and facilitated the speedy completion of my research. I acknowledge Resty Nabaterega for her contribution to my research work and writing. I am grateful to my research team Manveer Kaur, Mehdi Mohammed, Reim Soliman, Jibrael Odoom, and Erik Groenberg for their support and contributions to my research. Your help and friendship have been a great support to me. To my husband, Gbenga Obayemi, I am immensely grateful for your support, encouragement and motivation from day 1. You provided me with the strength I needed to continue and complete my program.

Contributions

The following scholarly contributions resulted from this MASc work:

1. Adekunle, A., Ukaigwe, S., dos Santos, A.B., Iorhemen, O.T. (2024). Potential for curdlan recovery from aerobic granular sludge wastewater treatment systems – A review. *Chemosphere.* 262: 142504.
2. Adekunle, A., Nabaterega, R., dos Santos, A.B., Iorhemen, O.T. Curdlan biosynthesis optimization in the granule matrix of aerobic granular sludge wastewater treatment systems. Submitted to *Bioresource Technology* (Manuscript ID: BITE-D-25-03143). Current Status*: Under Review*.

Details of contributions from the candidate and co-authors are listed below:

1. In this publication, the candidate conducted extensive review of related literature on circular economy and biorefinery concept, resource recovery from aerobic granular sludge (AGS), and the potential of curdlan recovery from AGS wastewater systems, manuscript writing, and proof reading. Prof. André Bezerra dos Santos provided reviewed and provided critical comments during manuscript preparation. Dr. Oliver Iorhemen provided significant contributions in terms of advice and corrections during manuscript preparation.
2. In this work, the candidate designed and performed all the experiments, collected and analyzed experimental data, wrote the first draft of the manuscript, revised the manuscript, and wrote the final manuscript. Dr Resty Nabaterega contributed to data analysis, proof reading with comments, and writing of the final manuscript draft. Dr. Andri Bezerra dos Santos assisted in the development of the curdlan recovery protocol and review of the draft. Dr. Oliver Iorhemen contributed with research guidance, funding acquisition, comments during manuscript writing, and proofreading.

Chapter 1 Introduction

1.1. Background and problem definition

The prospects of resource recovery from wastewater and its potential have gained attention over the past few decades. Resource recovery from wastewater treatment systems appears to give a promising future and offers potential collaboration between the wastewater, resource, and manufacturing sectors. Non-renewable resources such as phosphorite are at risk of depletion due to increasing industrial activities and population growth (Cordell et al., 2011; Chrispim et al., 2019). In the past decade, there has been extensive research on resource recovery and the potential for using the recovered high-value products alginate-like exopolysaccharide (ALE), polyhydroxyalkanoate (PHAs), phosphorus and tryptophan in industrial applications (De Sanctis et al., 2019; Karakas et al., 2020; Kehrein et al., 2020; Hamza et al., 2022). As an alternative means of production of resources, valuable resources such as biopolymers, bioplastics, biogas, and digestate are being extracted from wastewater to meet growing resource demands. As a result, wastewater is no longer viewed as a pollutant but as a valuable source of resources (Amann et al., 2018; Martí et al., 2017; De Sanctis et al., 2019; Karakas et al., 2020; Kehrein et al., 2020; Hamza et al., 2022).

For several decades, the floc-based conventional activated sludge (CAS) process has been the main technology used to treat municipal wastewater (Barrios-Hernández et al., 2020). However, CAS exhibits some notable drawbacks, including high energy consumption (CAS - 0.30 kWh per population equivalent and AGS - 0.19 kWh per population equivalent) (Ekholm et al., 2023), poor flocs settling properties, low biomass concentration, excess waste sludge production, and large space requirement due to the need for separate aeration tanks and clarifiers (Spinosa et al., 2011; Nancharaiah and Kiran Kumar Reddy, 2018; Hamza et al., 2022). Aerobic granular

sludge (AGS) biotechnology was developed to overcome these drawbacks. In the AGS system, microorganisms are self-immobilized into a matrix of compact granules that settle well, efficiently remove pollutants, and are comparatively more space efficient (De Sousa Rollemberg et al., 2018; Hamza et al., 2022). AGS biotechnology has garnered significant interest in the past two decades. During this period, the sequencing batch reactor (SBR) mode of operation has been widely used in AGS treatment systems (Nancharaiah & Kiran Kumar Reddy, 2018; Purba et al., 2020; Rosa-Masegosa et al., 2021). However, due to limitations such as inefficiency in handling high flow rates, the nature of continuous sewage flow in wastewater treatment plants (WWTPs) and the restricted amount of biomass retained through volume exchange, the adoption of continuous flow reactors (CFRs) is being explored as a promising alternative to the SBR mode of operation (Rosa-Masegosa et al., 2021; Yuan et al., 2021). Several recent studies have focused on different designs of CFRs for the formation of stable granules and effective wastewater treatment (Corsino et al., 2016; Lu et al., 2016). Presently, approximately 90 full-scale AGS-based WWTPs are operational globally, along with numerous laboratory- and pilot-scale installations (Sepúlveda-Mardones et al., 2019; Hamza et al., 2022).

Moreover, AGS shows strong potential as a resource reservoir due to its large extracellular polymeric substances (EPS) content (Liang et al., 2010; Barrios-Hernández et al., 2020; Zahra et al., 2022). The EPS matrix from AGS has been extensively investigated in various studies, revealing the presence of valuable substances such as tryptophan, polyhydroxyalkanoates (PHAs), alginate-like exopolysaccharide (ALE), and phosphorus (Karakas et al., 2020; de Carvalho et al., 2021; Ferreira et al., 2021; Hamza et al., 2022). Additional resources have been discovered in the EPS matrix of AGS, including curdlan (Ferreira et al., 2021), expanding the understanding of its chemical composition.

Curdlan is an insoluble, linear exopolysaccharide that consists of glucosyl residues interconnected by β-1,3 glycosidic bonds (Wu et al., 2012; Ganie et al., 2021). Curdlan is particularly valuable due to its properties such as biocompatibility, biodegradability, and nontoxicity to humans and the environment (Shih et al., 2009). Among other properties, curdlan is known to possess a gelling feature when heated, which improves its viscoelasticity, thermal stability, and water-holding capacity, all of which make it serve as a good food additive (Yang et al., 2016). In addition to its application in the food industry, curdlan and some of its derivatives serve as drug delivery polymer, as immune recognition sites of dectin-1, and as anti-AIDS agents to prevent HIV infection (Yang et al., 2016).

Considering the increasing areas of application of curdlan, it is inevitable for its demand to be on the rise. Currently, the global market value of curdlan is over 37 million US dollars, which is projected to grow to 57 million US dollars by 2030, at a Compound Annual Growth Rate (CAGR) of 7.3% during the forecast period (QY Research, 2024). However, the low conversion rate of glucose in curdlan production increases its overall production costs (Yuan et al., 2021). For instance, the fermentative production method for curdlan requires a minimum of 50 g/L of monomer sugars, which significantly increases the cost of production (Rofeal et al., 2023). Hence, an imperative need to recover curdlan from biosolids. AGS biotechnology has been identified as a promising avenue for the recovery of curdlan (Felz et al., 2020). This could create a system for integrating biorefinery into wastewater treatment systems. However, due to minimal research on this, issues regarding recovery techniques, quantification, optimization of production, and large-scale applications remain subjects of concern. Therefore, this research explores the potential of recovering curdlan from AGS treatment systems, aiming for future contributions to the curdlan market.

1.2. Research rationale and questions

The wide variety of exopolysaccharides that have been discovered in the aerobic granule matrix are currently being explored for more knowledge of their properties, efficient methods for extraction from the system, and purification protocols for the recovered products. As a result of the rheological and thermal properties, curdlan has gained increased interest, particularly due to the variety of industrial applications and the resulting high market demand. The commercial production of curdlan through microbial fermentation has been adopted extensively for decades. However, its recovery from AGS systems is yet to be explored. An important area that requires exploration is the optimization of key operational parameters and conditions such as feast-famine period ratio, carbon source, carbon-to-nitrogen (C/N) ratio, organic loading rate (OLR), hydraulic retention time (HRT), and feeding strategy for increased biosynthesis of curdlan in the granule matrix while maintaining the treatment performance of AGS-based wastewater treatment systems as well as maintaining granule stability. It will be worthwhile exploring how these parameters influence curdlan production by microorganisms and AGS bioreactor operational stability.

Therefore, the research project sought to answer the following research questions:

a) How does the C/N ratio (carbon measured in form of chemical oxygen demand – COD) impact the biosynthesis of curdlan in AGS treatment systems?
b) What is the impact of different feeding strategies on curdlan biosynthesis in AGS wastewater treatment systems?
c) Does varying organic loading rates influence the rate of curdlan biosynthesis in AGS wastewater treatment systems?

1.3. Research aim and objectives

This research project aimed to recovery curdlan from aerobic granule matrix while maintaining efficient wastewater treatment in AGS-based wastewater treatment systems. To achieve the aim, the specific objectives of the project were:

a) To determine the effect of C/N ratio on the biosynthesis of curdlan in AGS treatment systems.
b) To determine the impact of different feeding strategies on curdlan biosynthesis in AGS systems.
c) To determine the impact of varying organic loading rates on the rate of curdlan biosynthesis in AGS treatment systems.

1.4. Organization of thesis

This thesis is structured into five chapters:

Chapter 1, the current chapter, introduces the background of the resource recovery from wastewater and problem definition, the potential of curdlan recovery from AGS, discusses the research questions and rationale and concludes with the objectives of the research.

Chapter 2 covers an in-depth literature review of resource recovery and circular economy in the wastewater treatment sector, focusing on the potential of curdlan recovery from AGS. In this chapter, the properties, biosynthesis and microbial sources of curdlan were reviewed while identifying any research gaps. To understand the impact of various operational factors on curdlan biosynthesis, specific factors affecting the biosynthesis of curdlan were discussed in this chapter.

Chapter 3 outlines the experimental procedures for extracting curdlan from AGS systems, including bioreactor performance and biomass tests. The chapter details the use of Taguchi

orthogonal arrays in the experimental design to understand the relationships between variables and their effects on resource recovery. Pearson correlation analysis was also used to highlight the various correlations between each factor and curdlan biosynthesis. This combined approach aims to identify optimal conditions for resource recovery for further optimization studies.

Chapter 4 describes the results of biomass characteristics, performance of each experiment and the effects of C/N ratio, feeding strategy and OLR on curdlan recovery from AGS. The biomass characteristics focused on discussing the settling properties and biomass concentration in each experiment. The performance of each experiment was discussed to understand the removal efficiency trends over the experimental period and what factors may influence these results. The identification of the extracted biopolymer was discussed in this chapter. The various relationships between the studied factors (OLR, C/N ratio and feeding strategy) and curdlan biosynthesis were discussed to understand the trend of recovered curdlan. The factors and operational parameters that may have influenced these results were discussed in detail. The results of the statistical analysis (Taguchi and Pearson correlation analysis) were discussed and compared with previous studies.

Chapter 5 summarizes the research findings on the impact of each experimental factor on curdlan biosynthesis. This chapter compares the previous studies on resource recovery and AGS performance with this study and it concludes with recommendations for future research directions. The references supporting this thesis are listed at the end.

Chapter 2 Literature Review

2.1. Circular economy in wastewater management

The concept of a circular economy revolves around maximizing the lifespan of products and raw materials and minimizing waste by recognizing them as valuable secondary resources that can be reintegrated into the economy (Ghisellini et al., 2016; Neczaj and Grosser, 2018; Alhola et al., 2019). A major driver of this is resource depletion, scarcity and population growth. For instance, phosphorus recovery from WWTPs can reduce the dependence on phosphorite phosphate rock, which is a finite resource. The increasing world population and the corresponding increased demand for food make phosphorite depletion imminent (Cordell et al., 2011; Chrispim et al., 2019). The growing need for phosphorus in various industries, including fertilizer, textile, rubber, leather etc., underscores its need for recovery (Denning et al., 2014; Lu et al., 2016). Projections suggest that the global phosphorus reserve may be exhausted between 2070 and 2099 (Egle et al., 2016). Therefore, circular economy is acknowledged as a crucial element of sustainable development (Geissdoerfer et al., 2017). Within this framework, incorporating resource recovery can play a pivotal role in enhancing the value chain within the waste management industry and bolstering cost recovery (Kehrein et al., 2020).

Similarly, biorefinery aims to sustainably mine resources from wastewater, offering the opportunity to obtain high-value products from wastewater treatment systems (Iorhemen and Ukaigwe, 2023). This approach has made wastewater a valuable source of renewable energy, clean water, and, more importantly, raw materials. It also reduces the overall environmental impact of wastewater treatment by minimizing the release of pollutants into the environment and promoting

the reuse of valuable products. Moreover, biorefineries can promote economic viability, as the recovered products can generate revenues or offset the operational costs of treatment facilities.

Considering the significant benefits of a circular economy, all stakeholders have embraced the concept to primarily reduce dependence on raw materials and contribute to the United Nations' water and sanitation sustainable development objectives (Blomsma and Brennan, 2017; van Leeuwen et al., 2018; Campbell-Johnston et al., 2020). Adopting the biorefinery paradigm in wastewater management enhances sustainability and moves towards a circular economy.

2.2. Curdlan

Curdlan is an exopolysaccharide of high molecular weight residual sugar polymers secreted by different strains of non-pathogenic microorganisms, such as bacteria, yeast, and fungi. It is an insoluble, linear exopolysaccharide that consists of glucosyl residues interconnected by β-1,3 glycosidic bonds (Wu et al., 2012; Ganie et al., 2021). Curdlan was first synthesized from *Alcaligenes faecalis var myxogenes* 10C3 through glucose fermentation in 1966 (Zhan et al., 2012), but its demand increased over the years. Other strains including *Agrobacterium*, *Cellulomonas*, and *Bacillus* have also been selected for curdlan production (Martinez et al., 2015; Yu et al., 2011; Kalyanasundaram et al., 2012; Verma et al., 2020). Curdlan biosynthesis results from microbial response to nitrogen deficiency, leading to altering enzyme synthesis (Zhang et al., 2010). Curdlan biosynthesis can also be done through transmembrane proteins (synthases), but the process requires substantial energy and nutrient availability (Karnezis et al., 2003; Zhang et al., 2020). The industrial demand for curdlan has influenced the requirement for increased large-scale production. A major concern of curdlan production is the economic sustainability of the processes, primarily influenced by the raw materials, nitrogen, and carbon sources (Zhang and Nishinari,

2009; Salah et al., 2011; Verma et al., 2020). It is important to develop an efficient production method to ensure sustainable availability and continuously meet the demand for curdlan for industrial applications (Martinez et al., 2015).

2.3.Properties of curdlan

Curdlan is characterized by various properties that are important for its application and extraction protocol. It is a water-insoluble linear homopolysaccharide that consists of d-glucose-linked with repeated units of β-(1,3)-glucan (Chen and Wang, 2020; Yuan et al., 2021). The unique structure, solubility, rheological, and thermal gelling properties of curdlan make it suitable for various applications in the food and pharmaceutical industries (Martinez et al., 2015). Curdlan is a high molecular weight substance with a general chemical formula $(C_6H_{10}O_5)n$ (McIntosh et al., 2005; Kalyanasundaram et al., 2012; Verma et al., 2020). Curdlan consists of 90% carbohydrate, non-acidic, with numerous glucose subunits linked by β-bonds between the first and third carbon atoms of the ring (Liang et al., 2021). The d-glucose in curdlan is similar to that of cellulose although the chemical bonds are different (Harrison et al., 2023). Curdlan obtained from bacterial species is composed of glucose with a molecular weight that ranges between 5.3×10^4 Da and 5.8×10^6 Da in a 0.3 M alkaline solution (Kalyanasundaram et al., 2012). From fungal species, the molecular weight of curdlan obtained ranges between 2.06×10^4 Da to 5.0×10^6 Da (Verma et al., 2020). The β-arrangement gel in the infrared spectrum of curdlan exhibit a single peak at around 890/cm of the spectra (Kalyanasundaram et al., 2012).

The important properties of curdlan that make it particularly applicable in the food industry include thermal stability, gel syneresis, and freezing and thawing stability (Verma et al., 2020). Curdlan can form a thermo-reversible gel by heating its aqueous suspension to about 60 °C with subsequent cooling. A thermo-irreversible gel can also be formed by heating curdlan's aqueous

suspension to 80 °C with subsequent cooling (Zhang et al., 2002; Nishinari and Zhang, 2004; Chaudhari et al., 2021). The high-set curdlan (thermos-irreversible gel) is characterized by a triple helical structure through hydrophobic interactions, which is vital for the pharmaceutical industry in producing grafting co-polymers (Brodnjak, 2017) and drugs such as salbutamol sulfate, indomethacin, and prednisolone (Ichiyama et al., 2013). Meanwhile, the low-set curdlan (thermos-reversible gel) is characterized by a single helical structure through hydrogen bonds (Yan et al., 2020). Besides the high thermal stability, curdlan exhibits high freezing stability, making it commonly used in frozen foods (Chaudhari et al., 2021).

Curdlan is highly biodegradable and non-toxic to the environment and humans, making it widely used in different industries (Aquinas et al., 2022). It is a colorless, tasteless, and odorless compound with an appearance similar to white powder and shows stability in a wide pH range (3–9) (Shih et al., 2009; Verma et al., 2020; Harrison et al., 2023). Curdlan is a gelatinous and viscous substance with high tolerance to high temperatures and it is insoluble in water below 54 °C temperature (Jindal and Singh Khattar, 2018), as well as other organic solvents such as alcohol and acids. However, due to the ionization of hydrogen bonds, curdlan is soluble in alkaline solutions at pH 12, such as sodium hydroxide and trisodium phosphate (Dominguez-Martinez et al., 2017; West, 2020; Jia et al., 2021; Harrison et al., 2023).

2.4. Microbial sources of curdlan

Various microorganisms, including bacteria, yeast, fungi, mold, and algae secrete curdlan. While curdlan was first discovered in *Alcaligene faecalis* as one of the extracellular exogenous sugars produced (Prakash et al., 2018), the genus *Agrobacterium* secrets the highest amount of curdlan, particularly the linear 3-1 glucan (Venkatachalam et al., 2020). El-Sayed et al. (2016) reported that the media components, especially pH and temperature are primary factors for

optimizing curdlan production. These factors resulted in a yield of 2.34–4.82 g/L of curdlan from *Paenibacillus* sp. NBR-10.

The first curdlan-producing microorganism (*Alcaligene faecalis*) is found in soil, water, and human faeces. *Alcaligene faecalis* produces up to 72 g/L curdlan by feeding on ammonium phosphate and minimal nitrogen concentration (Wu et al., 2008). *Agrobacterium radiobacter*, first isolated from Australian soil, is another significant curdlan-producing bacterium used in commercial production (Verma et al., 2020). *A. radiobacter* produces curdlan in growth media using both continuous and batch methods with limited nitrogen (Dai et al., 2015; West, 2015; Verma et al., 2020). The strain - *Agrobacterium* sp. ATCC 31,749 produced the highest amount of curdlan when cultivated in a growth medium containing solids-hydrolysate and 2,2 mM ammonium phosphate as a nitrogen source (West, 2015). Additionally, when cultured in a growth medium containing whole hydrolysate and 3,3 mM ammonium phosphate, the curdlan produced was high. To improve the production of curdlan, Ying Liang et al. (2017) reported the strategy of combining a fungal strain (*Trichoderma harzianum* GIM 3.442) and *Agrobacterium* sp. ATCC 31,749 in a fermentation system to produce curdlan with low molecular weight. The system achieved the highest level of curdlan production by using wheat bran as a nitrogen source, significantly reducing the cost of biosynthesis of this curdlan.

Furthermore, the non-pathogenic gram-negative, rod-shaped *Agrobacterium* sp. is commonly utilized to produce curdlan. For commercial production purposes, curdlan is primarily generated on a large scale by two mutants, namely *Agrobacterium* sp. ATCC 31749 and *Agrobacterium* sp. ATCC 31750, with the latter being a variant of the former (Yu et al., 2015).

Paenibacillus polymyxa is another bacterium used for producing curdlan (Rafigh et al., 2014). For optimal curdlan yield, *P. polymyxa* is incubated at a temperature of 50 °C for 96 h and

a pH of 7. The culture media used contains 100 g/L of glucose and 3 g/L of yeast extract, giving a curdlan yield of about 6.89 g/L (Rafigh et al., 2014).

Date palm juice showed potential as a carbon source for curdlan production by *Rhizobium radiobacter* strain (Besbes et al., 2009). The bacteria demonstrated a strong ability to utilize the substrate in the culture media, producing 22.83 g/L of curdlan biopolymer under optimized conditions. These conditions included a culture media containing 2 g/L of ammonium sulfate, 120 mL/L of date glucose juice concentration, a pH of 7.0, a temperature of 30 °C, a shaking incubator speed of 180 rpm, and a fermentation time of 51 h, with curdlan of a molecular weight of 180 kDa (Salah et al., 2011). Additionally, Wang et al. (2016) found that the cell density of the bacteria increased with the total concentration of $(NH_4)_2HPO_4$ in the medium. Furthermore, adding a nitrogen source increased cell growth and curdlan production, particularly in the early fermentation stage.

Previous studies have investigated the microbial community in AGS systems and its impact on EPS composition and granule formation (Xia et al., 2018; Filho et al., 2019; Ekholm et al., 2024). The genus *Agrobacterium* has been identified as a significant producer of EPS in AGS systems. In a study by Shoda and Ishikawa (2014), *Alcaligene faecalis*, a functional heterotrophic nitrification and aerobic denitrification strain capable of removing high-strength ammonium, was found in freshwater wastewater treatment facilities. Furthermore, a bacterium belonging to the genus *Rhizobium* was isolated from CAS (Zhang et al., 2011). Based on phylogenetic analysis using the 16S rRNA gene sequence, it was discovered that the closest relative was *Rhizobium radiobacter* LMG 140T. Since these species have been detected in various wastewater treatment systems, particularly in floccular and granular sludge, further research is necessary to investigate their role in curdlan biosynthesis in AGS systems.

2.5. Factors affecting curdlan biosynthesis

The biosynthesis of curdlan is influenced by factors such as carbon source, pH, temperature, type of fermentation, and size of the bacterial inoculum (Jin et al., 2008; Pan et al., 2020; Gao et al., 2021). In Zhan et al. (2012), energy efficiency was the primary limiting factor affecting the high yield of curdlan biosynthesis using *Agrobacterium* species. This suggests the increase in glucose uptake as a primary method of optimization of curdlan production (Figure 2.1) (Zheng et al., 2007; Zhan et al., 2012). The most appropriate condition for enhancing curdlan biosynthesis was found to be when *Agrobacterium* sp. ATCC is exposed to sucrose as the carbon source at a concentration of 140 g/L, resulting in a curdlan yield of 32 g/L (Jiang, 2013). About 28.2 g/L curdlan yield was achieved when exposed to urea as the nitrogen source, while 15.2 g/L curdlan was produced with exposure to ammonium chloride after an incubation period of 95 h.

Additionally, the use of dried orange peels as the fermentation substrate in *A. faecalis* significantly influences curdlan production (Mohsin et al., 2019). In this study, the maximum sugar release of 72.3 g/L, with 95–98% removal of phenolics was achieved by drying orange peels at 120 °C after saccharification and detoxification, resulting in the production of 23.2 g/L curdlan under kinetic surveillance.

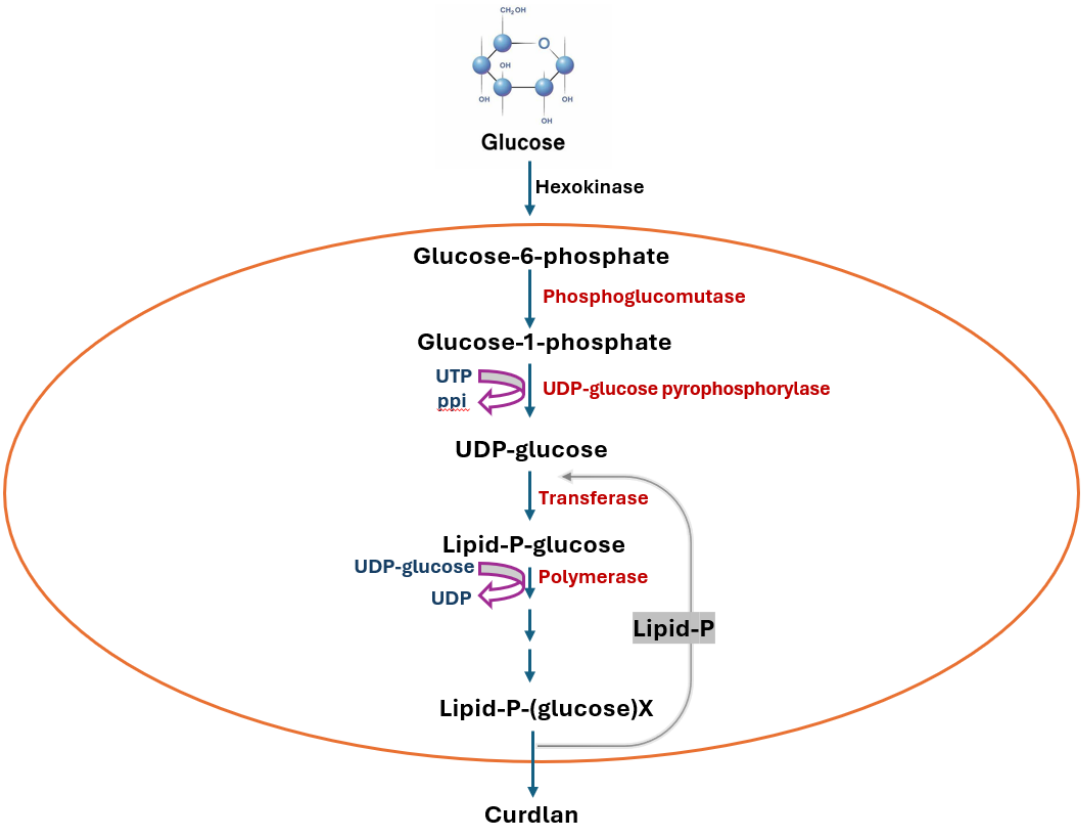

Figure 2. 1. Illustration of the metabolic pathway of curdlan biosynthesis

2.5.1. Carbon source

In the biosynthesis of curdlan, the selection of an appropriate carbon source is critical as it significantly influences both yield and quality. Studies have indicated that using dextrin as the carbon source can enhance the production of curdlan in *A. tumefaciens* ATCC31749 (Wan et al., 2022). Notably, the recombinant strain sp-AmyAXCC, which expresses IPTG-inducible α-amylase from *Xanthomonas campestris*, achieved a curdlan titer of 66.7 g/L with a yield of 0.56 g/g when dextrin was utilized, highlighting the substantial impact of the carbon source on curdlan production (Wan et al., 2022).

Additionally, research by Yu et al. (2024) examined the effects of various carbon sources, including maltose, glucose, maltodextrin, and hydrolysates of cassava starch treated with different

enzymes (α-amylase, β-amylase, and a combination of β-amylase and pullulanase). The findings revealed that maltose provided the highest curdlan yield of 32.5 g/L, while maltodextrin resulted in the lowest yield. With cassava starch hydrolysate at an initial sugar concentration of 90 g/L, curdlan production reached 28.4 g/L, yielding 0.79 g/g of consumed sugar and a molecular weight of 1.26×10^6 Da after 96 h.

The presence of specific carbon sources in the growth medium stimulates the secretion of enzymes crucial for curdlan biosynthesis (Al-Rmedh et al., 2023). Glucose enhances the activity of enzymes responsible for converting glucose to curdlan (Al-Rmedh et al., 2023). Furthermore, the increased expression of ATP-binding cassette transporters improves glucose uptake and its integration into the curdlan synthesis pathway (West, 2020). This indicates that the type of carbon source can significantly influence the metabolic pathways and enzyme activities involved in curdlan production.

2.5.2. Temperature

Temperature is a crucial factor for the biosynthesis of curdlan. Studies have indicated that the optimal temperature for curdlan production is about 30°C (El-Sehemy et al., 2012; West, 2020; Aquinas et al., 2024). At this temperature, the production of curdlan is maximized, likely due to the optimal enzymatic activities involved in its biosynthesis. When the temperature is increased beyond this optimal range, the production rate decreases, attributed to the denaturation of these enzymes and the destabilization of cellular processes. Additionally, temperature influences the gelling properties of curdlan. The heating of curdlan suspension to about 60°C results in the formation of a weak, thermo-reversible gel, which melts upon reheating (Zhan et al., 2012). However, when the temperature increases over 80°C, a strong, thermo-irreversible gel is formed. This temperature-induced gelation is essential for various applications of curdlan in the food

industry and biomedicine (Zhan et al., 2012). The precise control of temperature during the fermentation and gelation processes is therefore critical for optimizing curdlan production and its functional properties.

2.5.3. pH

Curdlan biosynthesis is influenced by the pH of the environment (Pan et al., 2020), which affects the activity of key enzymes involved in its production. For instance, at pH 5.5, the activity of the catalytic subunit of β-1,3-glucan synthase (crdS) is significantly higher compared to pH 7.0, with an increase of about 10-fold (Jin et al., 2008). Additionally, UTP-glucose-1-phosphate uridylyltransferase and phosphoglucomutase, which are essential for curdlan biosynthesis, resulted in more than 3 and 17 times respectively in an acidic pH of 5.5 (Jin et al., 2008; Yu et al., 2015). In an acidic environment, the metabolic pathways involving UTP-glucose and UDP-glucose are upregulated, ultimately increasing the yield of curdlan produced. Similarly, enzymes such as UTP-glucose-1-phosphate uridylytransferase and phosphoglucomutase also show increased activity at lower pH levels. This suggests that maintaining an optimal pH is essential for maximizing curdlan production. The biosynthesis of curdlan is likely controlled by a regulatory protein that modulates the expression of genes involved in its production. The activity of this regulatory protein is pH-dependent, with optimal activity observed at a specific pH level of 2. Studies have shown that the CrdR regulatory protein, which controls the expression of curdlan biosynthesis genes, functions more efficiently at lower pH levels (Lee et al., 1999; Jin et al., 2008; Yu et al., 2015). This pH-dependent regulation ensures that curdlan production is optimized under favorable conditions. In addition to the impact of pH on the quantity of curdlan synthesized, pH influences the quality of curdlan produced (West, 2020). Curdlan synthesized at different pH levels exhibits variations in its molecular weight and gelling properties. A lower pH indicated a higher molecular weight of

curdlan produced with stronger gelling properties compared to curdlan produced at a neutral pH (West, 2020).

2.5.4. Fermentation

The fermentation process employed plays a critical role in determining both the yield and quality of curdlan. Batch fermentation, where nutrients are supplied only at the beginning, often leads to lower curdlan yield due to nutrient depletion over time (Saudagar & Singhal, 2004). Meanwhile, fed-batch fermentation, which involves the periodic addition of nutrients, sustains microbial growth and enhances curdlan production. Studies indicate that fed-batch fermentation can increase curdlan yield compared to batch fermentation (Saudagar & Singhal, 2004; Zheng et al., 2014).

In the attempt to improve the fermentation process of curdlan, an optimized two-stage dissolved oxygen (DO) control based on the metabolic characterization of *Agrobacterium* sp. ATCC 31749 (Zhang et al. 2011) was used. In this study, a constant DO within the range of 5–75% was maintained during batch fermentation of curdlan, which was observed to influence the curdlan produced, the conversion efficiency of glucose to curdlan, and intracellular nucleotide concentrations. When compared with 15% DO, the optimal DO levels for curdlan fermentation ranged between 45 to 60%, resulting in an 80% improvement of average curdlan yield, 66% curdlan productivity and 32% glucose to curdlan conversion efficiency (Zhang et al., 2011).
Additionally, enhancing the oxygen levels during aerobic fermentation significantly enhances curdlan production, as aerobic conditions are conducive to both microbial growth and curdlan biosynthesis. In contrast, anaerobic conditions may alter these processes. Additionally, while enhancing oxygen levels in aerobic fermentation can greatly improve curdlan production, anaerobic conditions may alter microbial growth and curdlan biosynthesis. (Dhivya et al., 2014).

2.5.5. Size of the bacterial inoculum

The size of the bacterial inoculum directly influences curdlan production yields, with larger inoculum sizes leading to increased curdlan yields due to a higher number of microbial cells capable of synthesizing the biopolymer (Davis et al., 2005). In a study by Aquinas et al. (2024), it was demonstrated that an inoculum size of 10% (v/v) resulted in a maximum curdlan yield of 0.31 g/L after 96 h of fermentation. This finding indicates the importance of optimizing inoculum size to maximize curdlan production.

Furthermore, the size of the inoculum influences the growth kinetics of microorganisms responsible for curdlan biosynthesis. A larger inoculum accelerates the initial growth phase, leading to a quicker transition to the stationary phase, where curdlan production reaches its maximum (Aquinas et al., 2024). This accelerated growth improves the efficiency of the fermentation process, thereby increasing the total curdlan yield within a set period. Additionally, a larger inoculum enhances the metabolic activity of bacterial cells, resulting in more efficient substrate conversion into curdlan, which leads to higher yields and better biopolymer quality (Aquinas et al., 2024). Therefore, managing the inoculum size is essential for optimizing both the quantity and quality of curdlan produced.

2.6. Curdlan from wastewater

One of the major components of EPS is homopolysaccharides, a group of biopolymers including curdlan (More et al., 2014). In biofilm processes, curdlan was identified as part of the microbial EPS that is useful for biomedical applications (Mehta et al., 2017). Recently, curdlan has been identified in the aerobic granule matrix (Ferreira et al., 2021). Furthermore, microbial communities such as the genus *Agrobacterium*, *Rhizobium*, and *Alcaligene* sp., associated with

curdlan biosynthesis, have also been identified in the aerobic granule matrix (Zhang et al., 2011; Shoda and Ishikawa, 2014; Filho et al., 2019).

Apart from *Agrobacterium*, *Rhizobium*, and *Alcaligene* spp., other bacteria known to produce curdlan is *Paenibacillus* species (Liang et al., 2014). These species have been reported to be attractive for their interesting biotechnology potential in wastewater treatment (Rafigh et al., 2014). Curdlan forms a part of the naturally forming EPS, a primary by-product of the aerobic granule matrix, existing as a blend with gellan gum, glucomannan, or deoxycholic acid (Hussain et al., 2017). A total of 1083 high-quality metagenome-assembled genomes (MAGs) were obtained from 23 WWTPs (Dueholm et al., 2023). Putative gene clusters associated with the biosynthesis of various biopolymers, including curdlan, were identified and linked to some MAGs. This provides insight into the genome-resolved potential for curdlan and a better understanding of EPS composition in wastewater treatment systems.

Meanwhile, studies have shown that enzymes such as glycosyltransferases, polymerase, and transporter proteins determine the structural and functional diversity of the EPS (Vandana et al., 2023). In operons, these enzymes are encoded by specific genes, one of which is crd, a curdlan synthesizing gene, in microbes such as *Agrobacterium*. In the crdASC operon, curdlan biosynthesis is regulated (Yu et al., 2015). Hence, it can be deduced that the presence of these enzymes within the EPS of wastewater indicates the presence of curdlan synthesizing genes in wastewater treatment systems. This suggests that the recovery of curdlan from AGS biofilms is plausible (Figure 2.2). Given the presence of curdlan in the EPS of biological wastewater treatment systems and curdlan-producing microorganisms, it is worthwhile exploring the quantity of curdlan that can be obtained from AGS treatment systems.

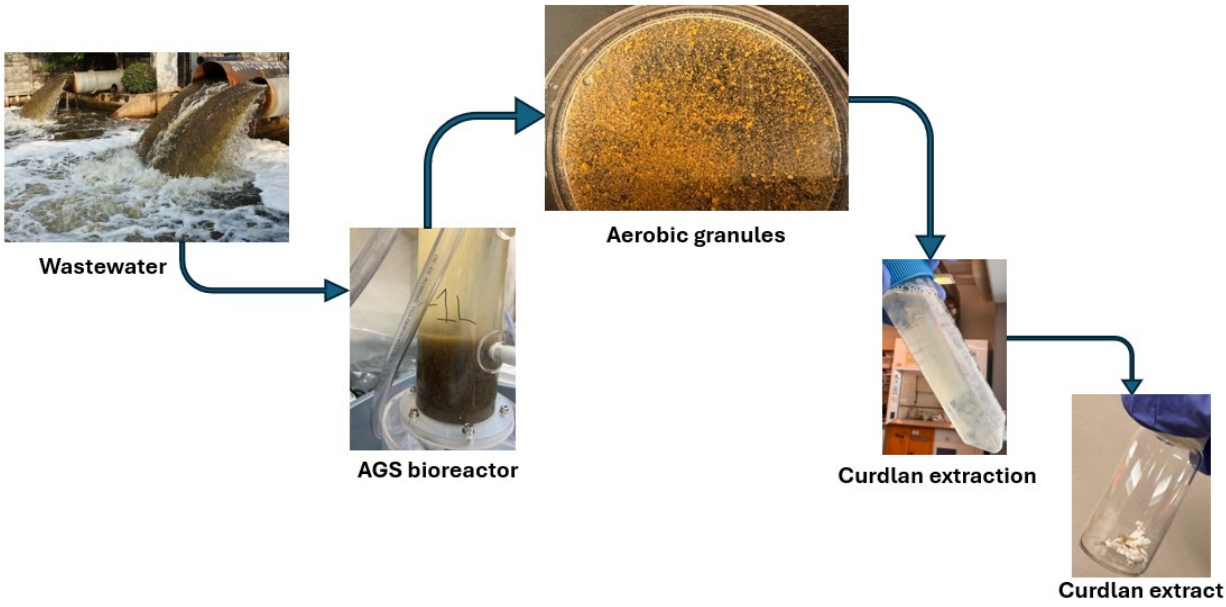

Figure 2. 2. Illustration of curdlan recovery from municipal wastewater using AGS treatment

In summary, the concept of a circular economy emphasizes the reuse of products and raw materials, reducing waste by treating it as a valuable resource. This approach is driven by resource depletion, scarcity, and population growth. The identification of curdlan in the AGS matrix gives an opportunity for curdlan recovery, however, this is yet to be explored. The efficiency of curdlan recovery from these systems is not well understood. Additionally, the role of specific microbial communities in curdlan biosynthesis in AGS systems requires further investigation. Addressing these gaps could enhance the feasibility of curdlan production from wastewater, contributing to a circular economy and sustainable development.

Chapter 3 Materials and Methods

3.1. Seed sludge

The AGS bioreactor was seeded with waste-activated sludge obtained from a WWTP in Western Canada. The sludge settling properties are presented as sludge volume index (SVI), which represents the amount of sludge that settles in 5 min and 30 min. The seed sludge had initial settling properties, SVI_{30} of 222 ± 20 mL/g and SVI_5 of 361 ± 11 mL/g and a mixed liquor suspended solids (MLSS) concentration of 23 ± 3 mg/L. The waste-activated sludge was acclimated for 10 d in batch mode before starting the system.

3.2. Feed wastewater

Synthetic wastewater was used for all the experiments. The synthetic wastewater was prepared using sodium acetate (NaAc) and sodium propionate (NaPr) as carbon sources and ammonium chloride (NH_4Cl) as a nitrogen source. Monobasic potassium phosphate (KH_2PO_4) and dibasic potassium phosphate (K_2HPO_4) were used to provide phosphorus. The composition of the wastewater for COD concentration of 2000 mg/L was as follows: NaAc anhydrous, 1.876 g/L; NaPr anhydrous, 0.417 g/L; NH_4Cl, 0.382 g/L; K_2HPO_4, 0.03 g/L; KH_2PO_4, 0.026 g/L; $CaCl_2 \cdot 2H_2O$, 0.03 g/L; $MgSO_4 \cdot 7H_2O$, 0.025 mg/L; $FeSO_4 \cdot 7H_2O$, 0.02 mg/L; and micronutrients stock solution of 1 mL/L. A micronutrients stock solution containing (in g/L): H_3BO_3, 0.05; $ZnCl_2$, 0.05; $CuCl_2$, 0.03; $MnSO_4.H_2O(NH_4)_6$, 0.05; $Mo_7O_{24}.4H_2O$, 0.05; $AlCl_3$, 0.05; $CoCl_2.6H_2O$, 0.05 and $NiCl_2$, 0.05, was used (Tay et al., 2003). The COD:N:P ratio was fixed at 100:5:1. This ratio was adjusted accordingly throughout the experiments.

3.3. Experimental design

Optimization studies were performed using the combination of Taguchi – orthogonal array (L9) and Pearson correlation analysis in Minitab 21 software. This determined the effect of

independent variables (C-to-N ratio – factor 1, feeding strategy – factor 2, and OLR – factor 3) on curdlan biosynthesis in the aerobic granule matrix. The responses or dependent variables were curdlan concentration (mass of curdlan in biomass, measured in mg/g), and wastewater treatment performance. The Taguchi design combination that was performed is shown in Table 3.1. The experimental runs and their corresponding operational conditions (C/N ratio, feeding strategy, and OLR) performed in the current study are summarized in Table 3.1

Table 3.1. Combinations of experimental factors for each run using Taguchi design.

Experimental Runs	**(C/N ratio)**	**(Feeding strategy)**	**(OLR – kg COD/m^3·d)**
R1	20	60 min feeding	2.1
R2	30	60 min feeding	1.5
R3	10	30 min feeding; 30 min resting phase	2.1
R4	30	10 min pulse feeding; 50 min resting phase	2.1
R5	10	10 min pulse feeding; 50 min resting phase	1.5
R6	20	30 min feeding; 30 min resting phase	1.5
R7	10	60 min feeding	0.8
R8	20	10 min pulse feeding; 50 min resting phase	0.8
R9	30	30 min feeding; 30 min resting phase	0.8

3.4. Experimental set-up and operation

In this experiment, R1, R3, R5 and R7 (Table 3.1) were run in one bioreactor one at a time, while R2, R4, R6 and R8 were run in another bioreactor one at a time. Meanwhile, R9 was run in a separate bioreactor. At the beginning of the experiment, the SVI_{30} and SVI_5 of R1, R3, R5, and R7 mixed liquor were 35 ± 1 mL/g and 37 ± 1 mL/g, while the SVI_{30} and SVI_5 of R2, R4, R6, and R8 mixed liquor were 41 ± 1 mL/g and 43 ± 1 mL/g respectively. The experiments were conducted at room temperature (21 ± 2°C).

The experiments were performed in three 5 L AGS bioreactors with a working volume of 4.5 L. The bioreactors were run for 30 weeks: 13 weeks for granule cultivation and maturation, and 17 weeks for optimization of curdlan biosynthesis experiments. For granule formation, the AGS bioreactors were seeded with waste-activated sludge from a municipal WWTP in Western Canada. Before the experimental runs began, the bioreactors were operated at an airflow velocity of 1.98 cm/s, starting with a 6-h cycles (to form granules) comprising 5 phases: feeding period of 60 min, aeration period of 4 h 20 min, settling time of 30 min (gradually reduced to 25 min, 20 min and 10 min as granules matured), decanting time of 8 min, and idle time of 2 min. For granulation and maturation of granules, the synthetic feed was formulated to achieve a COD concentration of 2000 mg/L, ammonia-nitrogen (NH_3-N) of 100 mg/L and phosphate (PO_4^3-P) of 20 mg/L. Over this period, COD, nitrogen and phosphorus removal performance profile and biomass performance were monitored. The schematic representation of AGS bioreactor set-up is shown in Figure 3.1 and the laboratory set-up is presented in Figure 3.2.

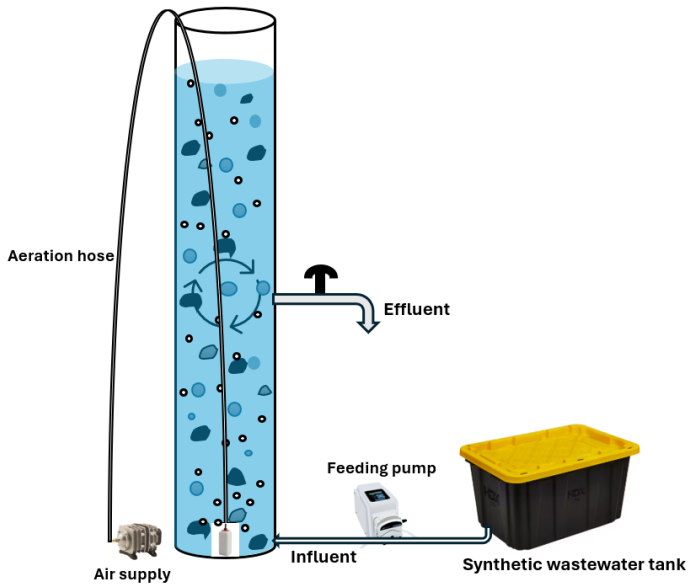

Figure 3. 2. Schematic representation of AGS bioreactor set-up.

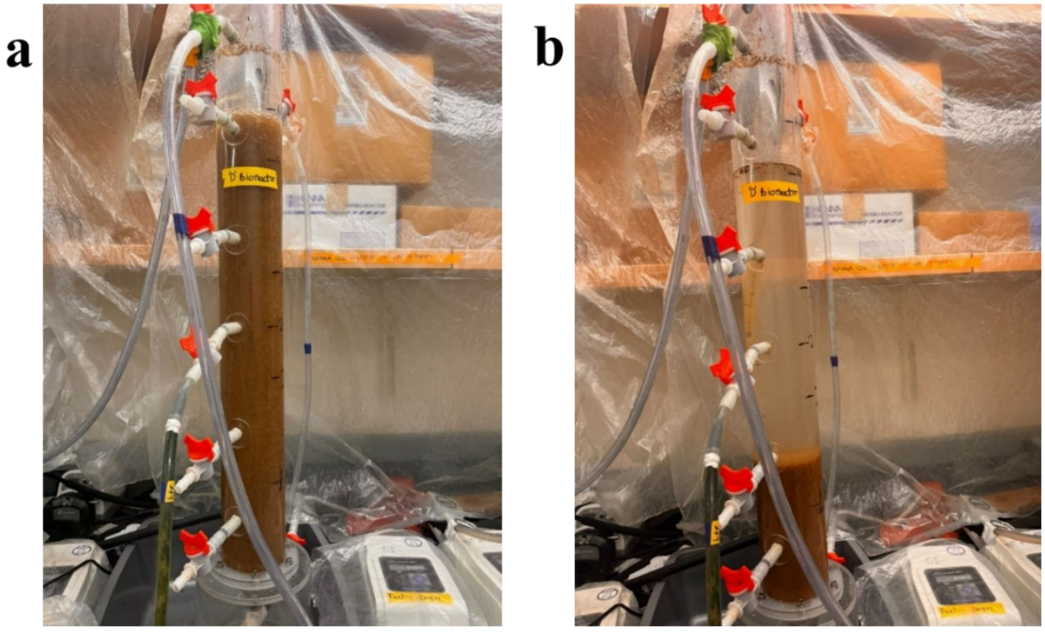

Figure 3. 3. An experimental set-up of AGS bioreactor in the laboratory. a) during aeration and b) during settling phase

Some indications of granulation and AGS stability are when the SVI_5 is closer to the SVI_{30} (de Kreuk et al., 2005; Nancharaiah and Raddy, 2018) and mature granules have SVI_{30} between 30 and 80 mL/g (Derlon et al., 2016). Once stable granules were cultivated, the cycle time was changed to 4 h comprising 5 phases: feeding period of 60 min (changed for every experiment to 10, 20 or 60 min), aeration period of 2 h 40 min, settling time of 10 min, decanting time of 8 min, and idle time of 2 min. The optimization experiments for curdlan biosynthesis were performed using the selected factors: C/N ratio – factor 1, feeding strategy – factor 2 and OLR – factor 3. The organic carbon, phosphorus and ammonia concentrations in SWW influent for each experiment are given in Table 3.2. These factors are crucial in AGS treatment systems because of their direct impact on microbial growth (Peng et al., 2022), granule stability (Vicente et al., 2021) and overall performance for nutrient and carbon removal (Kim et al., 2021). Using Taguchi design, three levels of the three factors were selected including C/N ratios of 10, 20 and 30, OLR of 0.8, 1.5, and 2.1 kg $COD/m^3 \cdot d$, and feeding strategy of 60 min feeding, 30 min feeding and 30 min resting phase, and 10 min pulse feeding and 50 min resting phase.

Table 3. 2. COD, ammonia and phosphorus concentration in SWW influent for each experiment.

Experimental run (OLR/C/N ratio/Feeding)	COD (mg/L)	NH_3 -N (mg/L)	PO_4^{3-}-P (mg/L)
R1 (2.1/20/60)	800	40	8
R2 (1.5/30/60)	550	27	6
R3 (2.1/10/30)	800	80	8
R4 (2.1/30/10)	800	27	8
R5 (1.5/10/10)	550	55	6
R6 (1.5/20/30)	550	27	6
R7 (0.8/10/60)	300	30	6
R8 (0.8/20/10)	300	15	3
R9 (0.8/30/30)	300	10	2

*OLR: Organic loading rate (2.1, 1.5 and 0.8 kg COD/m^3·d); C/N ration: Carbon-to-Nitrogen ratio (10, 20, 30); Feeding: feeding strategy (60 min, 30 min feeding and 30 min resting phase, and 10 min pulse feeding and 50 min resting phase).

3.5. Analytical methods

Performance testing was conducted twice per week, including COD, ammonia nitrogen (NH_3-N), nitrite-nitrogen (NO_2-N), nitrate-nitrogen (NO_3-N), and phosphate-phosphorus (PO_4^{3-}-P) to determine the removal efficiency of organic matter and nutrients during each experimental run. The procedures are described as follows:

3.5.1. COD

A closed reflux colorimetric method (5220D) was used to determine the total COD of the influent sample (APHA, 2023). Meanwhile, the USEPA reactor digestion method was used to determine the total COD of effluent samples. The standard method COD solution was prepared

for analyzing high-range COD (100 – 1500 mg/L), which is within the influent concentration for the experiments (300 – 800 mg/L). However, the pre-made USEPA solution used was <150 mg/L COD concentration. The chemical composition of the pre-made USEPA low-range solution was as follows: Concentrated sulfuric acid (H_2SO_4), disilver (1+) salt, Chromic acid and Mercury (2+) salt. The chemical composition of the prepared standard COD solution was as follows: Potassium dichromate ($K_2Cr_2O_7$), H_2SO_4, Silver sulphate (Ag_2SO_4) and Mercuric sulphate ($HgSO_4$).

In a 2 L pyrex storage glass bottle, 10.216 g 0f $K_2Cr_2O_7$ was added to 500 mL of deionized water. 167 mL of concentrated H_2SO_4 was added to the $K_2Cr_2O_7$ solution. 33.3 g of $HgSO_4$ and allowed to dissolve at room temperature. The solution was diluted by adding deionized water to 1000 mL of the beaker. The dichromate ion ($Cr_2O_7^{2-}$) in the digestion solution oxidizes the COD in the sample. That is, the amount of oxygen needed to oxidize organic material in the given sample is equal to the amount of $Cr_2O_7^{2-}$ oxidized to Cr^{3+}.

In another 2 L pyrex storage glass bottle, a catalyst solution was made by adding 10.1 g of Ag_2SO_4 to 1 L of H_2SO_4. The Ag_2SO_4 guarantees the complete oxidation of organic material, and the H_2SO_4 minimizes interferences from other compounds, such as bromine, chloride, and iodide. The solution was allowed to sit for 48 h to dissolve.

After 48 h, 1.2 mL of the $K_2Cr_2O_7$ digestion solution was pipetted into several 15 mL test tubes as needed. 2.8 mL of the H_2SO_4 reagent was added into the test tubes with the digestion solution. The test tubes were tightly capped and mixed thoroughly to give a homogenous COD digestion solution. COD standard solution (Hach, Germany) containing potassium hydrogen phthalate was used to obtain the standard calibration. The calibration curve derived is attached in Figure A1 in the appendix.

2 mL of SWW sample (influent and effluent) was added to the prepared COD digestion solution vial and mixed thoroughly to give a homogenized mixture. A digester DRB 200 (Hach, Canada) was pre-heated to a temperature of 150ºC and for 120 min. The COD mixture was placed in the pre-heated digester and heated at 150ºC for 120 min. The $Cr_2O_7^{2-}$ in the digestion solution oxidizes the COD in the sample, resulting in chromium changes from the 76 hexavalent to the trivalent state. This chemical reaction results in a color change that is measured by a spectrophotometer at 600 nm wavelength after allowing the digester to cool to about 120ºC and placed in a rack to cool to room temperature for result consistency. The COD concentration was calculated following the calibration standard curve which was derived from a known quantity of deionized water and potassium hydrogen phthalate.

To determine the effluent total COD concentration using the USEPA reactor digestion method, 2 mL of effluent sample was pipetted into the USEPA COD digestion solution test tube and mixed thoroughly to give a homogenized mixture. The digester DRB 200 (Hach, Canada) was pre-heated to a temperature of 150ºC for 120 min. The COD mixture was placed in the pre-heated digester and heated at 150ºC for 120 min. The $Cr_2O_7^{2-}$ in the digestion solution oxidizes the COD in the sample, resulting in a color change. After 120 min, the digester was allowed to cool to about 120ºC and placed in a rack to cool to room temperature for result consistency. Using a spectrophotometer single wavelength, the results were measured by a spectrophotometer at 420 nm wavelength.

3.5.2. Ammonia-nitrogen

NH_3 -N test was conducted using Hach Ammonia Nessler Method 8038. To achieve a dilution factor of 50, 0.5 mL of filtered (through a 0.45 μm filter) SWW sample (influent and effluent) was added to 24.5 mL of deionized water in a 50 mL vial to reduce the concentration of

the sample within the measuring range 0 to 2.5 mg/L. 3 drops of mineral stabilizer were added to the sample vials to stabilize the samples for result accuracy. The solution was mixed several times. 3 drops of polyvinyl alcohol dispersing agent were added to the mixed sample vial to prevent precipitation of interfering substances and mixed several times. Using a pipette, 1 mL of Nessler reagent was added to the sample mixture to enable a reaction with ammonia present in the sample. The solution was mixed several times. The mixture was allowed to react for 1 min. About 10 mL of the reacted sample mixture was poured into a sample cell to take the result in mg/L of NH_3-N at 380 using a spectrophotometer at the wavelength of 425 nm.

3.5.3. Nitrite nitrogen

NO_2-N was analyzed using Hach NitriVer®3 reagent. To achieve a dilution factor of 20, 0.5 mL of filtered effluent sample was added to 9.5 mL of deionized water in a 10 mL vial. The content of one NitriVer 3 reagent powder pillow was added to the 10 mL vial to activate the reaction of the nitrite present in the solution. The vial content was mixed thoroughly to dissolve the powder pillows completely. The mixture was allowed to react for 20 min. After 20 min, the content was poured into a sample cell, and the results were taken in mg/L of NO_2-N using a spectrophotometer at the wavelength of 507 nm.

3.5.4. Nitrate-nitrogen

NO_3-N was analyzed using Hach NitraVer®5 reagent. To achieve a dilution factor of 20, 0.5 mL of filtered (through a 0.45 μm) effluent sample was added to 9.5 mL of deionized water in a 10 mL vial. The content of one NitraVer 5 reagent powder pillow was added to the 10 mL vial to initiate the reaction with nitrate compounds present in the solution. The vial content was mixed thoroughly to dissolve the powder pillows completely. The mixture was allowed to react for 5 min.

After 5 min, the content was poured into a sample cell, and the results were taken in mg/L of NO_3-N using a spectrophotometer at the wavelength of 500 nm.

3.5.5. Phosphorus

PO_4^3-P was analyzed using, the PhosVer®3 Phosphate reagent. To achieve a dilution factor of 20, 0.5 mL of filtered (through a 0.45 μm). SWW sample (influent and effluent) was added to 9.5 mL of deionized water in a 10 mL vial. The content of one PhosVer 3 reagent powder pillow was added to the 10 mL vial to initiate the reaction with the phosphate present in the solution. The vial content was mixed thoroughly to dissolve the powder pillows completely. The mixture was allowed to react for 2 min. After 2 min, the content was poured into a sample cell, and the results were taken in mg/L of PO_4^{3-}-P using a spectrophotometer at the wavelength of 880 nm.

3.5.6. pH

The pH of the influent and effluent wastewater was tested twice a week. The method for pH measurement was the standard method (APHA, 2023). The pH for wastewater influent and effluent was monitored using a digital glass electrode pH meter. The glass electrode was used to measure the pH range from 1 to 14, and the results were determined by estimation. In a beaker, the wastewater was stirred thoroughly for homogeneity before measurement. The pH meter probe was dipped in the wastewater sample in the beaker and stirred continuously until a stable reading was reached on the digital display. The pH measurement was recorded upon stabilization of the reading.

3.5.7. Biomass characteristics

Biomass characteristics, including sludge volume index (SVI_{30}, and SVI_5), mixed liquor suspended solids (MLSS), and mixed liquor volatile suspended solids (MLVSS) were conducted using standard methods (APHA, 2023).

The MLSS and MLVSS were conducted by taking 10 mL of mixed liquor from each bioreactor during aeration. Using a 0.45-micron glass-fibre Millipore filter, the mixed liquor was filtered to obtain the wet biomass. This was placed in the pre-weighed crucible and allowed to dry in the oven for 24 h at 105^{o} C. After 24 h, the crucible was allowed to cool at room temperature in a desiccator and weighed. The MLSS result was calculated in mg/L using equation 3.1

$$MLSS\ (mg/L) = \frac{Filter\ Dry\ Weight\ (g) – Filter\ Tare\ Weight\ (g)}{Sample\ Volume\ (mL)} \times 1{,}000{,}000 \quad \text{Equation 3.1}$$

$$MLVSS\ (mg/L) = \frac{Filter\ Dry\ Weight\ (g) – Filter\ Ash\ Weight\ (g)}{Sample\ Volume\ (mL)} \times 1{,}000{,}000 \quad \text{Equation 3.2}$$

To determine the MLVSS result, the MLSS crucible was placed in a furnace for 45 min at a temperature of 550^{o}C. After 45 min, the crucible was allowed to cool to room temperature and weighed. The MLVSS result was calculated in mg/L using equation 3.2. The SVI_5, and SVI_{30} were conducted by taking 1L of mixed liquor from each bioreactor during aeration in a measuring cylinder. The settling biomass was timed for 5 and 30 min respectively to take the results. SVI results were calculated in mL/g of biomass using equation 3.3.

$$SVI\ (mL/g) = \frac{Settled\ sludge\ volume\ (mL/L)}{Suspended\ solids\ concentration\ (mg/L)} \times 1000\ mg/g \quad \text{Equation 3.3}$$

Images of sludge were taken once a week using a phone camera (48MP sensor, 2.44-micron quad pixels, 24 mm equivalent f/1.78-aperture lens, Dual Pixel AF, OIS). About 5 mL of mixed liquor was collected in a petri-dish and placed on a dark platform to enhance image quality. Photos were taken once a week to assess gradual granular growth.

3.6. Curdlan recovery and quantification

For curdlan recovery, 10 mL of AGS was collected (Figure 3.3). Approximately 18 mL of 0.143 mol/L of NaOH was added and placed in an orbital shaker for 60 min to dissolve the curdlan

gel within the granular sludge. The solution was centrifuged at 10,000 g at 4ºC for 15 min to collect the dissolved curdlan gel. The supernatant (dissolved curdlan gel) was collected, and its pH was adjusted to 4.8 – 5.2 by adding approximately 8 mL of 1.0 mol/L of acetic acid to allow the curdlan gel to precipitate (Laxmi et al., 2018). The solution was centrifuged at 10,000 g at 4 °C for 15 min to collect the wet precipitate settled at the bottom of the test tube. The gel precipitate was washed 3 times using deionized water and dried for 24 h using a freeze dryer at approximately -54 degrees and a pressure of 0.04 mbar. The amount of curdlan was measured in mg/g of the biosolids (Mangolim et al. 2017).

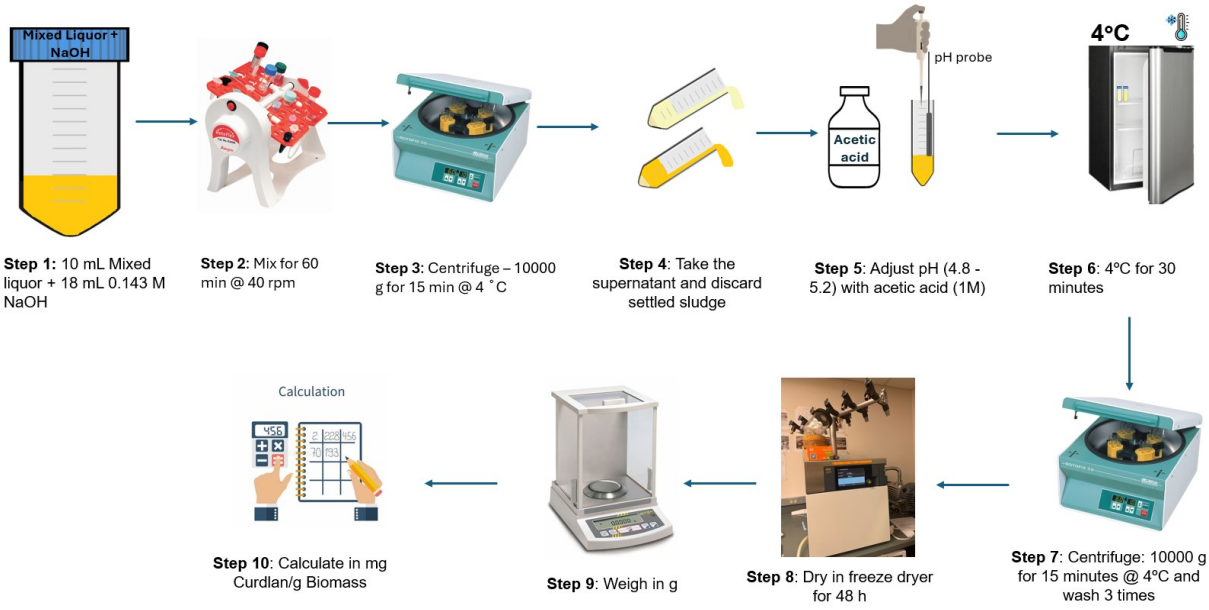

Figure 3.3. Method for curdlan extraction from AGS matrix modified from Mohsin et al. (2019)

3.6.1. Fourier transform infrared (FT-IR)

Fourier Transform Infrared (FT-IR) spectroscopy was used to acquire FT-IR spectra of both pure curdlan sample and dry curdlan extract. This method compares the curdlan extract with pure curdlan by analyzing the molecular vibration of both samples, generating a unique spectrum

of curdlan. The FT-IR spectra were recorded by Brucker Alpha II spectrometer (Brucker Inc., Switzerland) (Figure 3.4). About 0.002 mg of the sample was placed on the diamond crystal plate. The compression tip was released onto the sample on the diamond crystal plate to allow the infra-red light/radiation in and out and the sample. The FT-IR acquisition parameters were: number of scans (n = 32), scan range (4000 – 400 cm^{-1}), resolution (4 cm^{-1}), and aperture (1.5 mm). The FT-IR spectra displayed absorption bands corresponding to the different functional groups present in the chemical structure of curdlan. The specific scan range (4000 – 400 cm^{-1}) contained the absorption patterns unique to curdlan. The pattern observed in the pure curdlan sample was compared with the patterns obtained to confirm the structure of the extracted gel. The FT-IR spectra were acquired at room temperature.

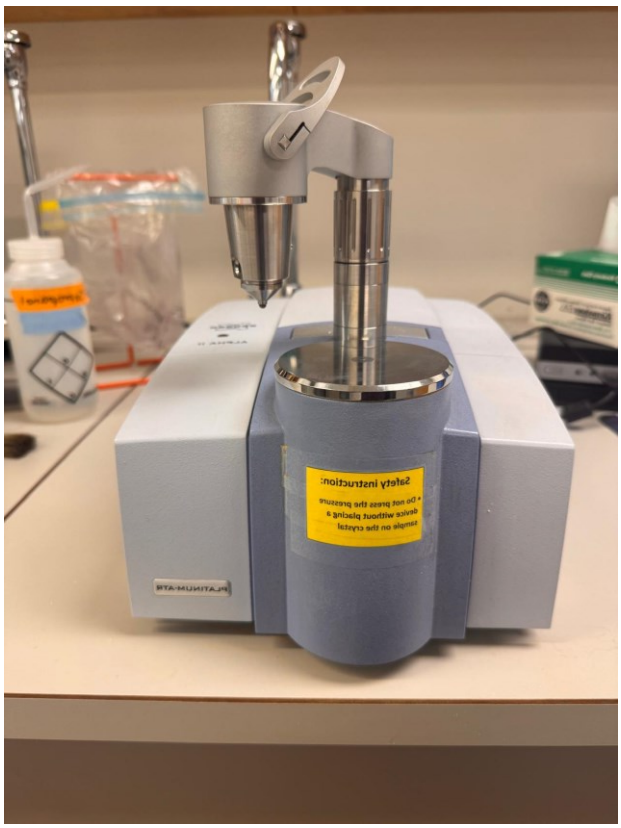

Figure 3.4. FT-IR spectrometer for identification of extracted biopolymer.

3.6.2. Aniline blue staining

Aniline blue WS (Rochester Medical Centre, USA) solution was prepared by adding 0.05 g of dry aniline WS into 100 mL of deionized water to make an aniline stock solution. About 10 mL of the stock solution was pipetted into another 90 mL of deionized water to dilute the dye (Mishra et al., 2024). About 0.5 mL of the diluted aniline was added to 100 mL of Thioglycollate medium agar (Oxoid, England) after bringing the solution to a boil. The agar was prepared by adding 2 g of dehydrated Leu broth to a conical flask with 100 mL of deionized water. This mixture was heated on the hot plate for about 7 min while stirring with a magnetic stirrer to enable the dry broth to dissolve completely. After the agar was dissolved, 0.5 mL of the diluted aniline was added to the agar solution, and mixed until a homogenized solution was achieved. About 30 mL of the warm agar solution was poured into petri dishes. Pure curdlan was sprinkled on the agar plate and allowed to sit for about 24 h. This procedure was repeated for gel extracts 3 times (Nakanishi et al., 1976; Wang et al., 2016).

3.6.3. Nuclear magnetic resonance (NMR) spectroscopy

The curdlan extract was compared with pure curdlan from *Alcaligene faecalis* (Sigma Aldrich, USA) by using Heteronuclear Single Quantum Coherence (^{1}H – ^{13}C HSQC) NMR spectroscopy to determine their similarity. The HSQC is a 2-dimensional proton-detecting homonuclear NMR experiment that is used to provide valuable structural information on ^{1}H - ^{13}C chemical bonds present in a compound. This technique uses the sensitivity of proton (H) for easy detection of carbon (Uematsu et al., 2025). The HSQC experiments were recorded using an Ascent Evo-400 MHz spectrometer (Bruker, Switzerland) equipped with a 5 mm BBO probe.

About 5 mg of pure curdlan and dry curdlan extract were weighed, dissolved in 0.7 mL of deuterated dimethyl sulfoxide (DMSO-d_6) and poured into separate NMR tubes. Each sample was placed in the NMR depth cage into the spectrometer one at a time to process the HSQC spectra. The NMR samples were equilibrated prior to acquisition at 298.0 K inside the spectrometer. The following parameters were used for the experiment: the pulse sequence program for HSQC was phase-sensitive hsqcedetgpsisp2.3; the number of collected data points was 2048 in F2 (H) and 256 in F1(C); the acquisition time was set to 0.195 s, and the increment delay was 60.2375 μs. The spectrum was acquired with 32 scans on a spectra width of 16602.352 ppm and 165 ppm. The integration of 2D peak volumes, data processing and analysis were carried out using Topspin 4.4 software for the comprehensive assignment of ^{1}H - ^{13}C signals for curdlan extract and pure sample.

3.7. Statistical analysis

The method of recovery of curdlan from AGS under different conditions involves changing one factor at a time and requires numerous experiments which may be inefficient, often leading to low optimization efficiency. To enhance this process, a design of experiment (DOE) approach was used to analyze the influence of independent variables and their respective responses, significantly reducing the number of experiments required.

Taguchi DOE is a statistical tool that uses orthogonal arrays to systematically study multiple factors and their interactions with a minimal number of experiments (Kalhori et al., 2018; Truong et al., 2022; Hisam et al., 2024). This approach identifies the optimal arrangement for experimental factors, ensuring the experiments are informative. It improves process performance, yield, and productivity, and achieves this by focusing on minimizing variation and enhancing quality (Hisam et al., 2024). Taguchi was used to determine the main effects of the independent factors, and the factors with the most significant effect on the response. The method uses signal-

to-noise (S/N) ratios to measure performance characteristics, assessing the effect of variables on removal efficiency (response). The S/N response is crucial for comparing the magnitude of the effects leading to a more accurate understanding of the specific impact of the factors on the system (Pourali et al., 2022, Seid-Mohammadi et al., 2019). Some commonly applied types of S/N analysis are: Smaller is better, Nominal is better, and Larger is better (Naseem and Kumar, 2017). However, the main goal of optimization in this study was to achieve maximum curdlan yield. Therefore, the S/N ratio for the "Larger is better" criterion was used in this experiment.

In combination with Taguchi, Pearson's correlation analysis was performed to evaluate the linear relationship between resource production at the different conditions and AGS stability during operation. A p-value of ≤ 0.05 was employed to indicate the rejection of the null hypothesis and statistical disparity between the data groups analyzed and to determine if the results obtained from the different treatment systems differ significantly.

Chapter 4 Results and Discussion

4.1. Treatment performance of the AGS system

4.1.1. Organic matter removal

Throughout the experimental period, the bioreactors consistently achieved COD removal efficiencies ranging from 91 ± 1% to 100 ± 0% (Figure 4.1). This demonstrates that the removal of organic matter remained notably high, regardless of variations in operational conditions. The reactors (R1 – R9) were operated with a high aeration time (2 h 40 min), an essential parameter for achieving high COD removal. The long aeration time ensures sufficient contact time and interaction between the wastewater and microbial granules, facilitating effective biodegradation of organic carbon, as corroborated by previous study (Rosman et al., 2014). The high COD degradation observed in this study aligns with other studies on the use of AGS for wastewater treatment (Franca et al., 2018; Iorhemen et al., 2022).

Similarly, high biomass concentration, the compact structure of aerobic granules, and good biomass settling enhance biomass retention in AGS systems (Świątczak and Cydzik-Kwiatkowska, 2018). The increased biomass concentration in AGS systems boosts microbial activity, leading to more efficient COD removal. Additionally, the dense and compact structure of AGS granules provides a large surface area for microbial activity and creates micro-environments for simultaneous COD and nutrient removal (Zeng et al., 2024), which facilitates the degradation process that results in improving the overall COD removal.

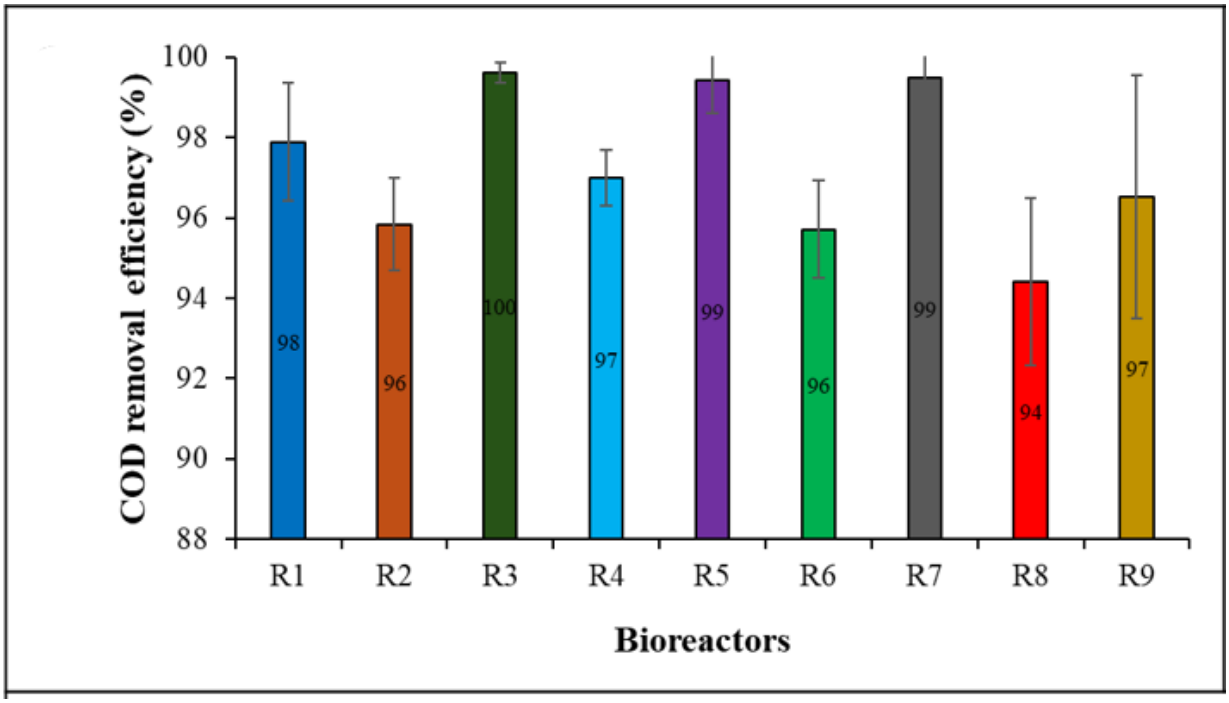

Figure 4.1. COD removal efficiency for bioreactors R1 to R9. ***R1 (C/N-20, 60 min feeding, OLR-2.1 kg COD/m³·d); R2 (C/N-30, 60 min feeding, OLR-1.5 kg COD/m³·d); R3 (C/N-10, 30 min feeding/30 min resting, OLR-2.1 kg COD/m³·d); R4 (C/N-30, 10 min pulse feeding/50 min resting, OLR-2.1 kg COD/m³·d); R5 (C/N-10, 10 min pulse feeding/50 min resting, OLR-1.5 kg COD/m³·d); R6 (C/N-20, 30 min feeding/30 min resting, OLR-1.5 kg COD/m³·d); R7 (C/N-10; 60 min feeding, OLR-0.8 kg COD/m³·d); R8 (C/N-20; 10 min pulse feeding/50 min resting, OLR-0.8 kg COD/m³·d); R9 (C/N-30; 30 min feeding/30 min resting, OLR-0.8 kg COD/m³·d).*

4.1.2. Nitrogen removal

The nitrogen removal efficiency across reactors R1 to R9 is illustrated in Figure 4.2. The NO_2^--N levels remained consistently low in all reactors, measuring less than 0.7 mg/L. The NH_3^--N removal efficiency for reactors R1 to R8 ranged from 80 ± 2% to 100 ± 1%, with reactor R9 (Figure 4.2) being the exception (< 60%). Notably, reactors R3, R6, and R8 exhibited the highest NH_3^--N removal efficiencies, with ranges of 90 ± 0% - 93 ± 1%, 91 ± 3% - 99 ± 0%, and 94 ± 2% - 98 ± 1%, respectively (Figure 4.2). These substantial removal rates suggest a complete nitrification process by ammonia-oxidizing bacteria, as evidenced by the low NO_2^--N concentrations in the effluent. This indicates a high and nearly complete conversion rate of NH_3-

N to NO_2^--N, followed by a successful conversion of NO_2^--N to NO_3^--N by nitrite-oxidizing bacteria (NOB). The nitrification process within the AGS systems can be attributed to the presence and activity of nitrifying bacteria and the 3-layered structure of the aerobic granules (aerobic, anoxic, and anaerobic layers), particularly the aerobic layer (Iorhemen et al., 2020; Yu and Wang, 2024). The layered structure of aerobic granules allows for the simultaneous processes of nitrification and denitrification, thereby enhancing the efficient removal of nitrogen.

Notably, reactor R8, even when operated at a low COD concentration of 300 mg/L, demonstrated a high ammonia-N removal efficiency (94 ± 2% - 98 ± 1%). This exceptional performance can be attributed to the metabolic flexibility of nitrifying bacteria within AGS systems, which enables them to transform from utilizing organic carbon sources (when depleted) to inorganic carbon source (CO_2) to achieve efficient NH_3^--N removal (Margot et al., 2016).

Meanwhile, reactors R7 and R9 exhibited lower NH_3^--N removal efficiencies, with ranges of 80 ± 2% - 83 ± 1% and 35 ± 5% - 57 ± 1%, respectively (Figure 4.2). While NO_2^--N levels remained low in all reactors, the incomplete nitrification process in reactor R9 resulted in lower NH_3^--N concentration. Furthermore, reactor R9 exhibited the lowest biomass concentration among all reactors, with a MLSS value as low as 6 g/L. This low biomass concentration indicates reduced biomass retention, which likely contributed to the diminished microbial population available for performing complete nitrification of NH_3^--N within the system (Liu, 2024).

Notably, the high NO_3^--N concentrations present in all bioreactors indicate the accumulation of NO_3^--N, as the NO_3^--N concentrations were occasionally higher than the NH_3^--N concentration in the SWW influent. While nitrification occurs in the aerobic layer of the granules, denitrification of NO_3^--N takes place in the anoxic layer (Yu and Wang, 2024).

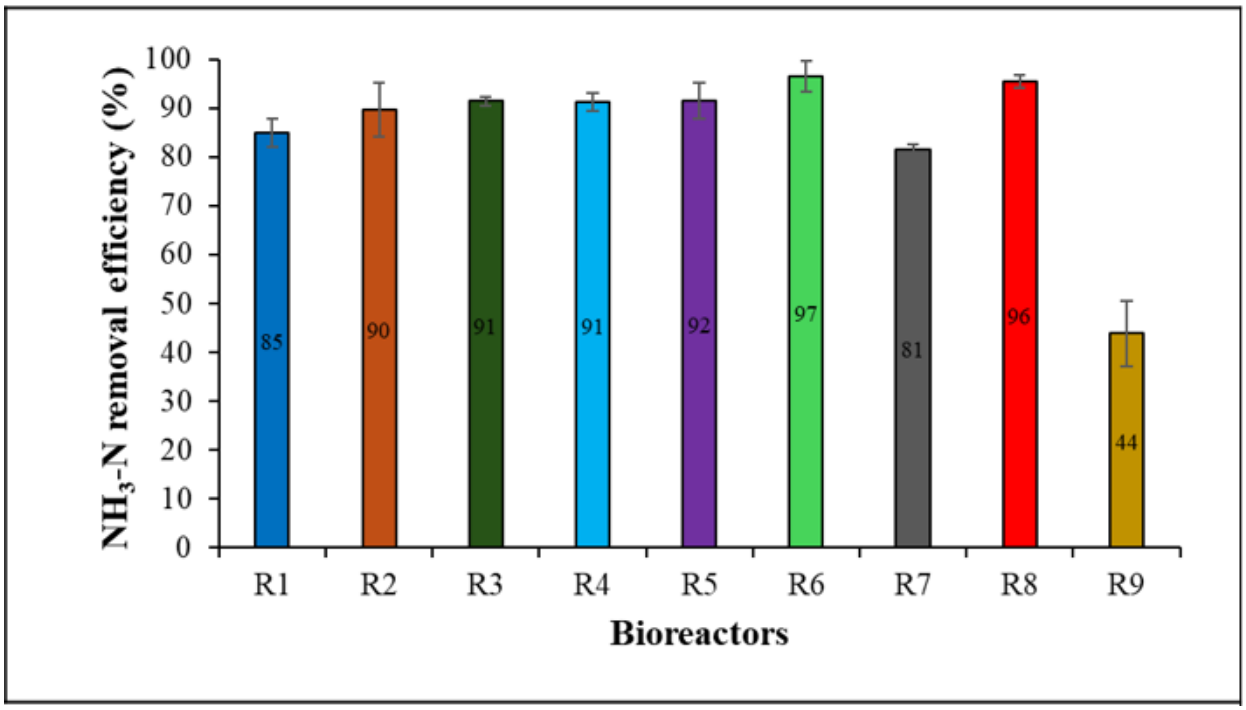

Figure 4.2. NH_3-N removal efficiency for bioreactors R1 to R9. ***R1 (C/N-20, 60 min feeding, OLR-2.1 kg COD/m³·d); R2 (C/N-30, 60 min feeding, OLR-1.5 kg COD/m³·d); R3 (C/N-10, 30 min feeding/30 min resting, OLR-2.1 kg COD/m³·d); R4 (C/N-30, 10 min pulse feeding/50 min resting, OLR-2.1 kg COD/m³·d); R5 (C/N-10, 10 min pulse feeding/50 min resting, OLR-1.5 kg COD/m³·d); R6 (C/N-20, 30 min feeding/30 min resting, OLR-1.5 kg COD/m³·d); R7 (C/N-10; 60 min feeding, OLR-0.8 kg COD/m³·d); R8 (C/N-20; 10 min pulse feeding/50 min resting, OLR-0.8 kg COD/m³·d); R9 (C/N-30; 30 min feeding/30 min resting, OLR-0.8 kg COD/m³·d)***

4.1.3. Phosphorus removal

The phosphorus removal efficiency observed across the experiments reached up to 96 ± 3%, particularly in reactors R3 and R5 (Figure 4.3). In R3, R5 and R6, there is a resting phase with no oxygen supply through aeration. R3 and R6 have a resting phase of 30 min, while R5 has a resting phase of 50 min. This period in the AGS system supports the growth and activity of phosphate-accumulating organisms (PAOs), which are the crucial microorganisms for phosphorus removal. This indicates that the feeding strategy (10 min pulse feeding and 30 min feeding with 30 min resting phase), contributed to the removal of phosphorus. The presence and activity of PAOs is important because they uptake and store phosphate as polyphosphate within their cells

(Nancharaiah and Reddy, 2018; Purba et al., 2020). In addition, the unique structure of the aerobic granule, including aerobic, anaerobic and anoxic layers play important role in phosphorus removal. This granule structure provides both aerobic and anaerobic conditions for oxygen diffusion limitation, which enables enhanced biological phosphorus removal (Iorhemen et al., 2022). Conversely, reactors R1, R2, R4, and R9 exhibited phosphate removal efficiencies of under 50% compared to other bioreactors (Figure 4.3). In R1 and R2, there is no resting phase (aeration begins immediately after the feeding phase). This prevents the interaction between the granular structure and the processes of anaerobic phosphorus release and uptake for efficient phosphorus removal. Similarly, reactors R9 and R4 exhibited lower phosphate removal efficiency. This reduction could be attributed to the presence of excessive glycogen-accumulating organisms (GAOs) competing for organic carbon, which may have suppressed the PAOs and decreased phosphate removal efficiency. This corresponds with a study on the relationship between GAOs and PAOs in biological systems (Tsertou et al., 2024). The interaction between GAOs and PAOs may have been influenced by the different feeding strategies employed (10-min pulse feeding with a 50-min resting phase, 30-min feeding with a 30-min resting phase, and 60-min feeding).

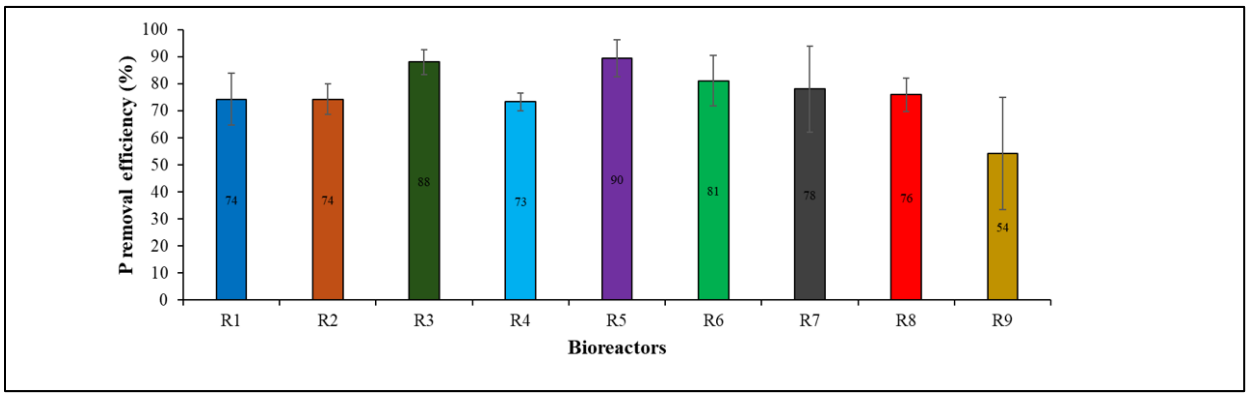

Figure 4.3. Phosphorus removal efficiency for bioreactors R1 to R9. ***R1 (C/N-20, 60 min feeding, OLR-2.1 kg COD/m³·d); R2 (C/N-30, 60 min feeding, OLR-1.5 kg COD/m³·d); R3 (C/N-10, 30 min feeding/30 min resting, OLR-2.1 kg COD/m³·d); R4 (C/N-30, 10 min pulse feeding/50 min resting, OLR-2.1 kg COD/m³·d); R5 (C/N-10, 10 min pulse feeding/50 min resting, OLR-1.5 kg COD/m³·d); R6 (C/N-20, 30 min feeding/30 min resting, OLR-1.5 kg COD/m³·d); R7 (C/N-10; 60 min feeding, OLR-0.8 kg COD/m³·d); R8 (C/N-20; 10 min pulse feeding/50 min resting, OLR-0.8 kg COD/m³·d); R9 (C/N-30; 30 min feeding/30 min resting, OLR-0.8 kg COD/m³·d)*

4.1.4. pH profile

Throughout the experiments, the pH of both influent and effluent wastewater remained relatively stable. The overall influent pH ranged from 7.43 to 8.03, while the effluent pH increased to a range of 7.95 to 8.86 (Table 4.1). To achieve this pH range, certain compounds in the SWW played crucial roles. Ammonium chloride (NH_4Cl), monopotassium phosphate (KH_2PO_4), and ferrous sulfate heptahydrate ($FeSO_4 \cdot 7H_2O$) contributed to the acidity of the influent. Meanwhile, sodium acetate (NaAc), dipotassium phosphate (K_2HPO_4), and sodium propionate (NaPr) contributed to its alkaline properties. Typically, the suitable pH range for aerobic granules to thrive successfully is between 7 and 9 (Ji et al., 2011; Niu et al., 2023). Maintaining the pH within this range throughout the experiment prevented filamentous growth, thereby facilitating the rapid formation of mature and stable granules.

The pH trend indicates that the mixed liquor in the reactors transitioned from a neutral-like condition to an alkaline condition, which explains the alkaline effluent observed throughout the experiment. During the nitrification process, nitrifying bacteria consume hydrogen ions (H^+), leading to an increase in pH within the reactors and subsequently in the effluent compared to the influent (De Vleeschauwer et al., 2021). Additionally, in the anoxic layer of the granules, where denitrification occurs, the process releases nitrogen gas, which produces alkalinity and further contributes to the increase in pH in the effluent (De Vleeschauwer et al., 2020).

Table 4.3. Summary of SWW influent and effluent pH values for each experimental run

Experimental run	Mean SWW Influent	Mean SWW Effluent
R1	7.74 ± 0.10	8.7 ± 0.09
R2	7.64 ± 0.09	8.43 ± 0.06
R3	7.78 ± 0.09	8.51 ± 0.12
R4	7.75 ± 0.11	8.7 ± 0.16
R5	7.75 ± 0.15	8.31 ± 0.10
R6	7.71 ± 0.09	8.53 ± 0.09
R7	7.8 ± 0.14	8.14 ± 0.13
R8	7.75 ± 0.07	8.31 ± 0.03
R9	7.8 ± 0.13	8.49 ± 0.12

*Number of observations – 8 per experimental run

4.2. Biomass characteristics of AGS

The bioreactors began with activated sludge biomass, whose SVI_{30}, SVI_5, MLSS and MLVSS were 222 ± 20 mL/g, 361 ± 11 mL/g, 2380 ± 340 mg/L and 2200 ± 210 mg/L, respectively. Figures 4.5 and 4.6 show the biomass characteristics of all 9 experiments (R1, R2, R3, R4, R5, R6, R7, R8 and R9 reactors), including the MLSS, MLVSS, SVI_5, SVI_{30}, and SVI_{30}-to-SVI_5 ratio. Each experiment (R1 to R9) was operated at various experimental conditions (Table 3.1). To reach granulation (that is R1 had SVI_{30} – 35 ± 1 mL/g; SVI_5 – 37 ± 1 mL/g and R2 had SVI_{30} 41 ± 1 mL/g; SVI_5 – 43 ± 1 mL/g), the bioreactors were operated for 106 d. The experiment began from the 107th day of operating the bioreactors. Images comparing the bioreactors at an early stage of operation around day 12 and around day 103 show the granule formation achieved over time (Figure 4.4).

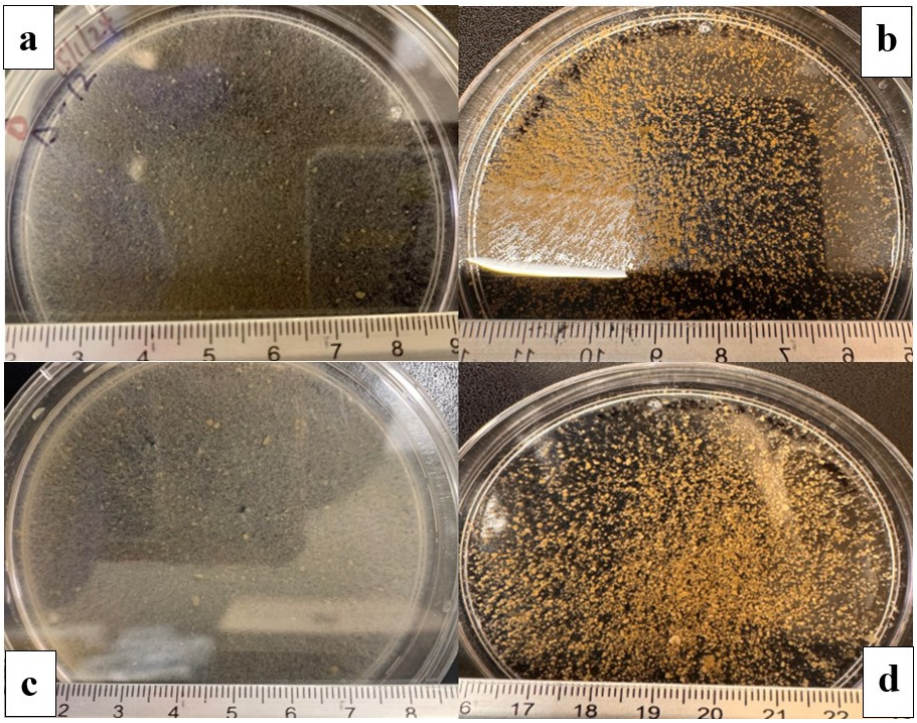

Figure 4.4. Images comparing reactor sludge during aerobic granule formation. a) day 12 of granule formation in R1. b) day 226 of granule formation in R1. c) day 12 of granule formation in R2. d) day 226 of granule formation in R2.

The reactors showed varying biomass results throughout the operational period. Though the biomass concentration of each bioreactor developed differently with time, R3, R5 and R6 achieved the highest MLSS and MLVSS concentrations (Figure 4.5). The highest MLSS and MLVSS were 17 ± 3 g/L and 13 ± 2 g/L respectively in reactor R3. This was close to the results in R5 (MLSS – 16 ± 1 g/L, MLVSS – 12 ± 1 g/L) and R6 (MLSS – 15 ± 1 g/L, MLVSS – 13 ± 1 g/L). Meanwhile, reactors R9 and R7 showed the lowest MLSS and MLVSS concentrations. R9 had MLSS and MLVSS of 6 ± 1 g/L and 5 ± 0 g/L respectively. R7 had MLSS and MLVSS concentrations of 11 ± 2 g/L and 8 ± 2 g/L respectively. The reactors with the highest biomass concentrations were operated at the higher OLR (2.1 and 1.5 kg COD/m^3·d), which corresponds with the previous study by Awang and Shaaban (2018). All 9 experiments were operated at a

suitable C/N ratio (10, 20 and 30) that support granule stability. The C/N ratio in the influent impacts the formation of stable granules, due to its effect of microbial population shift in AGS (Zhou and Sun, 2020). A high C/N ratio has been shown to cause granular instability by encouraging the growth of filaments in the granule. Though C/N ratio 20 and 30 are considered too high to support stable granule development (Gan et al., 2024), this was not the case in the experiments. In addition, the intensity of aeration may be attributed to the high biomass concentration. All bioreactors were operated at an airflow velocity of 1.98 cm/s, which is suitable for the appropriate hydrodynamic shear force required. The rate of oxygen transfer and shear forces within the reactor improves microbial activity and biomass growth, leading to higher MLSS concentrations (Adav et al., 2007). It is important to note that the observed decrease in biomass concentration in reactors R7, R8, and R9 at the start of these experiments was a result of the redistribution of sludge aimed at balancing the biomass levels across all bioreactors. Notably, this adjustment did not particularly impact the settling properties of the reactors as shown by SVI_{30}/SVI_5 ratio ranging from 0.95 to 1 (Figure 4.6).

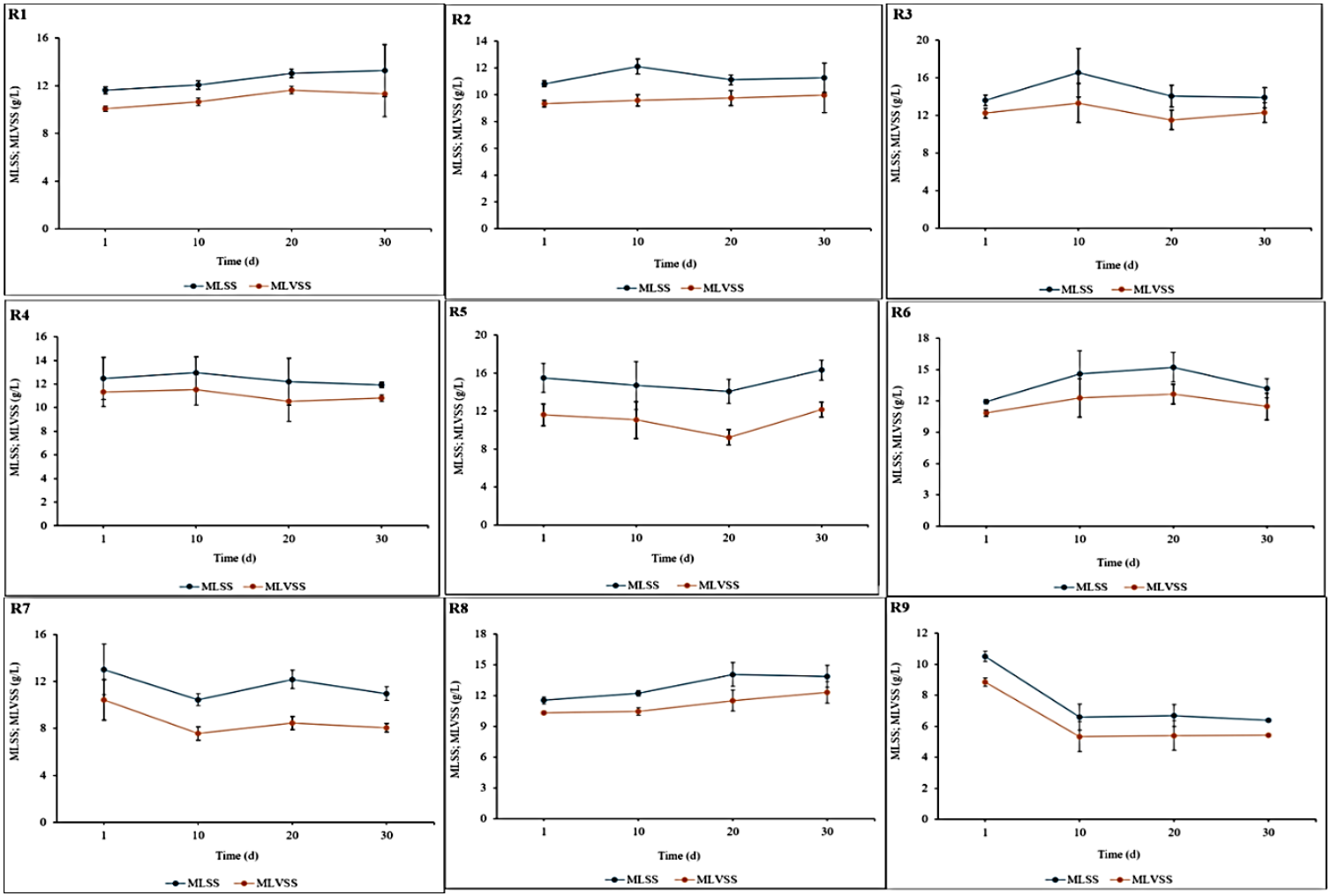

Figure 4.5. MLSS and MLVSS measured in g/L for bioreactors R1-9. **R1 (C/N-20, 60 min feeding, OLR-2.1 kg COD/m³·d); R2 (C/N-30, 60 min feeding, OLR-1.5 kg COD/m³·d); R3 (C/N-10, 30 min feeding/30 min resting, OLR-2.1 kg COD/m³·d); R4 (C/N-30, 10 min pulse feeding/50 min resting, OLR-2.1 kg COD/m³·d); R5 (C/N-10, 10 min pulse feeding/50 min resting, OLR-1.5 kg COD/m³·d); R6 (C/N-20, 30 min feeding/30 min resting, OLR-1.5 kg COD/m³·d); R7 (C/N-10; 60 min feeding, OLR-0.8 kg COD/m³·d); R8 (C/N-20; 10 min pulse feeding/50 min resting, OLR-0.8 kg COD/m³·d); R9 (C/N-30; 30 min feeding/30 min resting, OLR-0.8 kg COD/m³·d).*

In terms of settleability, the SVI_{30} and SVI_5 continuously reduced throughout the experiment, although there was some fluctuation from one experiment to another. The highest SVI_{30} was attained in R1 (35 ± 1 mL/g) and R2 (41 ± 1 mL/g), which indicates favorable settling performance from the start of the experiment (Figure 4.6). During the experimental period, the sludge settling at 5 and 30 min for each reactor remained consistently similar or nearly identical (Figure 4.7). The SVI_{30} further decreases throughout the experiment, favoring the performance of the reactors. This result may be attributed to the increase in granule size, as continuous growth of EPS improves the structure and size or aerobic granules (Wang et al., 2023). Additionally, the SVI_{30}-to-SVI_5 ratio consistently remained between the range of 0.95 to 1, another indication of good settleability and biomass stability and performance (Setianingsih et al., 2019).

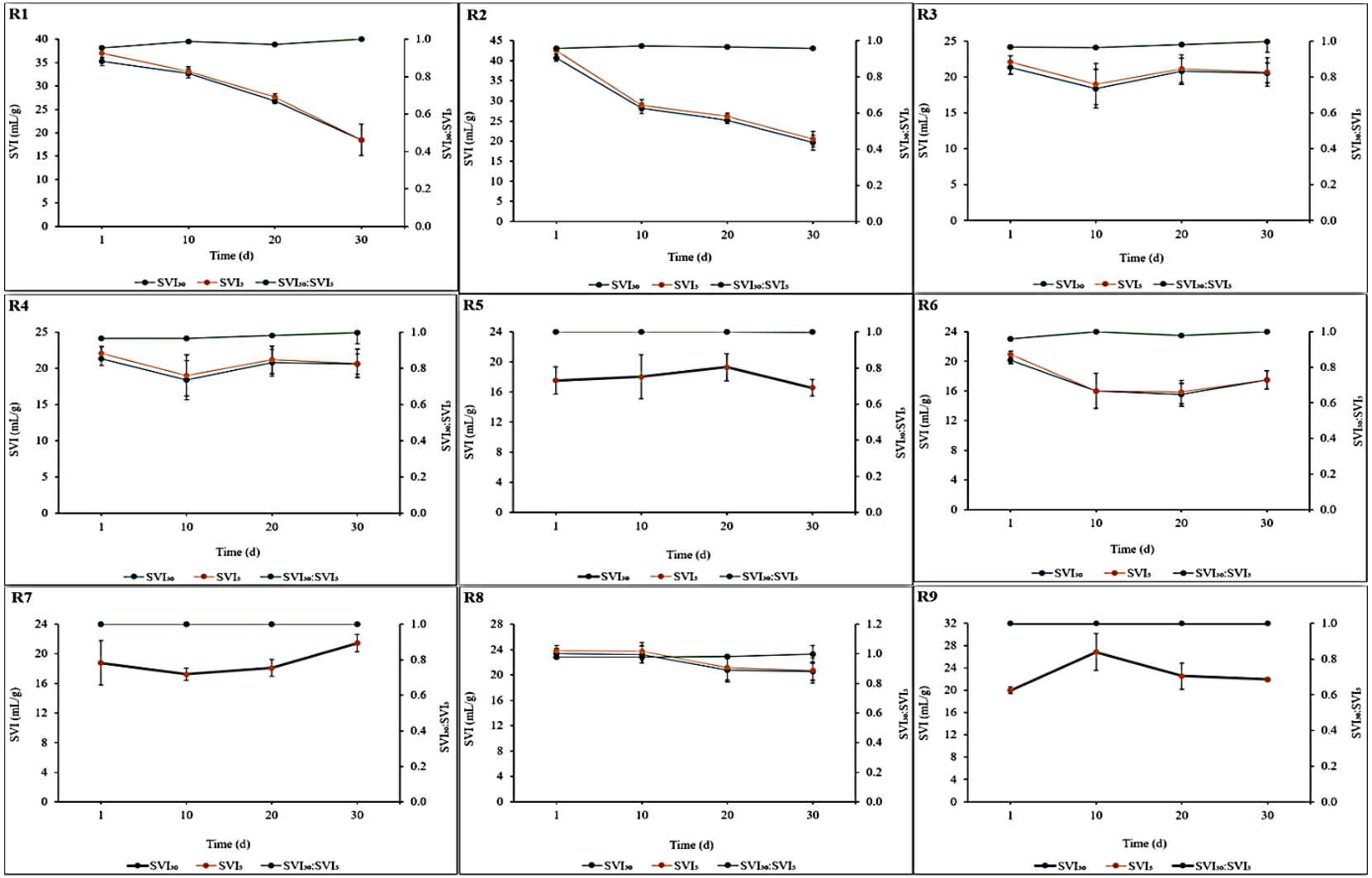

Figure 4.6. SVI_{30} and SVI_5 measured in mL/g and SVI_{30}-to-SVI_5 ratio for bioreactors R1-9. **R1 (C/N-20, 60 min feeding, OLR-2.1 kg COD/m³·d); R2 (C/N-30, 60 min feeding, OLR-1.5 kg COD/m³·d); R3 (C/N-10, 30 min feeding/30 min resting, OLR-2.1 kg COD/m³·d); R4 (C/N-30, 10 min pulse feeding/50 min resting, OLR-2.1 kg COD/m³·d); R5 (C/N-10, 10 min pulse feeding/50 min resting, OLR-1.5 kg COD/m³·d); R6 (C/N-20, 30 min feeding/30 min resting, OLR-1.5 kg COD/m³·d); R7 (C/N-10; 60 min feeding, OLR-0.8 kg COD/m³·d); R8 (C/N-20; 10 min pulse feeding/50 min resting, OLR-0.8 kg COD/m³·d); R9 (C/N-30; 30 min feeding/30 min resting, OLR-0.8 kg COD/m³·d).*

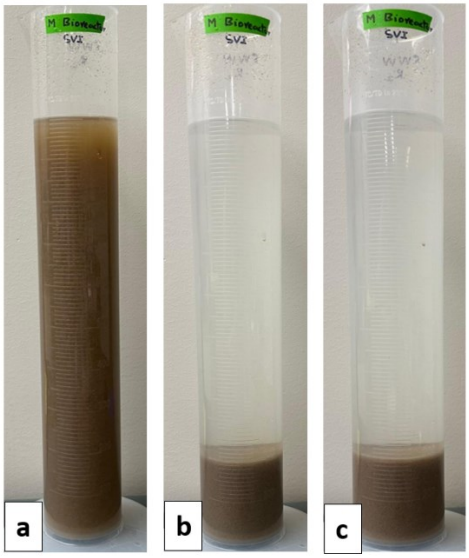

Figure 4.7. Reactor R8 settling. a) Sludge at 0 seconds b) sludge at 5 min c) sludge at 30 min.

4.3. Curdlan recovery

4.3.1. Identification of gel extract

To identify the gel extracted from AGS, a detailed analysis of its physical and chemical properties was conducted using various methods, including aniline blue staining, NMR, and FT-IR spectroscopy.

i. Aniline blue staining

In addition to the FT-IR analysis, aniline blue staining method was employed to test the presence of curdlan. Unlike other polysaccharides, curdlan can be stained by aniline blue solution, resulting in a distinct blue coloration. This is as a result of the affinity aniline stain has for β-1,3-glucan, present in curdlan structure (Stasinopoulos et al., 1999). Different from other polysaccharides, curdlan could be stained by aniline blue solution and show a clearly blue color. In this study, the biopolymer produced from AGS showed a positive aniline blue stain (Figure 4.18), indicating the gel extract was composed largely of β-1,3-glucosidic bond (Wood and

Fulcher, 1984), a typical characteristic of curdlan and curdlan-type biopolymer (Harada et al., 1968; Nakanishi et al., 1976; Wang et al., 2016).

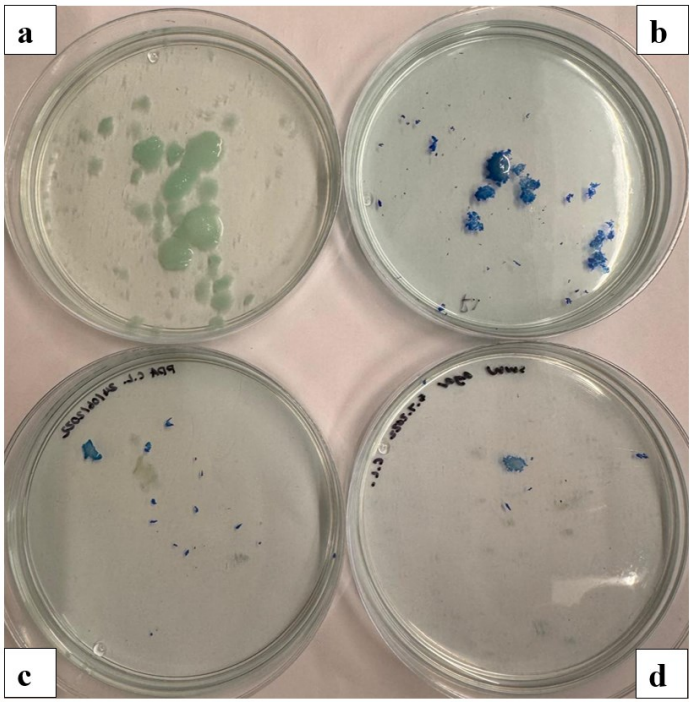

Figure 4.8. Aniline blue staining of curdlan. a) Curdlan without aniline; b) Aniline blue staining of commercial curdlan from *Alcaligene faecalis*; c) Aniline blue staining of curdlan gel extracted from R7 d) Aniline blue staining of curdlan extracted from R9.

ii. FT-IR spectroscopy

FT-IR spectroscopy is a valuable tool for analyzing biopolymers. Due to the complexity of the curdlan structure, there were multiple peaks at some regions of the spectrum - 1679.67 cm^{-1} (Siddique, 2024). As shown in Figure 4.17, the gel extract FT-IR spectrum displayed band transmittance at 3275.44 cm^{-1} and 2926.61 cm^{-1}, corresponding to the O-H group and C-H stretching, respectively. Additionally, an absorption band at 1025.30 cm^{-1} indicates the presence of the C-O group, closely aligning with the pure curdlan spectrum used as a standard and

corroborating previously reported findings by Martinez et al. (2015). The variation observed in the spectra may be due to the presence of impurities in the gel extract. This may lead to the shift in the vibrational energy levels of the sample and may introduce new peaks resulting in different absorption characteristics observed (Kupcewicz et al., 2013; Bhokare et al., 2022).

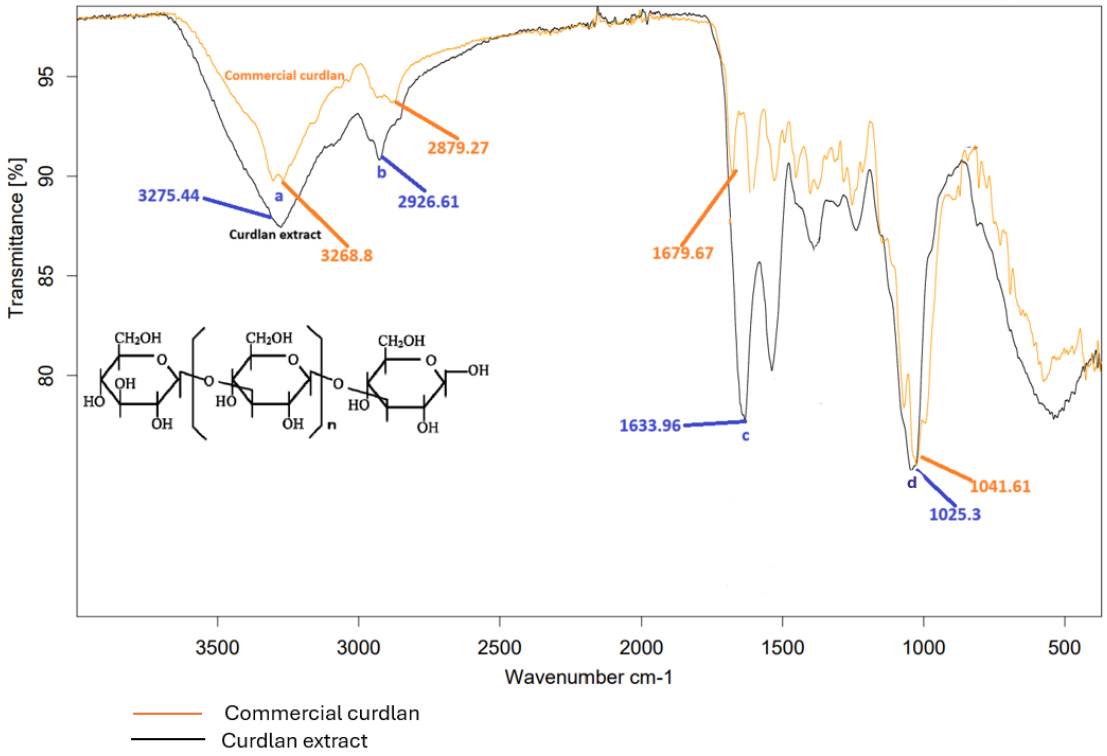

Figure 4.9. FT-IR spectra of commercial curdlan from *Alcaligene faecalis* and biopolymer extract from AGS system.

iii. $^{1}H - {}^{13}C$ HSQC NMR

The HSQC analysis of curdlan extract R7i and pure curdlan revealed the presence of correlations, as illustrated in Figure 4.10. Specifically, five distinct cross-peaks between the proton and carbon atoms were observed, indicating a strong similarity between the two samples (Table 4.2). In the ^{13}C spectrum of pure and extracted curdlan (Figure 4.10), the chemical shift at 103.73 ppm corresponds to the anomeric carbon C1 (Tang et al., 2018). Based on the $^{1}H–^{13}C$

HSQC spectrum (Figure 4.19), all chemical shifts of carbons and protons of pure curdlan were assigned. These cross-peak positions are similar to the observed chemical shifts in Tang et al. (2018). However, the presence of unrelated cross-peaks in the curdlan extracts suggests the existence of impurities within the samples. These impurities likely interfered with the spectral data, resulting in additional signals that were not present in the pure curdlan sample. Despite these impurities, the identified correlations at cross peaks a, b, c, d, and e (Table 4.2) between curdlan extract R7i and pure curdlan confirm the successful extraction of curdlan with some degree of contamination present.

In contrast, the HSQC analysis of curdlan extract R7ii did not exhibit the expected correlations with pure curdlan, making it difficult to interpret (Bryant et al., 2020). Rather than corresponding with a, b, c, d and e, R7ii exhibited cross-peaks f and g (Figure 4.10) including 61.51 ppm ^{13}C against 3.44 ppm ^{1}H, as well as 61.30 ppm ^{13}C against 3.70 ppm ^{1}H. These cross-peaks did not match those observed in R7i and pure curdlan. The discrepancy may be due to the presence of excessive by-products and impurities that were not present or less in the curdlan extract R7i, which could have altered the spectral profile.

To ensure the consistency and purity of curdlan extracts, it is essential to implement appropriate purification protocols during the recovery process. Further studies are needed to identify and mitigate the sources of by-products, thereby improving the quality and characterization of curdlan extracts.

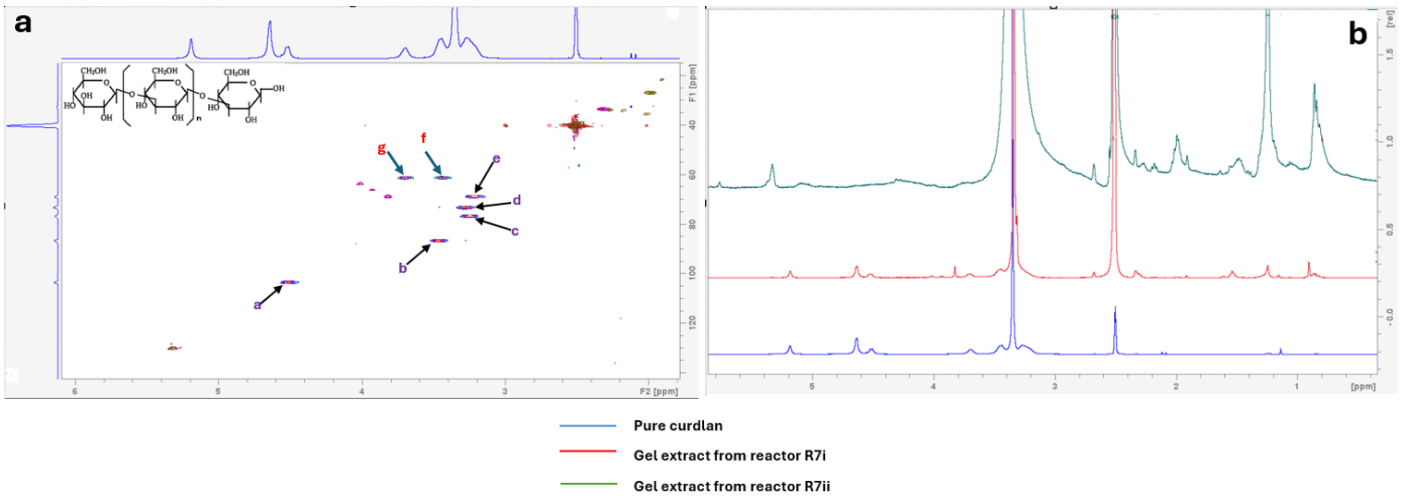

Figure 4.10. 2D ^{1}H - ^{13}C HSQC spectra of gel extract for AGS reactor and pure curdlan produced by *Alcaligene faecalis* in DMSO-d_6 (a); 1D ^{1}H NMR spectra showing gel extract from AGS reactor and pure curdlan (b).

Table 4.4. ^{13}C and ^{1}H NMR data for pure and R7i curdlan extract

Cross-peak points	**^{1}C δ Chemical shift (ppm)**		**^{13}H δ Chemical shift (ppm)**	
	Pure curdlan	Extract	Pure curdlan	Extract
a	103.73	103.73	4.51	4.51
b	86.99	86.99	3.46	3.47
c	76.83	77.13	3.26	3.26
d	73.24	73.84	3.28	3.28
e	69.05	69.05	3.21	3.21

4.3.2. Effect of C/N ratio on curdlan biosynthesis

The C/N ratio in the influent has been demonstrated to significantly influence the formation of stable granules. High C/N ratios can lead to the disintegration of AGS due to the proliferation of filamentous bacteria within the granules, thereby compromising their spherical structure and stability (Gan et al., 2024).

In the experiments, the C/N ratio was found to influence the production of high-quality and stable granules. However, the biomass concentration varied across experiments due to fluctuations in the microbial population. This variation in biomass concentration resulted in corresponding changes in EPS and the amount of curdlan extracted, as curdlan is one of the biopolymers present in the EPS.

To investigate the effect of the C/N ratio on curdlan biosynthesis, 9 experimental runs were operated under different conditions. The highest curdlan yields were observed in run R3 and R4, with yields of 74 ± 6 mg curdlan/g biomass and 69 ± 11 mg curdlan/g biomass, respectively, when operated at C/N ratios of 10 and 30 on day 30 of the experiments (Figure 4.12). Notably, run R1, R2, R3, and R4 exhibited an increasing trend in curdlan yield over days 10, 20, and 30, suggesting a positive effect of C/N ratios of 10, 20, and 30 on curdlan production (Figure 4.11).

Conversely, run R8, R2, R7, R6, and R5 showed low curdlan yields, with values below 20 mg curdlan/g biomass. These experimental runs were operated at C/N ratios of 20, 30, 10, 20, and 10, respectively. These results did not particularly follow a trend. This indicates that the C/N ratio, whether high or low, did not directly influence the high yield of curdlan in these experiments, contrary to studies suggesting that EPS yield decreases with a lower C/N ratio (Cui et al., 2017; Su et al., 2023).

Pearson correlation analysis revealed that there is no correlation between the C/N ratio and curdlan yield (r = -0.07) (Table 4.3). A similar observation was obtained in a study on the impact of C/N ratio on EPS synthesis in wastewater (Erkan et al., 2016). However, this result was not statistically significant (p = 0.852). Considering the main effects analysis, it was observed that C/N ratio of 10 was the optimal in this experiment for curdlan yield ($p \leq 0.05$). Among all factor-levels, C/N ratio of 10 was the third most effective factor level in the experiment (Figure 4.13). The observation indicates that despite its low impact on curdlan production, it may be worthwhile to study further the optimization of C/N ratio 10 for curdlan recovery.

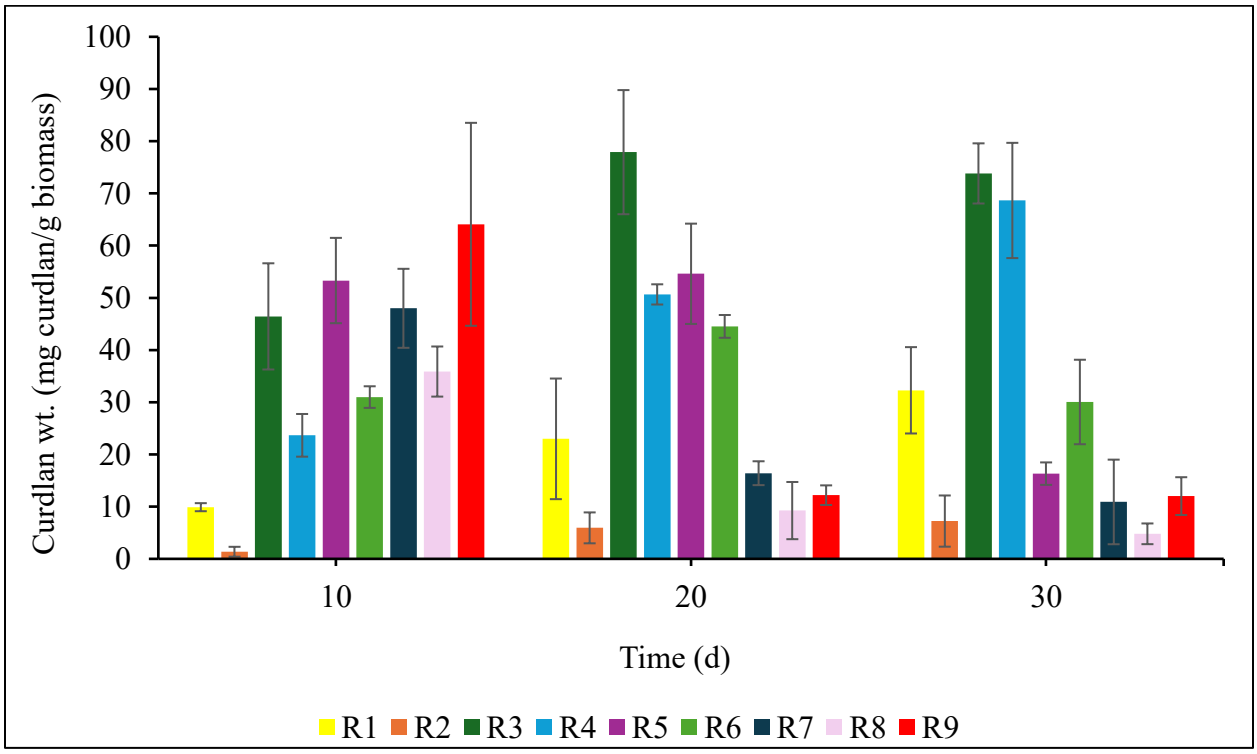

Figure 4.11. Curdlan gel extracted from AGS biomass for days 10, 20 and 30 of 9 experimental runs. **R1 (C/N-20, 60 min feeding, OLR-2.1 kg COD/m³·d); R2 (C/N-30, 60 min feeding, OLR-1.5 kg COD/m³·d); R3 (C/N-10, 30 min feeding/30 min resting, OLR-2.1 kg COD/m³·d); R4 (C/N-30, 10 min pulse feeding/50 min resting, OLR-2.1 kg COD/m³·d); R5 (C/N-10, 10 min pulse feeding/50 min resting, OLR-1.5 kg COD/m³·d); R6 (C/N-20, 30 min feeding/30 min resting, OLR-1.5 kg COD/m³·d); R7 (C/N-10; 60 min feeding, OLR-0.8 kg COD/m³·d); R8 (C/N-20; 10 min pulse feeding/50 min resting, OLR-0.8 kg COD/m³·d); R9 (C/N-30; 30 min feeding/30 min resting, OLR-0.8 kg COD/m³·d).*

4.3.3. Effects of OLR on curdlan biosynthesis

The OLR in this study corresponds to the concentration of organic carbon, measured as COD, fed into the bioreactor in a day. The experimental runs were operated at OLRs of 0.8, 1.5, and 2.1 kg COD/m³·d, which correspond to COD concentrations of 300, 550, and 800 mg/L, respectively.

From the experiments, run R3, R4, and R1 exhibited the highest curdlan yields of 74 ± 6, 69 ± 11, and 32 ± 8 mg curdlan/g biomass on day 30, respectively. These experimental runs were operated at the highest OLR of 2.1 kg COD/m³·d. Additionally, run R6, which was operated at an OLR of 1.5 kg COD/m³·d achieved a curdlan yield of 30 ± 8 mg curdlan/g biomass on day 30.

It is well established that high EPS production results in high curdlan yields. The high OLR studied likely led to an increase in biomass concentration, which in turn enhanced EPS synthesis. This increased EPS synthesis is the primary reason behind the high curdlan yields observed in these experimental runs. Higher OLR provides more substrates for microbial growth, leading to enhanced EPS synthesis, which subsequently increases the amount of curdlan extracted from the AGS system. These findings are consistent with previous studies (Cydzik-Kwiatkowska, 2021; Peng et al., 2022).

Meanwhile, lower OLR resulted in lower curdlan yields in run R2, R5, R7, R8, and R9, with yields of 7 ± 5, 16 ± 2, 11 ± 8, 5 ± 2, and 12 ± 4 mg curdlan/g biomass, respectively (Figuren 4.12). These results align with other studies on the effect of low OLR on EPS biosynthesis in AGS systems (Traina et al., 2022). Notably, run R7, R8, and R9, operated at an OLR of 0.8 kg COD/m³·d, showed a consistent decrease in curdlan yield from day 10 to day 30 by approximately 77%, 87%, and 81%, respectively. This observation further supports the notion that OLR significantly influences curdlan biosynthesis in AGS systems.

Statistical analysis revealed a significant positive correlation ($p = 0.007$) at 0.05 level of siginifcance between OLR and curdlan yield, indicating that an increase in OLR promotes higher curdlan production. This observation is supported by studies on biopolymer recovery from AGS (Traina et al., 2022; Liu et al., 2023). These findings show the critical role of OLR in optimizing curdlan yield in AGS systems, providing valuable insights for future research and practical applications in wastewater treatment. Regarding the main effects analysis (Figure 4.13), it was observed that OLR ($p \leq 0.05$) 2.1 kg COD/m^3·d was the optimal in this experiment for curdlan yield. Though this study shows the impact of OLR on curdlan production, the factor-level of OLR of 2.1 kg COD/m^3·d stood out, making it crucical to study further on how this OLR can be combined with other optimal factors for curdlan production optimization study.

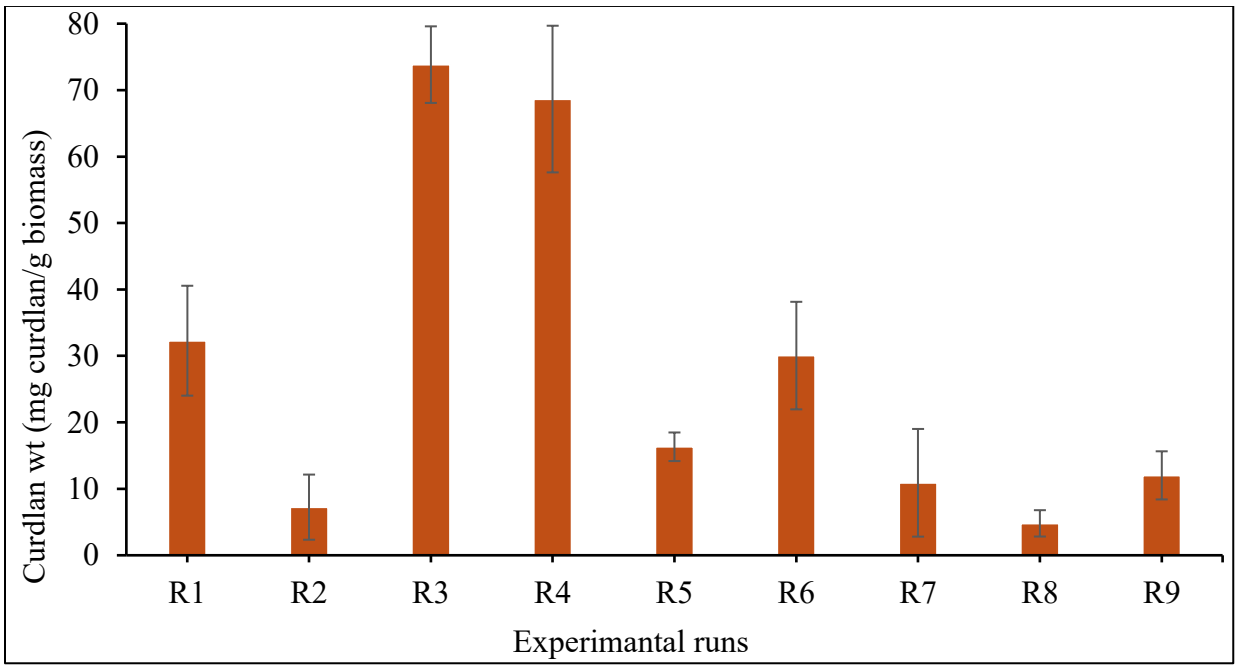

Figure 4.12. Curdlan gel extracted from AGS biomass on day 30 of 9 experiments. **R1 (C/N-20, 60 min feeding, OLR-2.1 kg COD/m³·d); R2 (C/N-30, 60 min feeding, OLR-1.5 kg COD/m³·d); R3 (C/N-10, 30 min feeding/30 min resting, OLR-2.1 kg COD/m³·d); R4 (C/N-30, 10 min pulse feeding/50 min resting, OLR-2.1 kg COD/m³·d); R5 (C/N-10, 10 min pulse feeding/50 min resting, OLR-1.5 kg COD/m³·d); R6 (C/N-20, 30 min feeding/30 min resting, OLR-1.5 kg COD/m³·d); R7 (C/N-10; 60 min feeding, OLR-0.8 kg COD/m³·d); R8 (C/N-20; 10 min pulse feeding/50 min resting, OLR-0.8 kg COD/m³·d); R9 (C/N-30; 30 min feeding/30 min resting, OLR-0.8 kg COD/m³·d).*

Table 4.3. Pearson correlation analysis showing the relationship between the experimental factors (C/N ratio, OLR, and feeding strategy) and curdlan biosynthesis in AGS.* C/N ratio ($p = 0.516$), OLR ($p = 0.007$), and feeding strategy ($p = 0.852$)

	C/N	Feeding	OLR	Curdlan
C/N	1			
Feeding strategy	*	1		
OLR	*	*	1	
Curdlan	-0.07	-0.25	0.82	1

4.3.4. Effect of feeding strategy on curdlan biosynthesis

The feeding strategy in this study was measured by the time it takes to feed the bioreactors per cycle. Considering the 9 experimental runs, the impact of feeding strategy on curdlan yield did not particularly show a clear trend, however, it is noticeable that the slow feeding (60 min feeding time) run R2 and R7, with the exception to R1, gave low mean curdlan yield of 7 ± 5, and 11 ± 8 mg curdlan/g biomass (Figure 4.12). This may be an indication of the negative effect slow feeding has on biopolymer synthesis in AGS systems, as slow feeding rates has been associated with the disruption of the protein-polysaccharide balance in EPS (Vicente et al., 2021). This disruption increases protein content, leading to improved mechanical strength and stability of the granules, however, results in drop in biopolymers in the AGS system (Vicente et al., 2021).

On the other hand, the higher curdlan yield can be associated with pulse and fairly fast (30 min) feeding strategies. For instance, R3 (74 ± 6 mg curdlan/g biomass) and R4 (69 ± 11 mg curdlan/g biomass), being the highest curdlan yielding experimental runs were operated at 30 and 10 min feeding time, allowing for a resting period, which contributes to granules stability and EPS synthesis (Weissbrodt et al., 2012), resulting from the feast-famine regime created by 10 min pulse feeding and 30 min feeding thereby promoting the production of EPS, in turn, curdlan production.

Whereas, R5, R8 and R9 produced low curdlan despite their operating feeding strategy being 10 min pulse and 30 min feeding. This may be due to the influence of the combined effect of other operating factors, leading to the drop in curdlan production. Statisitcally, there was a no correlation ($r = -0.25$) between feeding strategy and curdlan yield. However, this result is not statistically significant ($p = 0.852$), which agrees with a study on the impact of feeding strategy on AGS stability (Vicente et al., 2021). In contrast, Sun et al. (2024) reported that feeding strategies play a dominant role in shaping the structure of the microbial community and altering the properties of the EPS, which directly affects curdlan recovery.

Furthermore, considering the mean effect analysis (Figure 4.13), it was observed that the feeding strategy of 30 min feeding/30 min resting phase was the optimal feeding strategy in this experiment for curdlan yield ($p \leq 0.05$). Among all factor-levels, C/N ratio of 10 was the third most effective factor level in the experiment (Figure 4.13). The observation indicates that the 30 min feeding strategy is above the average mean of the overall effects of factors, which indicates that 30 min feeding/30 min resting phase has the overall second highest impact on curdlan yield in the study. Therefore, it may be worthwhile to perform further studies to optimize the feeding strategy levels to improve the overall performance of your system. Due to the varying observations regarding the impact of feeding strategies employed, it is crucial to explore the intrinsic mechanisms of how feeding strategies make differences in curdlan synthesis in AGS systems. In addition, future research should focus on investigating the combined effects of the optimal factors identified in this study on curdlan biosynthesis within the AGS matrix. Specifically, the optimal conditions include an OLR of 2.1 kg COD/m^3·d, a C/N ratio of 10, and a feeding strategy involving a 30 min feeding phase followed by a 30 min resting phase. By examining the interactions between these factors, it will be possible to gain insight of their synergistic impact on curdlan production.

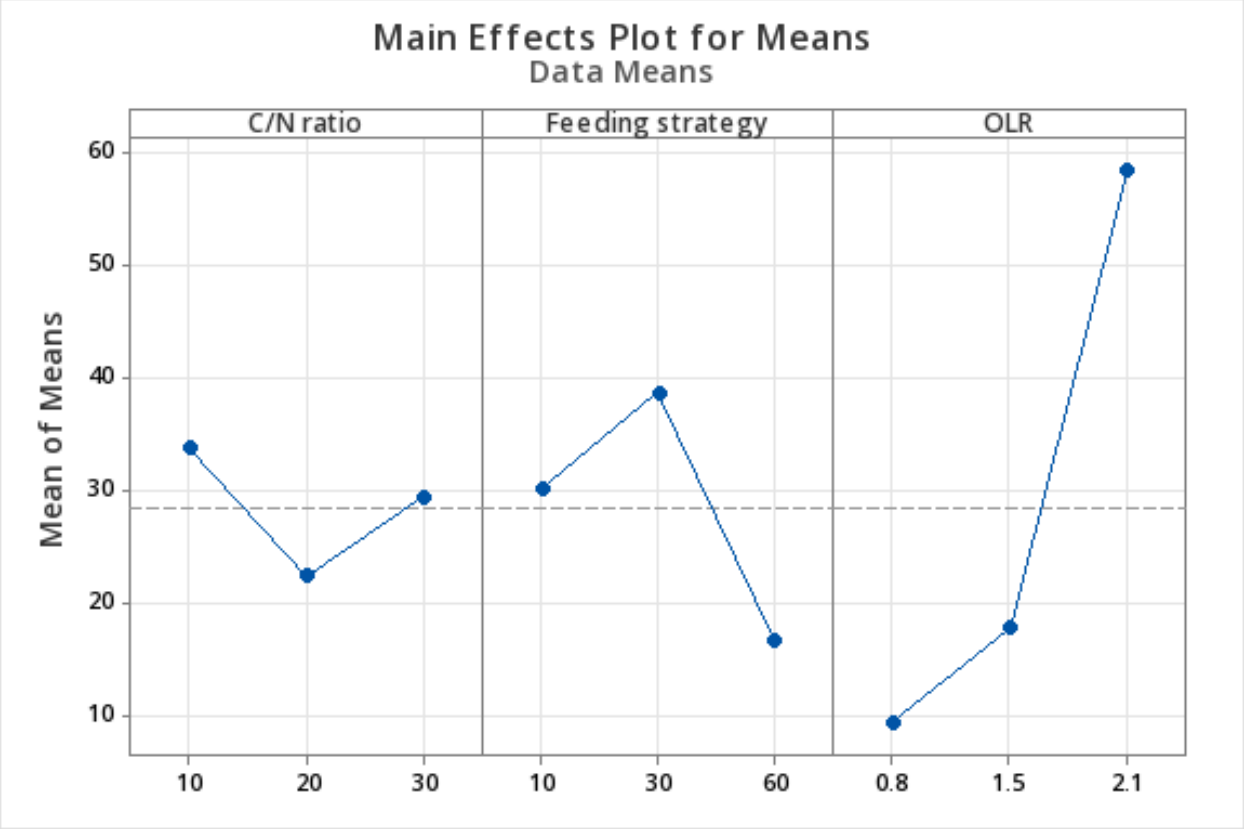

Figure 4.13. Main effect analysis of experimental factors at different levels on curdlan biosynthesis from AGS matrix

Chapter 5 Conclusions and Recommendations

5.1. Conclusions

With the emergence of the wastewater biorefinery concept, WWTPs are now viewed as wastewater-resource factories inserted into circular cities to achieve sustainability. The AGS biotechnology has particularly gained increased interest in this regard due to its enhanced wastewater treatment performance and potential for resource recovery. In the present study, the effect of OLR, C/N ratio, and feeding strategy on the biosynthesis of curdlan in the aerobic granule matrix during wastewater treatment in AGS-based wastewater treatment system were determined. The main conclusions drawn from this research are outlined below:

- Curdlan was identified in the aerobic granule matrix
- The C/N ratio showed no effect on curdlan yield. Pearson correlation analysis revealed no correlation ($r = -0.07$) between C/N ratio and curdlan yield. This result was not statistically significant at 95% confidence level ($p=0.516$).
- The OLR was identified as the most influential factor affecting curdlan production in the aerobic granule matrix. Curdlan yield increased with increasing OLR, attaining an optimum yield of 74 ± 6 mg curdlan/g biomass. Pearson correlation analysis revealed a significant positive correlation ($r = 0.82$) between OLR and curdlan yield; and this was statistically significant at 95% confidence level ($p=0.007$). This observation highlights the crucial role of OLR on curdlan production in AGS systems.
- The feeding strategy showed minimal effect on curdlan yield. Pearson correlation analysis revealed a weak negative correlation ($r = -0.25$) between feeding strategy and curdlan yield. However, this result was not statistically significant at 95% confidence level ($p = 0.852$).

This implies that variations in the feeding regime have minimal effect on curdlan production.

- Taguchi mean effect analysis showed that OLR of 2.1 kg COD/m^3·d, C/N ratio of 10, and feeding strategy of 30 min feeding/30 min resting phase were optimal for curdlan production in the aerobic granule matrix.
- The AGS systems achieved COD, NH_3-N, and PO_4^{3-}–P removal efficiencies reaching 99.6 ± 0.6%, 97 ± 1%, and 91 ± 6%, respectively.
- The AGS system achieved stability throughout the experimental period as both SVI_5 and SVI_{30} values in all the experimental runs were in the range 16 ± 2 – 43 ± 1 mL/g and the SVI_{30}/SVI_5 ratio was consistently between 0.9 and 1.0 throughout the experimental duration.

5.2. Limitations

The present study had some limitations. These include:

- This study was limited to the use of synthetic municipal wastewater in a laboratory-controlled environment. Since the synthetic wastewater was produced using sodium acetate and sodium propionate as the carbon sources, almost all the carbon is biodegradable which would result in a BOD:COD ratio of about 1. In real municipal wastewater, there are some refractory organics as well as non-biodegradable organics which would alter the BOD:COD ratio. The presence of refractory and non-biodegradable organic matter as well as other constituents in real wastewater may alter the EPS composition which would have an impact of curdlan production.
- The present study focused on the effect of OLR, COD/N ratio, and feeding strategy on curdlan production in the aerobic granule matrix. However, other key parameters such as

substrate type, solids retention time, hydrodynamic shear force, temperature, feast-famine period ratio, volumetric exchange ratio, and hydraulic retention time were not studied. These factors play a crucial role in EPS production; and, they may also have a salient impact on curdlan biosynthesis in the aerobic granule matrix.

5.3. Recommendations

Based on the results obtained from this thesis, it is imperative to conduct further research in the following areas:

(i) Future research should consider validating the findings in the present study using actual municipal wastewater at pilot- and eventually full-scales. This will provide insights into the impacts of a mixture of different carbon sources and different constituents as well as variable wastewater loads on curdlan yield.

(ii) Future studies should determine the effect of other AGS operational factors such as substrate type, solids retention time, hydrodynamic shear force, temperature, feast-famine period ratio, volumetric exchange ratio, and hydraulic retention time on curdlan biosynthesis in the aerobic granule matrix in AGS-based wastewater treatment systems

(iii) Further study to understand EPS production trends in AGS systems should be conducted. It is crucial to conduct thorough monitoring using cycle tests to gain insights into microbial interactions at different stages of the AGS process. This understanding can lead to more targeted and effective recovery strategies, ultimately improving overall yield and optimizing curdlan recovery.

(iv) Research should be conducted on the development of purification protocols for the curdlan extracted from waste aerobic granules.

(v) Based on these results, research is recommended on the optimization of curdlan production in the aerobic granule matrix where both individual effects and interactive effects of the different factors can be studied. Such studies should be done using experimental designs such as central composite design.

References

Adav, S. S., Lee, D. J., & Lai, J. Y. (2007). Effects of aeration intensity on formation of phenol-fed aerobic granules and extracellular polymeric substances. *Applied Microbiology and Biotechnology*, *77*(1), 175–182. https://doi.org/10.1007/S00253-007-1125-3/FIGURES/4

Alhola, K., Ryding, S. O., Salmenperä, H., & Busch, N. J. (2019). Exploiting the Potential of Public Procurement: Opportunities for Circular Economy. *Journal of Industrial Ecology*, *23*(1), 96–109. https://doi.org/10.1111/JIEC.12770

Al-Rmedh, Y. S. S., Ali, H. I., & Al-Sahlany, S. T. G. (2023). Curdlan Gum, Properties, Benefits and Applications. *IOP Conference Series: Earth and Environmental Science*, *1158*(11). https://doi.org/10.1088/1755-1315/1158/11/112011

Amann, A., Zoboli, O., Krampe, J., Rechberger, H., Zessner, M., & Egle, L. (2018). Environmental impacts of phosphorus recovery from municipal wastewater. *Resources, Conservation and Recycling*, *130*, 127–139.

Amorim de Carvalho, C. de, Ferreira dos Santos, A., Tavares Ferreira, T. J., Sousa Aguiar Lira, V. N., Mendes Barros, A. R., & Bezerra dos Santos, A. (2021). Resource recovery in aerobic granular sludge systems: is it feasible or still a long way to go? *Chemosphere*, *274*, 129881. https://doi.org/10.1016/j.chemosphere.2021.129881

Aquinas, N., Bhat, R. M., & Selvaraj, S. (2021). A review presenting production, characterization, and applications of biopolymer curdlan in food and pharmaceutical sectors. Polymer Bulletin, 79, 6905–6927.

Aquinas, N., Bhat, R. M., & Selvaraj, S. (2024). Submerged Fermentation and Kinetics of Newly Isolated Priestia megaterium for the Production of Biopolymer Curdlan. *Journal of Polymers*

and the Environment, *32*(9), 4683–4698. https://doi.org/10.1007/S10924-024-03224-6/FIGURES/12

Awang, N. A., & Shaaban, Md. G. (2018). *Effect of Variable and Low Organic Loading Rate on Formation Aerobic Granular Sludge in Sewage Treatment*.

Barrios-Hernández, M. L., Pronk, M., Garcia, H., Boersma, A., Brdjanovic, D., van Loosdrecht, M. C. M., & Hooijmans, C. M. (2020). Removal of bacterial and viral indicator organisms in full-scale aerobic granular sludge and conventional activated sludge systems. *Water Research X*, *6*, 100040. https://doi.org/10.1016/J.WROA.2019.100040

Besbes, S., Drira, L., Blecker, C., Deroanne, C., & Attia, H. (2009). Adding value to hard date (Phoenix dactylifera L.): Compositional, functional and sensory characteristics of date jam. *Food Chemistry*, *112*(2), 406–411. https://doi.org/10.1016/J.FOODCHEM.2008.05.093

Bhokare, S. S., Biradar, V. R., Chakole, R. D., Charde, M. S., Swarupa, M., & Bhokare, S. (2022). Applications of FTIR Spectroscopy: Review. *Ijsdr.Org International Journal of Scientific Development and Research*, *7*, 213. www.ijsdr.org

Blomsma, F., & Brennan, G. (2017). The Emergence of Circular Economy: A New Framing Around Prolonging Resource Productivity. *Journal of Industrial Ecology*, *21*(3), 603–614. https://doi.org/10.1111/JIEC.12603

Bokhary, A., Leitch, M., & Liao, B. Q. (2022). Effect of organic loading rates on the membrane performance of a thermophilic submerged anaerobic membrane bioreactor for primary sludge treatment from a pulp and paper mill. *Journal of Environmental Chemical Engineering*, *10*(3), 107523. https://doi.org/10.1016/J.JECE.2022.107523

Bryant, N., G. Yoo, C., Pu, Y., & Ragauskas, A. J. (2020). 2D HSQC Chemical Shifts of Impurities from Biomass Pretreatment. *ChemistrySelect*, *5*(11), 3359–3364. https://doi.org/10.1002/SLCT.202000406

Campbell-Johnston, K., Vermeulen, W. J. V., Reike, D., & Brullot, S. (2020). The Circular Economy and Cascading: Towards a Framework. *Resources, Conservation & Recycling: X*, *7*, 100038. https://doi.org/10.1016/J.RCRX.2020.100038

Chaudhari, V., Buttar, H. S., Bagwe-Parab, S., Tuli, H. S., Vora, A., & Kaur, G. (2021). Therapeutic and industrial applications of curdlan with overview on its recent patents. *Frontiers in Nutrition*, 8, 646988.

Chen, Y., & Wang, F. (2020). Review on the preparation, biological activities and applications of curdlan and its derivatives. *European Polymer Journal*, *141*, 110096. https://doi.org/10.1016/J.EURPOLYMJ.2020.110096

Chrispim, M. C., Scholz, M., & Nolasco, M. A. (2019). Phosphorus recovery from municipal wastewater treatment: Critical review of challenges and opportunities for developing countries. *Journal of Environmental Management*, *248*, 109268.

Cognitive Market Research. (2024). Curdlan Market Report. Available from: https://www.cognitivemarketresearch.com/curdlan-market-report

Cordell, D., Rosemarin, A., Schröder, J. J., & Smit, A. L. (2011). Towards global phosphorus security: A systems framework for phosphorus recovery and reuse options. *Chemosphere*, *84*(6), 747–758. https://doi.org/10.1016/J.CHEMOSPHERE.2011.02.032

Corsino, S. F., Campo, R., Di Bella, G., Torregrossa, M., & Viviani, G. (2016). Study of aerobic granular sludge stability in a continuous-flow membrane bioreactor. Bioresource Technology, 200, 1055–1059. https://doi.org/10.1016/J.BIORTECH.2015.10.065

Cui, Y. W., Shi, Y. P., & Gong, X. Y. (2017). Effects of C/N in the substrate on the simultaneous production of polyhydroxyalkanoates and extracellular polymeric substances by Haloferax mediterranei via kinetic model analysis. *RSC Advances*, *7*(31), 18953–18961. https://doi.org/10.1039/C7RA02131C

Cydzik-Kwiatkowska, A. (2021). Biopolymers in Aerobic Granular Sludge—Their Role in Wastewater Treatment and Possibilities of Re-Use in Line with Circular Economy. *Energies 2021, Vol. 14, Page 7219*, *14*(21), 7219. https://doi.org/10.3390/EN14217219

Dai, X., Yang, L., Zheng, Z., Chen, H., & Zhan, X. (2015). [Proteomic analysis of curdlan-producing Agrobacterium sp. ATCC 31749 in response to dissolved oxygen]. *Wei Sheng Wu Xue Bao = Acta Microbiologica Sinica*, *55*(8), 1018–1025.

Davis, K. E. R., Joseph, S. J., & Janssen, P. H. (2005). Effects of growth medium, inoculum size, and incubation time on culturability and isolation of soil bacteria. *Applied and Environmental Microbiology*, *71*(2), 826–834

De Kreuk, M. K. et al. Simultaneous COD, nitrogen, and phosphate removal by aerobic granular sludge. *Biotechnology and Bioengineering*, v. 90, n. 6, p. 761-769, 2005.

Denning, G., Kabambe, P., Sanchez, P., Malik, A., Flor, R., Harawa, R., Nkhoma, P., Zamba, C., Banda, C., Magombo, C., Keating, M., Wangila, J., & Sachs, J. (2014). Global availability of phosphorus and its implications for global food supply: An economic overview. *PLoS Biology*, *7*(1). https://doi.org/10.1371/JOURNAL.PBIO.1000023

De Sanctis, M., Altieri, V. G., Piergrossi, V., & Di Iaconi, C. (2019). Aerobic granular-based technology for water and energy recovery from municipal wastewater. *New Biotechnology*, *56*, 71–78. https://doi.org/10.1016/J.NBT.2019.12.002

De Sousa Rollemberg, S. L., Mendes Barros, A. R., Milen Firmino, P. I., & Bezerra dos Santos, A. (2018). Aerobic granular sludge: Cultivation parameters and removal mechanisms. *Bioresource Technology*, *270*, 678–688. https://doi.org/10.1016/J.BIORTECH.2018.08.130

Derlon, N., Wagner, J., da Costa, R. H. R., & Morgenroth, E. (2016). Formation of aerobic granules for the treatment of real and low-strength municipal wastewater using a sequencing batch reactor operated at constant volume. *Water Research*, *105*, 341–350. https://doi.org/10.1016/J.WATRES.2016.09.007

De Vleeschauwer, F., Caluwé, M., Dobbeleers, T., Stes, H., Dockx, L., Kiekens, F., Copot, C., & Dries, J. (2020). A dynamic control system for aerobic granular sludge reactors treating high COD/P wastewater, using pH and DO sensors. *Journal of Water Process Engineering*, *33*, 101065. https://doi.org/10.1016/J.JWPE.2019.101065

De Vleeschauwer, F., Caluwé, M., Dobbeleers, T., Stes, H., Dockx, L., Kiekens, F., Copot, C., & Dries, J. (2021). A dynamically controlled anaerobic/aerobic granular sludge reactor efficiently treats brewery/bottling wastewater. *Water Science and Technology*, *84*(12), 3515–3527. https://doi.org/10.2166/WST.2021.470

Dhivya, C., Benny, I. S., Gunasekar, V., & Ponnusami, V. (2014). A review on development of fermentative production of curdlan. *International Journal of ChemTech Research*

Dueholm, M. K. D., Besteman, M., Zeuner, E. J., Riisgaard-Jensen, M., Nielsen, M. E., Vestergaard, S. Z., Heidelbach, S., Bekker, N. S., & Nielsen, P. H. (2023). Genetic potential for exopolysaccharide synthesis in activated sludge bacteria uncovered by genome-resolved metagenomics. *Water Research*, *229*, 119485. https://doi.org/10.1016/J.WATRES.2022.119485

Ekholm, J., Persson, F., de Blois, M., Modin, O., Gustavsson, D. J. I., Pronk, M., van Loosdrecht, M. C. M., & Wilén, B. M. (2024). Microbiome structure and function in parallel full-scale aerobic granular sludge and activated sludge processes. *Applied Microbiology and Biotechnology*, *108*(1), 1–15. https://doi.org/10.1007/S00253-024-13165-8/FIGURES/7

Ekholm, J., de Blois, M., Persson, F., Gustavsson, D. J. I., Bengtsson, S., van Erp, T., & Wilén, B. M. (2023). Case study of aerobic granular sludge and activated sludge—Energy usage, footprint, and nutrient removal. *Water Environment Research*, *95*(8). https://doi.org/10.1002/WER.10914

Egle, L., Rechberger, H., Krampe, J., & Zessner, M. (2016). Phosphorus recovery from municipal wastewater: An integrated comparative technological, environmental and economic assessment of P recovery technologies. *Science of The Total Environment*, *571*, 522–542. https://doi.org/10.1016/J.SCITOTENV.2016.07.019

El-Sayed, M. H., Arafat, H. H., Elsehemy, I. A., & Basha, M. (2016). Optimization, purification and physicochemical characterization of curdlan produced by paenibacillus sp. Strain NBR-10. *Biosciences Biotechnology Research Asia*, *13*(2), 901–909. https://doi.org/10.13005/BBRA/2113

El-Sehemy IA, Haroun BM, El-Diwany AI, El-Shahed KY, & Tolba IM. (2012). Statistical optimization of curdlan production by local Egyptian agrobacterium isolates. *Al-Azhar Journal of Pharmaceutical Sciences*, *45*(1), 413–424.

Erkan, H. S., Onkal Engin, G., Ince, M., & Bayramoglu, M. R. (2016). Effect of carbon to nitrogen ratio of feed wastewater and sludge retention time on activated sludge in a submerged membrane bioreactor. Environmental Science and Pollution Research, 23(11), 10742–10752. https://doi.org/10.1007/S11356-016-6215-2/TABLES/7

Felz, S., Kleikamp, H., Zlopasa, J., van Loosdrecht, M. C. M., & Lin, Y. (2020). Impact of metal ions on structural EPS hydrogels from aerobic granular sludge. *Biofilm*, *2*, 100011. https://doi.org/10.1016/J.BIOFLM.2019.100011

Ferreira dos Santos, A., Amancio Frutuoso, F. K., de Amorim de Carvalho, C., Sousa Aguiar Lira, V. N., Mendes Barros, A. R., & Bezerra dos Santos, A. (2022). Carbon source affects the resource recovery in aerobic granular sludge systems treating wastewater. *Bioresource Technology*, *357*, 127355. https://doi.org/10.1016/J.BIORTECH.2022.127355

Filho, N. P., Lage, I., Morais, H., Carneiro, L., Silva, F., Silva, C. M., Carlos, J., Dias, T., Canedo Da Silva, C., & Oliveira De Paula, S. (2019). Production of Extracellular Polymeric Substances by Isolate Consortia Obtained from Mesophilic Aerobic Granules from the Treatment of Paper Mill Effluent. *BioResources*, *14*(3), 5845–5861. https://jtatm.textiles.ncsu.edu/index.php/BioRes/article/view/BioRes_14_3_5845_Filho_Extracellular_Polymeric_Substances

Franca, R. D. G., Pinheiro, H. M., van Loosdrecht, M. C. M., & Lourenço, N. D. (2018). Stability of aerobic granules during long-term bioreactor operation. *Biotechnology Advances*, *36*(1), 228–246. https://doi.org/10.1016/J.BIOTECHADV.2017.11.005

Fujii, R., Iwamoto, H., & Nagata, Y. (2024). A new method to deal with missing data using Taguchi's T-method. *Total Quality Science*, 10(2). https://doi.org/10.17929/tqs.10.44

Gan, C., Cheng, Q., Chen, R., Chen, X., Chen, Y., Wu, Y., Li, C., Xu, S., & Chen, Y. (2024). Rapid Formation and Performance of Aerobic Granular Sludge Driven by a Sodium Alginate Nucleus under Different Organic Loading Rates and C/N Ratios. *Water 2024, Vol. 16, Page 1336*, *16*(10), 1336. https://doi.org/10.3390/W16101336

Ganie, S. A., Rather, L. J., & Li, Q. (2021). Review on Anti-cancer and Anti-microbial Applications of Curdlan Biomaterials. *Journal of Polymers and the Environment 2021 30:4*, *30*(4), 1284–1299. https://doi.org/10.1007/S10924-021-02299-9

Gao, M. J., Liu, L. P., Li, S., Lyu, J. L., Jiang, Y., Zhu, L., Zhan, X. B., & Zheng, Z. Y. (2020). Multi-stage glucose/pachymaran co-feeding enhanced endo-β-1,3-glucanase production by Trichoderma harzianum via simultaneous increases in cell concentration and inductive effect. *Bioprocess and Biosystems Engineering*, *43*(8), 1479–1486. https://doi.org/10.1007/S00449-020-02341-5

Gao, M., Yang, G., Li, F., Wang, Z., Hu, X., Jiang, Y., Yan, J., Li, Z., & Zhan, X. (2021). Efficient endo-β-1,3-glucanase expression in Pichia pastoris for co-culture with Agrobacterium sp. for direct curdlan oligosaccharide production. *International Journal of Biological Macromolecules*, *182*, 1611–1617. https://doi.org/10.1016/J.IJBIOMAC.2021.05.142

Geissdoerfer, M., Savaget, P., Bocken, N. M. P., & Hultink, E. J. (2017). The Circular Economy – A new sustainability paradigm? *Journal of Cleaner Production*, *143*, 757–768. https://doi.org/10.1016/J.JCLEPRO.2016.12.048

Ghisellini, P., Cialani, C., & Ulgiati, S. (2016). A review on circular economy: the expected transition to a balanced interplay of environmental and economic systems. *Journal of Cleaner Production*, *114*, 11–32. https://doi.org/10.1016/J.JCLEPRO.2015.09.007

Global Curdlan Market Insights, Forecast to 2030. (n.d.). Retrieved November 5, 2024, from https://www.qyresearch.com/reports/2720723/curdlan

Hamza, R., Rabii, A., Ezzahraoui, F. zahra, Morgan, G., & Iorhemen, O. T. (2022). A review of the state of development of aerobic granular sludge technology over the last 20 years: Full-

scale applications and resource recovery. *Case Studies in Chemical and Environmental Engineering*, *5*, 100173. https://doi.org/10.1016/J.CSCEE.2021.100173

Harada, T., Misaki, A., & Saito, H. (1968). Curdlan: a bacterial gel-forming -1, 3-glucan. Archives of Biochemistry and Biophysics, 124, 292–298.

Harrison, J., Akers, R., Allan, S., -, al, Wang, X., Sakakura, M., Miura, K., Tia, M., & Garcia, G. (2023). Curdlan Gum, Properties, Benefits and Applications. *IOP Conference Series: Earth and Environmental Science*, *1158*(11), 112011. https://doi.org/10.1088/1755-1315/1158/11/112011

Hisam, M. W., Dar, A. A., Elrasheed, M. O., Khan, M. S., Gera, R., & Azad, I. (2024). The Versatility of the Taguchi Method: Optimizing Experiments Across Diverse Disciplines. *Journal of Statistical Theory and Applications*, 23(4), 365–389. https://doi.org/10.1007/S44199-024-00093-9/FIGURES/4

Hussain, A., Zia, K. M., Tabasum, S., Noreen, A., Ali, M., Iqbal, R., & Zuber, M. (2017). Blends and composites of exopolysaccharides; properties and applications: A review. *International Journal of Biological Macromolecules*, *94*, 10–27. https://doi.org/10.1016/J.IJBIOMAC.2016.09.104

Iorhemen, O. T., & Ukaigwe, S. (2023). Biorefinery Paradigm in Wastewater Management: Opportunities for Resource Recovery from Aerobic Granular Sludge Systems. *Lecture Notes in Civil Engineering*, *363 LNCE*, 1319–1334. https://doi.org/10.1007/978-3-031-34593-7_84

Iorhemen, O. T., Ukaigwe, S., Dang, H., & Liu, Y. (2022). Phosphorus Removal from Aerobic Granular Sludge: Proliferation of Polyphosphate-Accumulating Organisms (PAOs) under Different Feeding Strategies. *Processes 2022, Vol. 10, Page 1399*, *10*(7), 1399. https://doi.org/10.3390/PR10071399

Iorhemen, O. T., Zaghloul, M. S., Hamza, R. A., & Tay, J. H. (2020). Long-term aerobic granular sludge stability through anaerobic slow feeding, fixed feast-famine period ratio, and fixed SRT. *Journal of Environmental Chemical Engineering*, *8*(2), 103681. https://doi.org/10.1016/J.JECE.2020.103681

Ji SL, Li JT, Qin ZP, Liu ZP, Cui DH (2011) Bacteria composition of aerobic granular sludge under filamentous bulking and control method of filamentous bulking. *J Beijing Univ Technol* 37:1530–1535

Jia, X., Wang, C., Du, X., Peng, H., Liu, L., Xiao, Y., & He, C. (2021). Specific hydrolysis of curdlan with a novel glycoside hydrolase family 128 β-1,3-endoglucanase containing a carbohydrate-binding module. *Carbohydrate Polymers*, *253*, 117276. https://doi.org/10.1016/J.CARBPOL.2020.117276

Jiang, L. (2013). Effect of nitrogen source on curdlan production by Alcaligenes faecalis ATCC 31749. *International Journal of Biological Macromolecules*, *52*(1), 218–220. https://doi.org/10.1016/J.IJBIOMAC.2012.10.010

Jin, L. H., Um, H. J., Yin, C. J., Kim, Y. H., & Lee, J. H. (2008). Proteomic analysis of curdlan-producing Agrobacterium sp. in response to pH downshift. *Journal of Biotechnology*, *138*(3–4), 80–87. https://doi.org/10.1016/J.JBIOTEC.2008.08.010

Jindal, N., & Singh Khattar, J. (2018). Microbial Polysaccharides in Food Industry. *Biopolymers for Food Design*, 95–123. https://doi.org/10.1016/B978-0-12-811449-0.00004-9

Kalhori, E. M., Ghahramani, E., Al-Musawi, T. J., Saleh, H. N., Sepehr, M. N., & Zarrabi, M. (2018). Effective reduction of metronidazole over the cryptomelane-type manganese oxide octahedral molecular sieve (K-OMS-2) catalyst: facile synthesis, experimental design and modeling, statistical analysis, and identification of by-products. *Environmental Science and*

Pollution Research, *25*(34), 34164–34180. https://doi.org/10.1007/S11356-018-3352-9/FIGURES/11

Kalyanasundaram, G. T., Doble, M., & Gummadi, S. N. (2012). Production and downstream processing of (1→3)-β- D-glucan from mutant strain of Agrobacterium sp. ATCC 31750. *AMB Express*, *2*(1), 1–10. https://doi.org/10.1186/2191-0855-2-31/FIGURES/6

Karakas, I., Sam, S. B., Cetin, E., Dulekgurgen, E., & Yilmaz, G. (2020). Resource recovery from an aerobic granular sludge process treating domestic wastewater. *Journal of Water Process Engineering*, *34*, 101148. https://doi.org/10.1016/J.JWPE.2020.101148

Karnezis, T., Epa, V. C., Stone, B. A., & Stanisich, V. A. (2003). Topological characterization of an inner membrane (1→3)-β-D-glucan (curdlan) synthase from Agrobacterium sp. strain ATCC31749. *Glycobiology*, *13*(10), 693–706. https://doi.org/10.1093/GLYCOB/CWG093

Kehrein, P., Van Loosdrecht, M., Osseweijer, P., & Posada, J. (2020). Exploring resource recovery potentials for the aerobic granular sludge process by mass and energy balances – energy, biopolymer and phosphorous recovery from municipal wastewater. *Environmental Science: Water Research & Technology*, *6*(8), 2164–2179. https://doi.org/10.1039/D0EW00310G

Kim, H., Kim, J., & Ahn, D. (2021). Effects of carbon to nitrogen ratio on the performance and stability of aerobic granular sludge. *Environmental Engineering Research*, *26*(1), 1–8. https://doi.org/10.4491/EER.2019.284

Kim, M. K., Ryu, K. E., Choi, W. A., Rhee, Y. H., & Lee, I. Y. (2003). Enhanced production of (1,3)--d-glucan by a mutant strain of Agrobacterium species. *Biochemical Engineering Journal*, 16, 163–168

Kupcewicz, B., Ronowicz, J., Balcerowska-Czerniak, G., Walasek, A., & Budzisz, E. (2013). Evaluation of impurities in simvastatin drug products with the use of FT-IR spectroscopy and

selected chemometric techniques. *Central European Journal of Chemistry*, *11*(8), 1320–1329. https://doi.org/10.2478/S11532-013-0264-X/METRICS

Laxmi, V.M., Latha, D., and Jayasree, A. S. (2018). Production and characterization of curdlan from *agrobacterium sp*. *IJPSR*; Vol. 9(11): 4871-4874.

Lee, J. H., Lee, I. Y., Kim, M. K., & Park, Y. H. (1999). Optimal pH control of batch processes for production of curdlan by Agrobacterium species. *Journal of Industrial Microbiology and Biotechnology*, 23(2), 143–148. https://doi.org/10.1038/SJ.JIM.2900714

Liang, Y., Qu, Z., Liu, M., Zhu, M., Zhang, X., Wang, L., Jia, F., Zhan, X., & Wang, J. (2021). Further interpretation of the strengthening effect of curdlan on frozen cooked noodles quality during frozen storage: Studies on water state and properties. *Food Chemistry*, *346*, 128908. https://doi.org/10.1016/J.FOODCHEM.2020.128908

Liang, Y., Zhu, L., Ding, H., Gao, M., Zheng, Z., Wu, J., & Zhan, X. (2017). Enhanced production of curdlan by coupled fermentation system of Agrobacterium sp. ATCC 31749 and Trichoderma harzianum GIM 3.442. *Carbohydrate Polymers*, *157*, 1687–1694. https://doi.org/10.1016/J.CARBPOL.2016.11.055

Liang, Z., Li, W., Yang, S., & Du, P. (2010). Extraction and structural characteristics of extracellular polymeric substances (EPS), pellets in autotrophic nitrifying biofilm and activated sludge. *Chemosphere*, *81*(5), 626–632. https://doi.org/10.1016/J.CHEMOSPHERE.2010.03.043

Lu, Y. Z., Wang, H. F., Kotsopoulos, T. A., & Zeng, R. J. (2016). Advanced phosphorus recovery using a novel SBR system with granular sludge in simultaneous nitrification, denitrification and phosphorus removal process. *Applied Microbiology and Biotechnology*, *100*(10), 4367–4374. https://doi.org/10.1007/S00253-015-7249-Y/TABLES/2

Liu, Y. Q. (2024). Environmental Protection through Aerobic Granular Sludge Process. *Processes 2024, Vol. 12, Page 243*, *12*(2), 243. https://doi.org/10.3390/PR12020243

Liu, Z., Zhang, D., Yang, R., Wang, J., Duan, Y., Gao, M., Wang, J., Zhang, A., & liu, yongjun. (2023). Investigation of Increasing Organic Loading Rate in the Aerobic Sludge Granulation: Performance, Extracellular Polymeric Substances and Microbial Community Behaviors. https://doi.org/10.2139/SSRN.4563336

Mangolim, C. S., Silva, T. T. Da, Fenelon, V. C., Koga, L. N., De Ferreira, S. B. S., Bruschi, M. L., & Matioli, G. (2017). Description of recovery method used for curdlan produced by Agrobacterium sp. IFO 13140 and its relation to the morphology and physicochemical and technological properties of the polysaccharide. *PLOS ONE*, 12(2), e0171469. https://doi.org/10.1371/JOURNAL.PONE.0171469

Martí, N., Barat, R., Seco, A., Pastor, L., & Bouzas, A. (2017). Sludge management modeling to enhance P-recovery as struvite in wastewater treatment plants. *Journal of Environmental Management*, *196*, 340–346. https://doi.org/10.1016/J.JENVMAN.2016.12.074

Margot, J., Lochmatter, S., Barry, D. A., & Holliger, C. (2016). Role of ammonia-oxidizing bacteria in micropollutant removal from wastewater with aerobic granular sludge. *Water Science and Technology*, *73*(3), 564–575. https://doi.org/10.2166/WST.2015.514

Martinez, C. O., Ruiz, S. P., Nogueira, M. T., Bona, E., Portilho, M., & Matioli, G. (2015). Effective immobilization of Agrobacterium sp. IFO 13140 cells in loofa sponge for curdlan biosynthesis. *Molecules*, 20, 7957–7973.

McIntosh, M., Stone, B. A., & Stanisich, V. A. (2005). Curdlan and other bacterial (1→3)-beta-D-glucans. *Applied Microbiology and Biotechnology*, 68, 163–173.

Mehta, K., Shukla, A., & Saraf, M. (2017). Articulating the exuberant intricacies of bacterial exopolysaccharides to purge environmental pollutants. *Heliyon*, e08446. https://doi.org/10.1016/j.heliyon.2021.e08446

Mishra, U. K., Chandel, V. S., Yadav, A. K., Gautam, A. K., Anand, A. D., Varun, J., Rai, A. K., & Singh, S. P. (2024). Synthesis, characterization, and study of photocatalytic degradation of aniline blue dye using copper oxide nanoparticles prepared by Santa Maria feverfew leaf extract. *Nanotechnology for Environmental Engineering*, *9*(3), 473–482. https://doi.org/10.1007/S41204-024-00378-5/FIGURES/10

Mohsin, A., Sun, J., Khan, I. M., Hang, H., Tariq, M., Tian, X., Ahmed, W., Niazi, S., Zhuang, Y., Chu, J., Mohsin, M. Z., Salim-ur-Rehman, & Guo, M. (2019). Sustainable biosynthesis of curdlan from orange waste by using Alcaligenes faecalis: A systematically modeled approach. *Carbohydrate Polymers*, *205*, 626–635. https://doi.org/10.1016/J.CARBPOL.2018.10.047

More, T. T., Yadav, J. S. S., Yan, S., Tyagi, R. D., & Surampalli, R. Y. (2014). Extracellular polymeric substances of bacteria and their potential environmental applications. *Journal of Environmental Management*, 144, 1–25.

Nancharaiah, Y. V., & Kiran Kumar Reddy, G. (2018). Aerobic granular sludge technology: Mechanisms of granulation and biotechnological applications. *Bioresource Technology*, *247*, 1128–1143. https://doi.org/10.1016/J.BIORTECH.2017.09.131

Nakanishi, I., Kimura, K., Suzuki, T., Ishikawa, M., Banno, I., Sakane, T., & Harada, T. (1976). Demonstration of curdlan-type polysaccharide and some other β-1, 3-glucan in microorganisms with aniline blue. *The Journal of General and Applied Microbiology*, 22(1), 1–11. https://doi.org/10.2323/JGAM.22.1

Naseem, M., & Kumar, C. (2017). QSLB: Queue size based single path load balancing routing protocol for MANETs. *International Journal of Ad Hoc and Ubiquitous Computing*, *24*(1–2), 90–100. https://doi.org/10.1504/IJAHUC.2017.080918

Neczaj, E., & Grosser, A. (2018). Circular Economy in Wastewater Treatment Plant–Challenges and Barriers. *Proceedings 2018, Vol. 2, Page 614*, *2*(11), 614. https://doi.org/10.3390/PROCEEDINGS2110614

Nishinari, K., & Zhang, H. (2004). Recent advances in the understanding of heat set gelling polysaccharides. *Trends in Food Science & Technology*, *15*(6), 305–312. https://doi.org/10.1016/J.TIFS.2003.05.001

Niu, X., Han, X., Jin, Y., Yue, J., Zhu, J., Xie, W., & Yu, J. (2023). Aerobic granular sludge treating hypersaline wastewater: Impact of pH on granulation and long-term operation at different organic loading rates. *Journal of Environmental Management*, *330*, 117164. https://doi.org/10.1016/J.JENVMAN.2022.117164

Pan, L., Chen, X. S., Wang, K. F., & Mao, Z. G. (2020). Mechanisms of response to pH shock in microbial fermentation. *Bioprocess and Biosystems Engineering*, *43*(3), 361–372. https://doi.org/10.1007/S00449-019-02232-4/FIGURES/5

Peng, J., Zhao, L., Wang, Q., Song, W., Wang, Z., Li, J., Zhang, X., Yuan, F., Chen, S., Peng, J., Zhao, L., Wang, Q., Song, W., Wang, Z., Li, J., Zhang, X., and Yuan, F. (2022). Enhancing the Stability of Aerobic Granular Sludge Process Treating Municipal Wastewater by Adjusting Organic Loading Rate and Dissolved Oxygen Concentration. Separations 2022, Vol. 9, Page 228, 9(8), 228.

Pourali, P., Fazlzadeh, M., Aaligadri, M., Dargahi, A., Poureshgh, Y., & Kakavandi, B. (2022). Enhanced three-dimensional electrochemical process using magnetic recoverable of

Fe3O4@GAC towards furfural degradation and mineralization. *Arabian Journal of Chemistry*, *15*(8), 103980. https://doi.org/10.1016/J.ARABJC.2022.103980

Prakash, S., Rajeswari, K., Divya, P., Ferlin, M., Rajeshwari, C. T., & Vanavil, B. (2018). Optimization and production of curdlan gum using Bacillus cereus PR3 isolated from rhizosphere of leguminous plant. *Preparative Biochemistry & Biotechnology*, *48*(5), 408–418. https://doi.org/10.1080/10826068.2018.1451886

Purba, L. D. A., Ibiyeye, H. T., Yuzir, A., Mohamad, S. E., Iwamoto, K., Zamyadi, A., & Abdullah, N. (2020). Various applications of aerobic granular sludge: A review. *Environmental Technology & Innovation*, *20*, 101045. https://doi.org/10.1016/J.ETI.2020.101045

Rafigh, S. M., Yazdi, A. V., Vossoughi, M., Safekordi, A. A., & Ardjmand, M. (2014). Optimization of culture medium and modeling of curdlan production from Paenibacillus polymyxa by RSM and ANN. *International Journal of Biological Macromolecules*, *70*, 463–473. https://doi.org/10.1016/J.IJBIOMAC.2014.07.034

Rakić , T.; Kasagić -Vujanović , I.; Jovanović , M.; Jančˇ ić -Stojanović , B.; Ivanović , D. Comparison of Full Factorial Design,Central Composite Design, and Box-Behnken Design in Chromato-graphic Method Development for the Determination of Fluconazoleand Its Impurities. *Anal. Lett*. 2014, 47, 1334−1347.

Rofeal, M., Abdelmalek, F., Pietrasik, J., & Steinbüchel, A. (2023). Sustainable curdlan biosynthesis by Rahnella variigena ICRI91 via alkaline hydrolysis of Musa sapientum peels and its edible, active and modified hydrogel for Quercetin controlled release. *International Journal of Biological Macromolecules*, *225*, 416–429. https://doi.org/10.1016/J.IJBIOMAC.2022.11.080

Rosa-Masegosa, A., Muñoz-Palazon, B., Gonzalez-Martinez, A., Fenice, M., Gorrasi, S., & Gonzalez-Lopez, J. (2021). New Advances in Aerobic Granular Sludge Technology Using Continuous Flow Reactors: Engineering and Microbiological Aspects. *Water 2021, Vol. 13, Page 1792*, *13*(13), 1792. https://doi.org/10.3390/W13131792

Rosman, N. H., Nor Anuar, A., Chelliapan, S., Md Din, M. F., & Ujang, Z. (2014). Characteristics and performance of aerobic granular sludge treating rubber wastewater at different hydraulic retention time. *Bioresource Technology*, *161*, 155–161. https://doi.org/10.1016/J.BIORTECH.2014.03.047

Salah, R., Jaouadi, B., Bouaziz, A., Chaari, K., Blecker, C., Derrouane, C., Attia, H., & Besbes, S. (2011). Fermentation of date palm juice by curdlan gum production from Rhizobium radiobacter ATCC 6466^{TM}: Purification, rheological and physico-chemical characterization. *LWT - Food Science and Technology*, *44*(4), 1026–1034.

Saudagar, P. S., & Singhal, R. S. (2004). Fermentative production of curdlan. *Applied Biochemistry and Biotechnology - Part A Enzyme Engineering and Biotechnology*, *118*(1–3), 21–31. https://doi.org/10.1385/ABAB:118:1-3:021/METRICS

Seid-Mohammadi, A., Ghorbanian, Z., Asgari, G., & Dargahi, A. (2019). Degradation of CEX antibiotic from aqueous environment by US/S2O82–/NiO process: optimization using Taguchi method and kinetic studies. *Desalination and Water Treatment*, *171*, 444–455. https://doi.org/10.5004/DWT.2019.24777

Sepúlveda-Mardones, M., Campos, J. L., Magrí, A., & Vidal, G. (2019). Moving forward in the use of aerobic granular sludge for municipal wastewater treatment: an overview. *Reviews in Environmental Science and Bio/Technology 2019 18:4*, *18*(4), 741–769. https://doi.org/10.1007/S11157-019-09518-9

Setianingsih, N. I., Hadiyanto, Sudarno, Yuliasni, R., Setianingsih, N. I., Hadiyanto, Sudarno, & Yuliasni, R. (2019). Performance of Aerobic Microbial Granules in Organic Carbon Removal as a Method in the Treatment of Biodegradable Wastewater. *E3SWC*, *125*, 03014. https://doi.org/10.1051/E3SCONF/201912503014

Shih, I. L., Yu, J. Y., Hsieh, C., & Wu, J. Y. (2009). Production and characterization of curdlan by Agrobacterium sp. *Biochemical Engineering Journal*, *43*(1), 33–40. https://doi.org/10.1016/J.BEJ.2008.08.006

Shoda, M., & Ishikawa, Y. (2014). Heterotrophic nitrification and aerobic denitrification of high-strength ammonium in anaerobically digested sludge by Alcaligenes faecalis strain No. 4. *Journal of Bioscience and Bioengineering*, *117*(6), 737–741. https://doi.org/10.1016/J.JBIOSC.2013.11.018

Siddique, I. (2024). Exploring Functional Groups and Molecular Structures: A Comprehensive Analysis using FTIR Spectroscopy. Chemistry Research Journal, 2024(2), 70–76. https://doi.org/10.5281/zenodo.11281698

Sniatala, B., Kurniawan, T. A., Sobotka, D., Makinia, J., & Othman, M. H. D. (2023). Macro-nutrients recovery from liquid waste as a sustainable resource for production of recovered mineral fertilizer: Uncovering alternative options to sustain global food security cost-effectively. *Science of The Total Environment*, *856*, 159283. https://doi.org/10.1016/J.SCITOTENV.2022.159283

Spinosa, L., Ayol, A., Baudez, J. C., Canziani, R., Jenicek, P., Leonard, A., Rulkens, W., Xu, G., & van Dijk, L. (2011). Sustainable and Innovative Solutions for Sewage Sludge Management. *Water 2011, Vol. 3, Pages 702-717*, *3*(2), 702–717. https://doi.org/10.3390/W3020702

Standard Methods for the Examination of Water and Wastewater, 24th Edition. Published by the American Public Health Association (APHA), American Water Works Association (AWWA), and Water Environment Federation (WEF). ISBN: 978-0-87553-299-8

Stasinopoulos, S. J., Fisher, P. R., Stone, B. A., & Stanisich, V. A. (1999). Detection of two loci involved in (1→3)-β-glucan (curdlan) biosynthesis by Agrobacterium sp. ATCC31749, and comparative sequence analysis of the putative curdlan synthase gene. *Glycobiology*, *9*(1), 31–41. https://doi.org/10.1093/GLYCOB/9.1.31

Su, L., Li, Y., Chao, L., Li, Q., & Hu, Z. (2023). Enhanced Simultaneous Nitrogen and Phosphorus Removal Performance of the AGS-SBR Reactor Based on the Effects of the C/N Ratio and Microbial Community Change. *Sustainability 2023, Vol. 15, Page 7691*, *15*(9), 7691. https://doi.org/10.3390/SU15097691

Sun, S., Chen, Z., Wang, X., Wang, S., Liu, L., Yan, P., Chen, Y., Fang, F., & Guo, J. (2024). Effect of different feeding strategies on performance of aerobic granular sludge: From perspective of extracellular polymeric substances and microorganisms. Journal of Environmental Chemical Engineering, 12(1), 111688. https://doi.org/10.1016/J.JECE.2023.111688

Świątczak, P., & Cydzik-Kwiatkowska, A. (2018). Performance and microbial characteristics of biomass in a full-scale aerobic granular sludge wastewater treatment plant. *Environmental Science and Pollution Research*, *25*(2), 1655–1669. https://doi.org/10.1007/S11356-017-0615-9/FIGURES/6

Tang, R., Hao, J., Zong, R., Wu, F., Zeng, Y., & Zhang, Z. (2018). Oxidation pattern of curdlan with TEMPO-mediated system. *Carbohydrate Polymers*, *186*, 9–16. https://doi.org/10.1016/J.CARBPOL.2017.12.080

Tay, J. H., Tay, S. T. L., Ivanov, V., Pan, S., Jiang, H. L., & Liu, Q. S. (2003). Biomass and porosity profiles in microbial granules used for aerobic wastewater treatment. Letters in *Applied Microbiology*, 36(5), 297–301. https://doi.org/10.1046/J.1472-765X.2003.01312.X

Traina, F., Corsino, S. F., Torregrossa, M., & Viviani, G. (2022). Biopolymer Recovery from Aerobic Granular Sludge and Conventional Flocculent Sludge in Treating Industrial Wastewater: Preliminary Analysis of Different Carbon Routes for Organic Carbon Utilization. *Water 2023, Vol. 15, Page 47*, *15*(1), 47. https://doi.org/10.3390/W15010047

Truong, H. T. B., Bui, H. N., Nguyen, H. T., Pham, T. L., Nguyen, D. N., Perng, Y. S., Lam, L. T. M., Vo, T. D. H., Nguyen, V. T., & Bui, H. M. (2022). A Taguchi approach with electron-beam irradiation to optimize the efficiency of removing enrofloxacin from aqueous media. *Korean Journal of Chemical Engineering*, *39*(4), 973–985. https://doi.org/10.1007/S11814-021-0995-X/METRICS

Tsertou, E., Caluwé, M., Goettert, D., Goossens, K., Suazo, K. S., Vanherck, C., & Dries, J. (2024). Impact of low and high temperatures on aerobic granular sludge treatment of industrial wastewater. *Water Science and Technology*, *89*(3), 548–561. https://doi.org/10.2166/WST.2024.024

van Leeuwen, K., de Vries, E., Koop, S., & Roest, K. (2018). The Energy & Raw Materials Factory: Role and Potential Contribution to the Circular Economy of the Netherlands. *Environmental Management*, *61*(5), 786–795. https://doi.org/10.1007/S00267-018-0995-8/FIGURES/2

Vandana, Priyadarshanee, M., & Das, S. (2023). Bacterial extracellular polymeric substances: Biosynthesis and interaction with environmental pollutants. *Chemosphere*, *332*, 138876. https://doi.org/10.1016/J.CHEMOSPHERE.2023.138876

Venkatachalam, G., Arumugam, S., & Doble, M. (2020). Industrial production and applications of α/β linear and branched glucans. *Https://Doi.Org/10.1080/00194506.2020.1798820*, *63*(5), 533–547.

Verma, D. K., Niamah, A. K., Patel, A. R., Thakur, M., Singh Sandhu, K., Chávez-González, M. L., Shah, N., & Noe Aguilar, C. (2020). Chemistry and microbial sources of curdlan with potential application and safety regulations as prebiotic in food and health. *Food Research International*, *133*, 109136. https://doi.org/10.1016/J.FOODRES.2020.109136

Vicente, V. E., de Sousa Rollemberg, S. L., & Bezerra dos Santos, A. (2021). Impact of feeding strategy on the performance and operational stability of aerobic granular sludge treating high-strength ammonium concentrations. *Journal of Water Process Engineering*, 44, 102378. https://doi.org/10.1016/J.JWPE.2021.102378

Wan, J., Shao, Z., Jiang, D., Gao, H., & Yang, X. (2022). Curdlan production from cassava starch hydrolysates by Agrobacterium sp. DH-2. *Bioprocess and Biosystems Engineering*, *45*(5), 969–979. https://doi.org/10.1007/S00449-022-02718-8/FIGURES/8

Wang, G., Fang, F., Huang, X., Yang, F., Sun, S., Yan, P., Chen, Y.-P., & Guo, J. (2023). The Effect of Food-to-Microoriganisms On Aerobic Granular Sludge Settleability: Microbial Community, Potential Roles And Sequential Responses of Extracellular Proteins and Polysaccharides. https://doi.org/10.2139/SSRN.4485862

Wang, X. Y. Z., Dong, J. J., Xu, G. C., Han, R. Z., & Ni, Y. (2016). Enhanced curdlan production with nitrogen feeding during polysaccharide synthesis by Rhizobium radiobacter. *Carbohydrate Polymers*, 150, 385–391. https://doi.org/10.1016/J.CARBPOL.2016.05.036

Weissbrodt, D. G., Lochmatter, S., Ebrahimi, S., Rossi, P., Maillard, J., & Holliger, C. (2012). Bacterial selection during the formation of early-stage aerobic granules in wastewater

treatment systems operated under wash-out dynamics. Frontiers in Microbiology, 3(SEP), 34106. https://doi.org/10.3389/FMICB.2012.00332/BIBTEX

West, T. P. (2015). Effect of nitrogen source concentration on curdlan production by Agrobacterium sp. ATCC 31749 grown on prairie cordgrass hydrolysates. *Http://Dx.Doi.Org/10.1080/10826068.2014.985835*, *46*(1), 85–90.

West, T. P. (2020). Production of the Polysaccharide Curdlan by Agrobacterium species on Processing Coproducts and Plant Lignocellulosic Hydrolysates. *Fermentation 2020, Vol. 6, Page 16*, *6*(1), 16. https://doi.org/10.3390/FERMENTATION6010016

Wood, P. J., & Fulcher, R. G. (1984). Specific interaction of aniline blue with (1 → 3)-β-d-glucan. Carbohydrate Polymers, 4(1), 49–72. https://doi.org/10.1016/0144-8617(84)90044-4

Wu, C., Peng, S., Wen, C., Wang, X., Fan, L., Deng, R., & Pang, J. (2012). Structural characterization and properties of konjac glucomannan/curdlan blend films. *Carbohydrate Polymers*, *89*(2), 497–503. https://doi.org/10.1016/J.CARBPOL.2012.03.034

Wu, J., Zhan, X., Liu, H., & Zheng, Z. (2008). Enhanced Production of Curdlan by Alcaligenes faecalis by Selective Feeding with Ammonia Water during the Cell Growth Phase of Fermentation. *Chinese Journal of Biotechnology*, *24*(6), 1035–1039. https://doi.org/10.1016/S1872-2075(08)60049-7

Xia, J., Ye, L., Ren, H., & Zhang, X. X. (2018). Microbial community structure and function in aerobic granular sludge. *Applied Microbiology and Biotechnology 2018 102:9*, *102*(9), 3967–3979. https://doi.org/10.1007/S00253-018-8905-9

Yang, H., Li, W., Chen, S., Guo, X., Huang, F., & Zhu, P. (2021). Optimization and Modeling of Curdlan Production under Multi-physiological-parameters Process Control by Agrobacterium

radiobacter Mutant A-15 at High Initial Glucose. *Biotechnology and Bioprocess Engineering*, *26*(6), 1012–1022. https://doi.org/10.1007/S12257-021-0028-Y/METRICS

Yang, M., Zhu, Y., Li, Y., Bao, J., Fan, X., Qu, Y., Wang, Y., Hu, Z., & Li, Q. (2016). Production and optimization of curdlan produced by Pseudomonas sp. QL212. *International Journal of Biological Macromolecules*, *89*, 25–34.

Yu, L., Wu, J., Liu, J., Zhan, X., Zheng, Z., & Lin, C. C. (2011). Enhanced curdlan production in Agrobacterium sp. ATCC 31749 by addition of low-polyphosphates. *Biotechnology and Bioprocess Engineering*, *16*(1), 34–41.

Yu, T., Wang, Y., Wang, W., Zhang, Y., Zhang, Y., Han, H., Liu, Y., Zhou, S., & Dong, X. (2024). Optimizing Curdlan Synthesis: Engineering Agrobacterium tumefaciens ATCC31749 for Enhanced Production Using Dextrin as a Carbon Source. *Fermentation 2024, Vol. 10, Page 240*, *10*(5), 240. https://doi.org/10.3390/FERMENTATION10050240

Yu, X., Zhang, C., Yang, L., Zhao, L., Lin, C., Liu, Z., & Mao, Z. (2015). CrdR function in a curdlan-producing Agrobacterium sp. ATCC31749 strain. *BMC Microbiology*, *15*(1), 1–10. https://doi.org/10.1186/S12866-015-0356-1/FIGURES/6

Yuan, M., Fu, G., Sun, Y., & Zhang, D. (2021). Biosynthesis and applications of curdlan. *Carbohydrate Polymers*, *273*, 118597. https://doi.org/10.1016/J.CARBPOL.2021.118597

Yu, C., & Wang, K. (2024). Continuous flow aerobic granular sludge: recent developments and applications. *Water Science and Technology*, *89*(5), 1155–1178. https://doi.org/10.2166/WST.2024.055

Zahra, S. A., Abdullah, N., Iwamoto, K., Yuzir, A., & Mohamad, S. E. (2022). Alginate-like exopolysaccharides in aerobic granular sludge: A review. *Materials Today: Proceedings*, *65*, 3046–3053. https://doi.org/10.1016/J.MATPR.2022.04.032

Zeng, P. ;, Liu, Y.-Q. ;, Li, J. ;, Liao, M., Zeng, P., Liu, Y.-Q., Li, J., & Liao, M. (2024). The Aerobic Granules Process for Wastewater Treatment: From Theory to Engineering. Processes 2024, Vol. 12, Page 707, 12(4), 707. https://doi.org/10.3390/PR12040707

Zhai, W., Danjo, T., & Iwata, T. (2017). Synthesis and physical properties of Curdlan branched Ester derivatives. *Journal of Polymer Research*, *24*(11), 1–7. https://doi.org/10.1007/S10965-017-1348-7/METRICS

Zhang, H., & Nishinari, K. (2009). Characterization of the conformation and comparison of shear and extensional properties of curdlan in DMSO. *Food Hydrocolloids*, *23*(6), 1570–1578. https://doi.org/10.1016/J.FOODHYD.2008.11.001

Zhang, H., Nishinari, K., Williams, M. A. K., Foster, T. J., & Norton, I. T. (2002). A molecular description of the gelation mechanism of curdlan. *International Journal of Biological Macromolecules*, *30*(1), 7–16. https://doi.org/10.1016/S0141-8130(01)00187-8

Zhang H-T, Zhan X-B, Zheng Z-Y, Wu J-R, English N, Yu X-B, Lin C-C (2011) Improved curdlan fermentation process based on optimization of dissolved oxygen combined with pH control and metabolic characterization of *Agrobacterium* sp. ATCC 31749. *Appl Microbiol Biotechnol.* doi:10.1007/s00253-011-3448-3

Zhang, H., Zhan, X., Zheng, Z., Wu, J., & Chen, D. (2010). A new strategy for enhancement curdlan biosynthesis in alcaligenes faecalis by activating gene expression. 2010 4th International Conference on Bioinformatics and Biomedical Engineering, ICBBE 2010. https://doi.org/10.1109/ICBBE.2010.5517254

Zhang, W., Gao, H., Huang, Y., Wu, S., Tian, J., Niu, Y., Zou, C., Jia, C., Jin, M., Huang, J., Chang, Z., Yang, X., & Jiang, D. (2020). Glutamine synthetase gene glnA plays a vital role in

curdlan biosynthesis of Agrobacterium sp. CGMCC 11546. *International Journal of Biological Macromolecules*, *165*, 222–230. https://doi.org/10.1016/J.IJBIOMAC.2020.09.152

Zheng, Z. Y., Lee, J. W., Zhan, X. B., Shi, Z., Wang, L., Zhu, L., Wu, J. R., & Lin, C. C. (2007). Effect of metabolic structures and energy requirements on curdlan production by Alcaligenes faecalis. *Biotechnology and Bioprocess Engineering*, *12*(4), 359–365. https://doi.org/10.1007/BF02931057/METRICS

Zhou, J., & Sun, Q. (2020). Performance and microbial characterization of aerobic granular sludge in a sequencing batch reactor performing simultaneous nitrification, denitrification and phosphorus removal with varying C/N ratios. *Bioprocess and Biosystems Engineering*, *43*(4), 663–672. https://doi.org/10.1007/S00449-019-02264-W/FIGURES/7

Zhan, X. B., Lin, C. C., & Zhang, H. T. (2012). Recent advances in curdlan biosynthesis, biotechnological production, and applications. *Applied Microbiology and Biotechnology*, 93(2), 525–531. https://doi.org/10.1007/S00253-011-3740-2/FIGURES/2

Appendices

Appendix A Calibration curve for COD solution

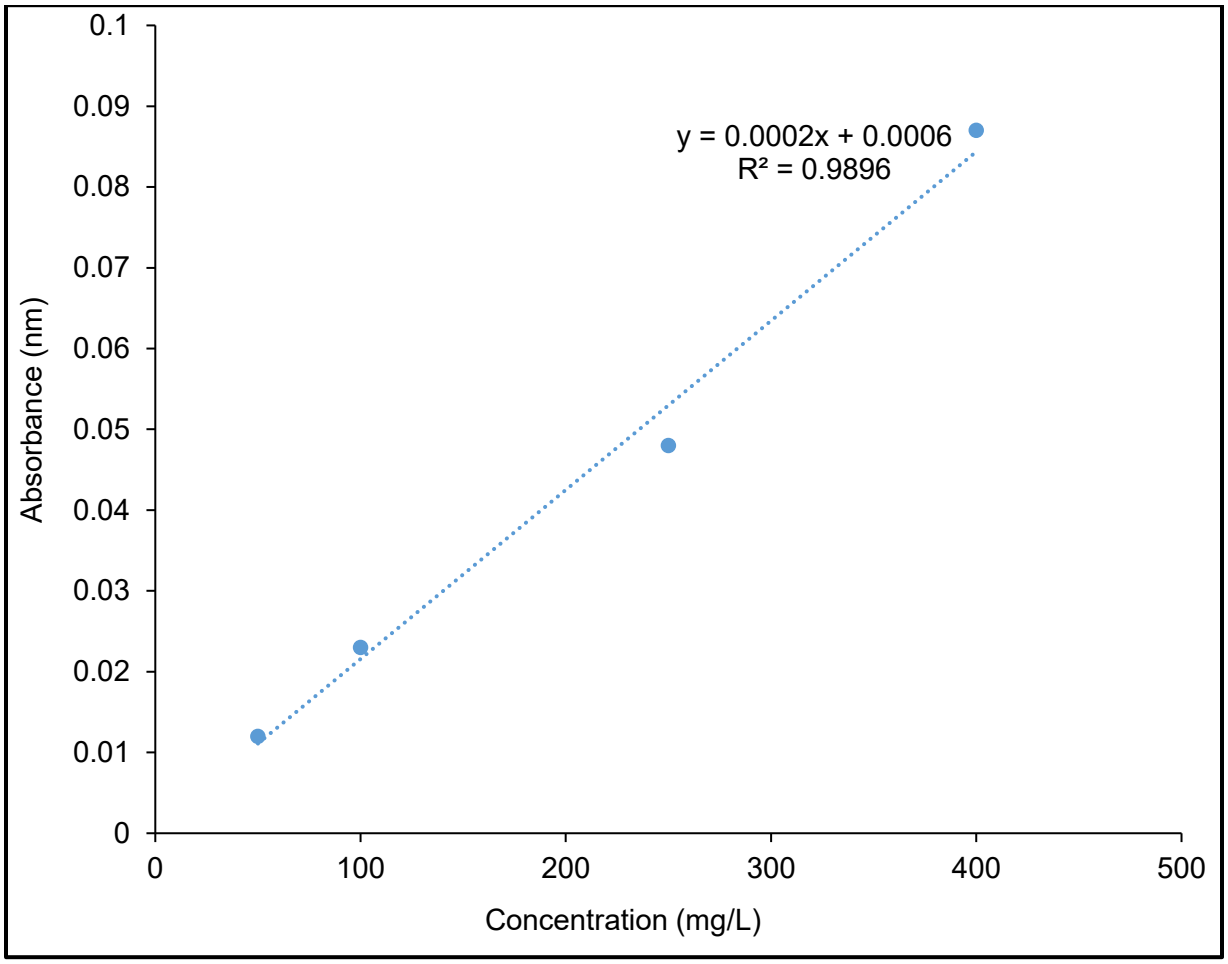

Figure A1: Calibration curve for COD solution

Appendix B Curdlan recovery from AGS system

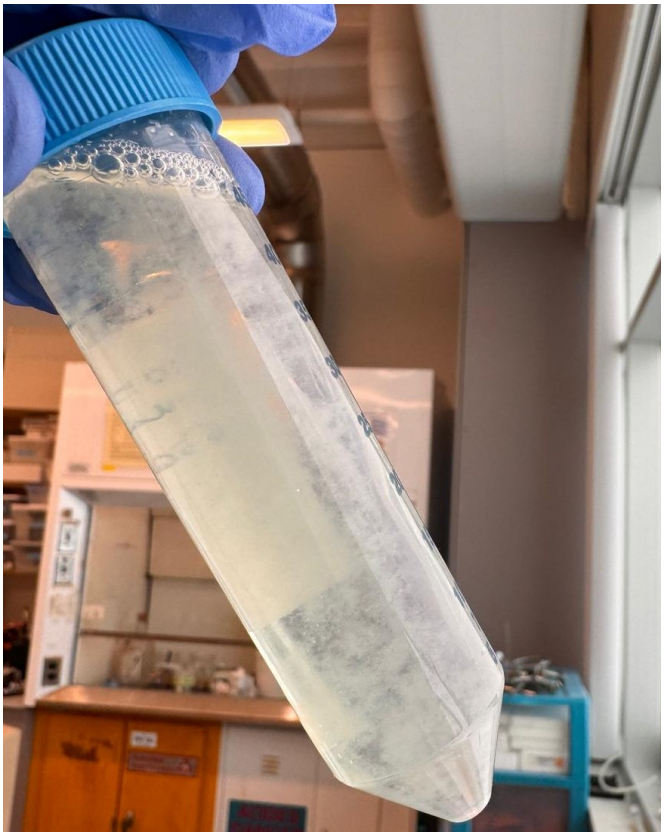

Figure B1. Curdlan gel precipitate at pH of 4.8 in diluted NaOH solution.

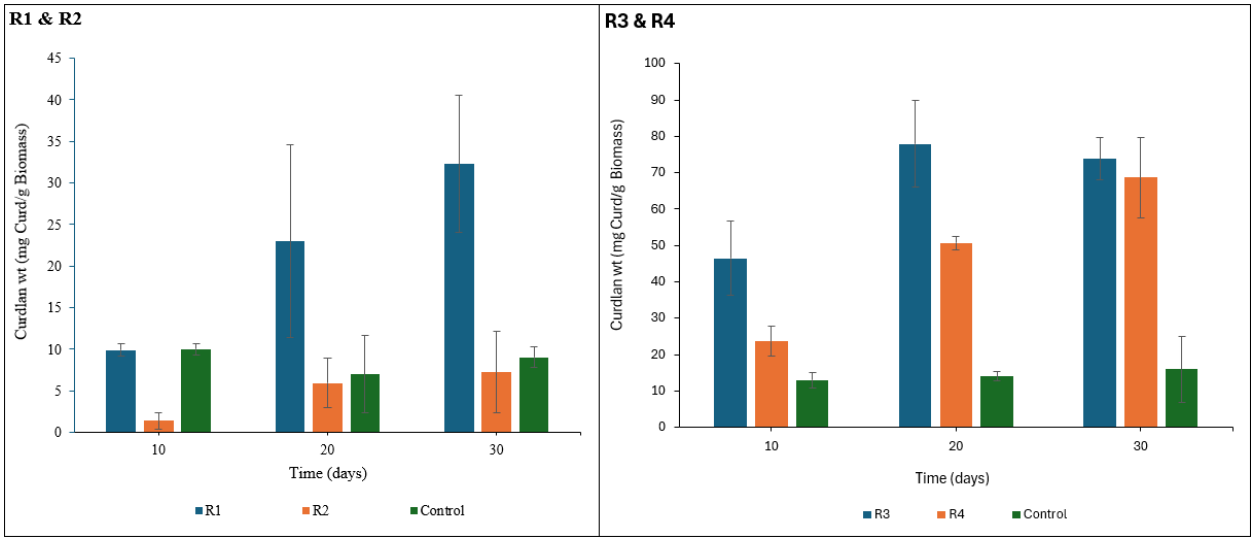

Figure B2: Bar graph of curdlan recovery from R1 - R4 with the respective control

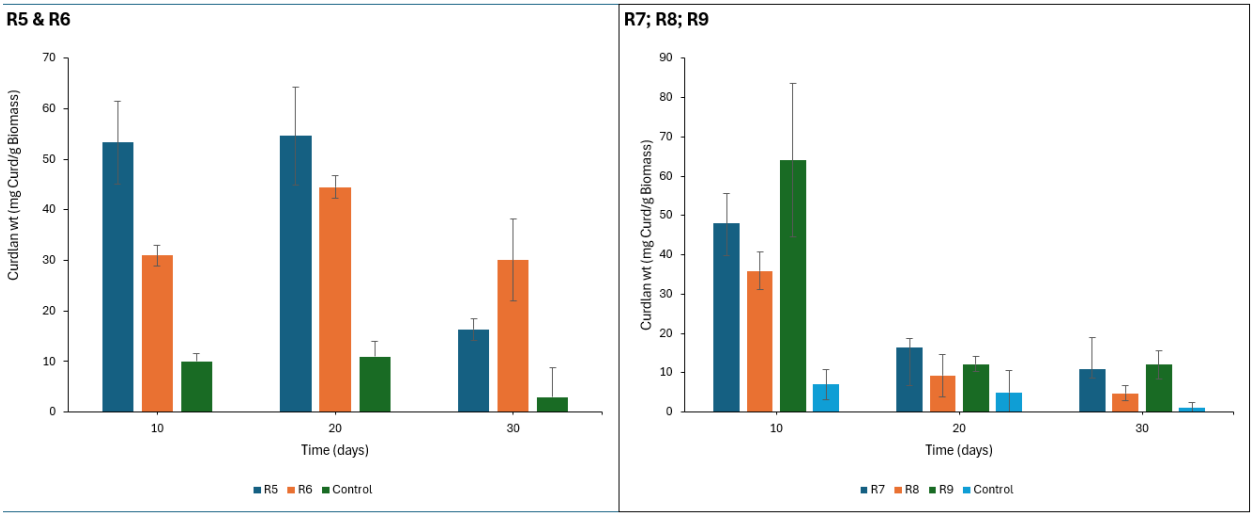

Figure B3: Bar graph of curdlan recovery from R5 – R9 with the respective control

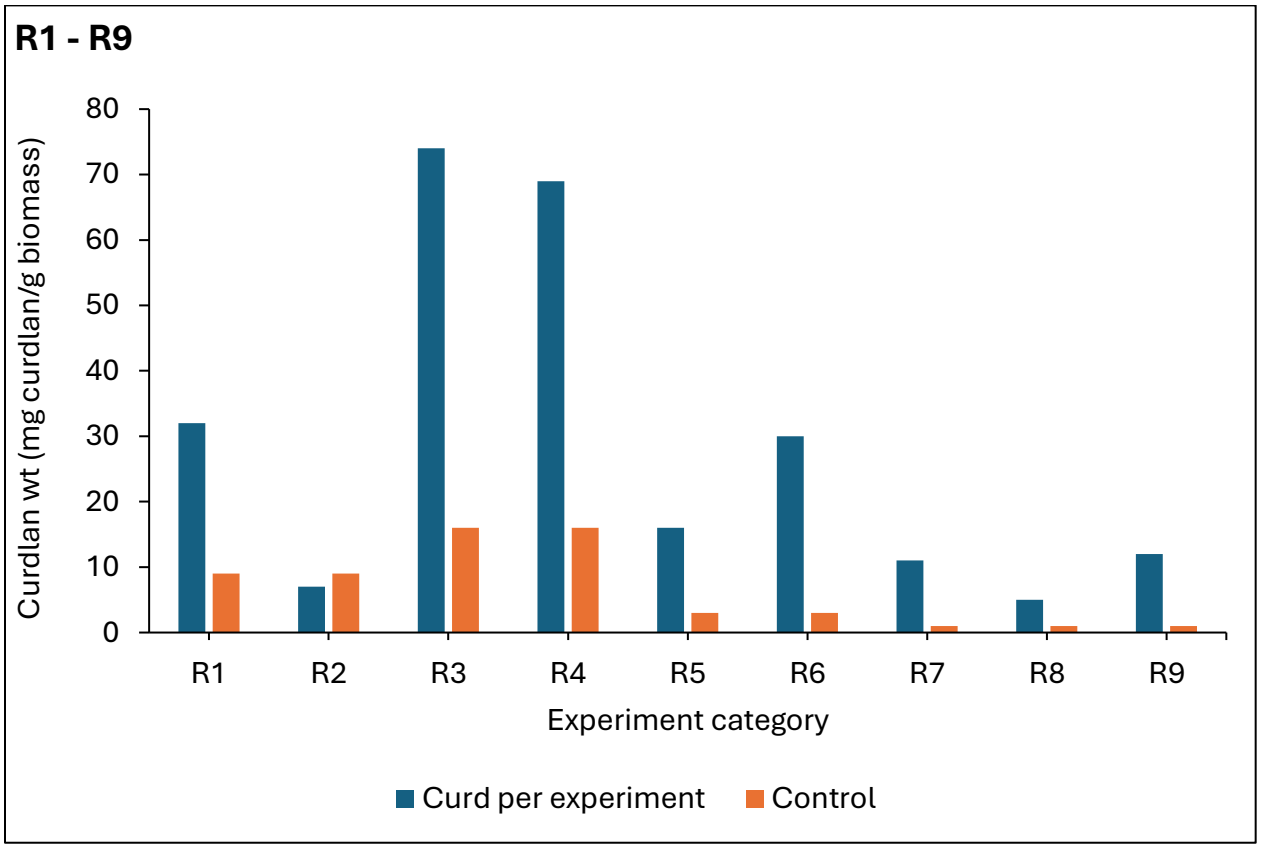

Figure B4: Bar graph of curdlan recovery at day 30 of each experimental run (R1 – R9) with the respective control.

Appendix C Permissions to include published paper and submitted manuscript in the thesis

Figure C1. Review paper journal permission proof

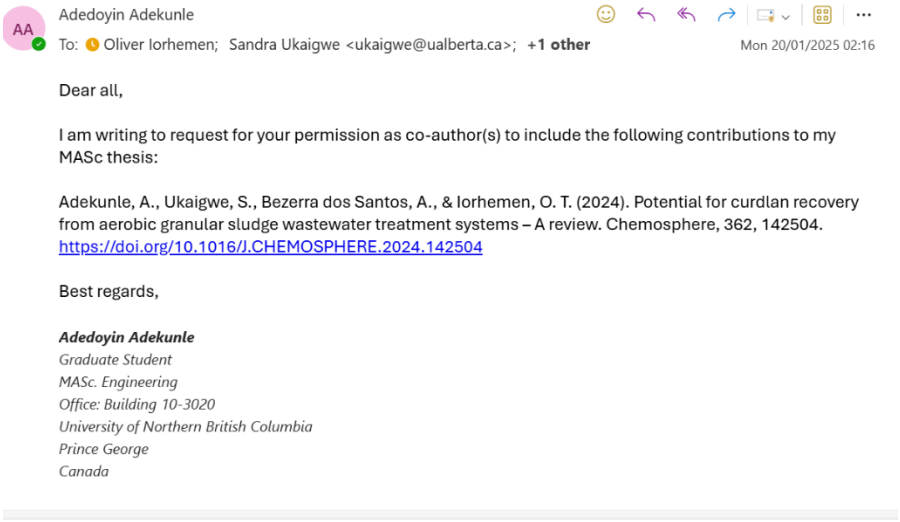

Figure C2. Review paper co-author 1 permission request

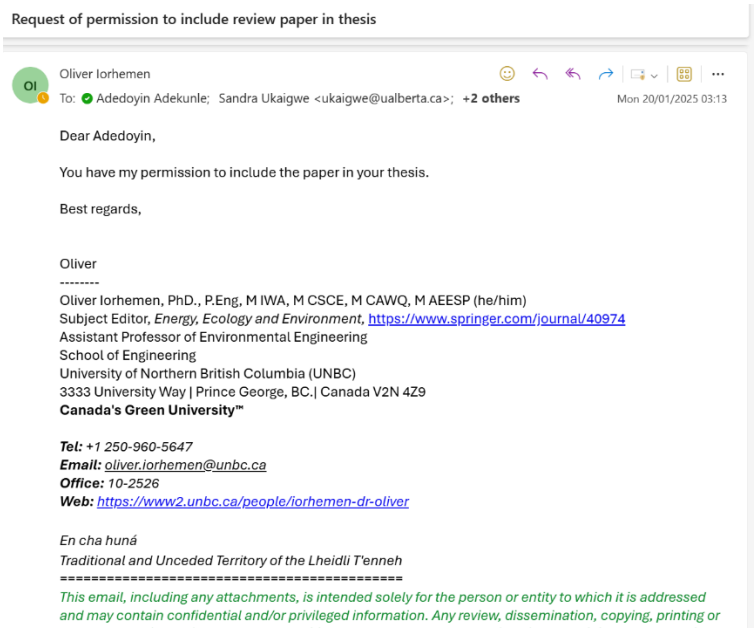

Request of permission to include review paper in thesis

Oliver Iorhemen

To: Adedoyin Adekunle; Sandra Ukaigwe <ukaigwe@ualberta.ca>; **+2 others** Mon 20/01/2025 03:13

Dear Adedoyin,

You have my permission to include the paper in your thesis.

Best regards,

Oliver

Oliver Iorhemen, PhD., P.Eng, M IWA, M CSCE, M CAWQ, M AEESP (he/him)
Subject Editor, *Energy, Ecology and Environment*, https://www.springer.com/journal/40974
Assistant Professor of Environmental Engineering
School of Engineering
University of Northern British Columbia (UNBC)
3333 University Way | Prince George, BC.| Canada V2N 4Z9
Canada's Green University™

Tel: *+1 250-960-5647*
Email: *oliver.iorhemen@unbc.ca*
Office: *10-2526*
Web: *https://www2.unbc.ca/people/iorhemen-dr-oliver*

En cha huná
Traditional and Unceded Territory of the Lheidli T'enneh
==========
This email, including any attachments, is intended solely for the person or entity to which it is addressed and may contain confidential and/or privileged information. Any review, dissemination, copying, printing or

Figure C3. Review paper co-author 2 permission request

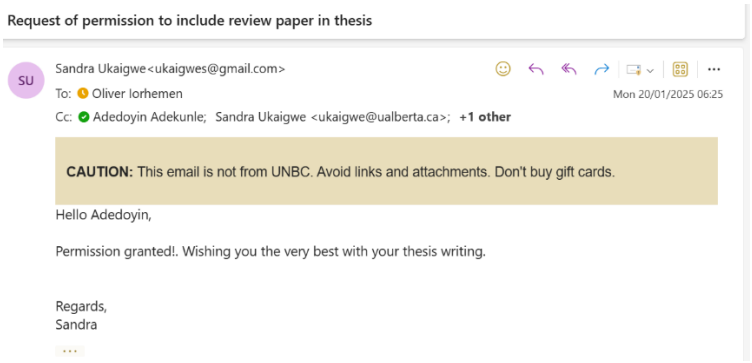

Request of permission to include review paper in thesis

Sandra Ukaigwe<ukaigwes@gmail.com>

To: Oliver Iorhemen Mon 20/01/2025 06:25

Cc: Adedoyin Adekunle; Sandra Ukaigwe <ukaigwe@ualberta.ca>; **+1 other**

CAUTION: This email is not from UNBC. Avoid links and attachments. Don't buy gift cards.

Hello Adedoyin,

Permission granted!. Wishing you the very best with your thesis writing.

Regards,
Sandra

Figure C4. Review paper co-author 3 permission request

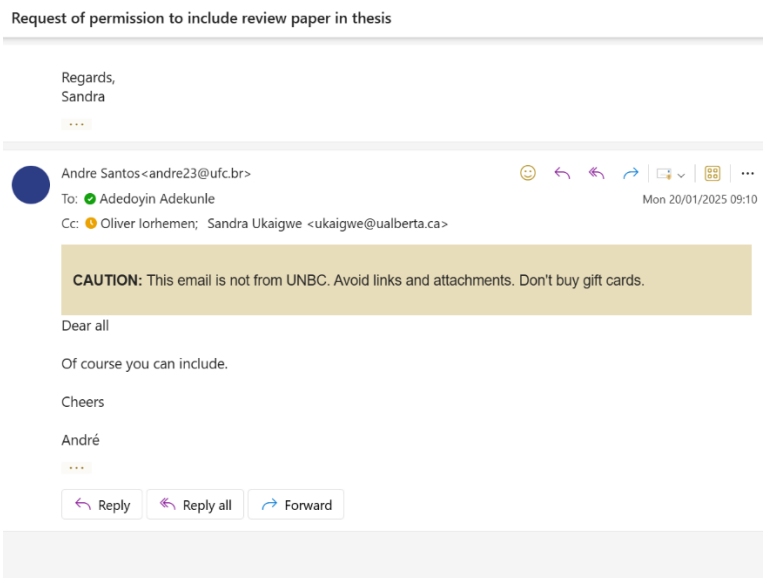

Figure C5. Review paper co-author 4 permission request

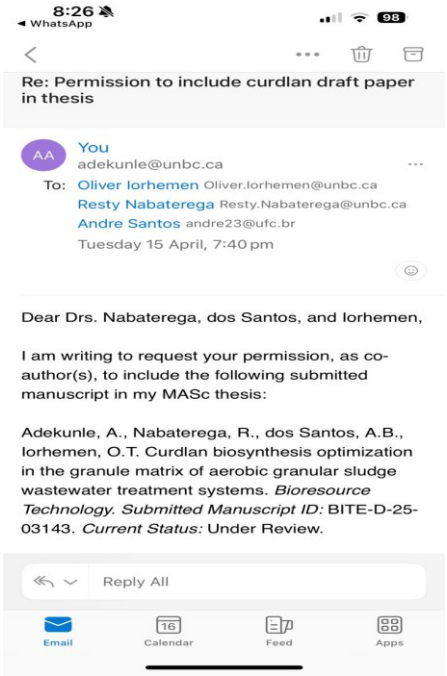

Figure C6. Research manuscript paper co-author request

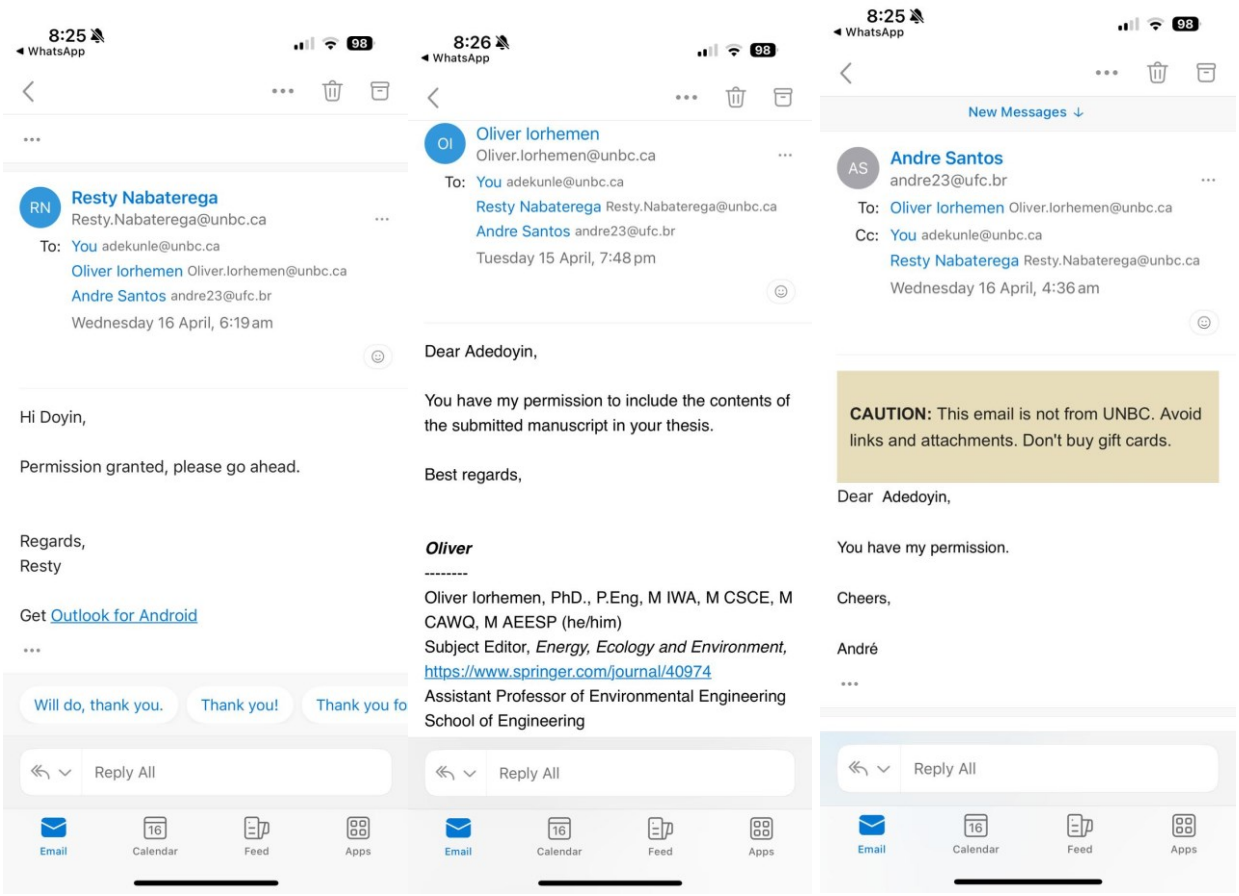

Figure C7. Research manuscript co-author permission request 1, 2 and 3